Spatial Localisation of Oxidative and Inflammatory Markers within Advanced Atherosclerotic Plaques

---

A thesis submitted in partial fulfilment of the
Requirements for the degree of
Master of Science
in Biochemistry
At the
School of Biological Sciences
University of Canterbury
New Zealand

Elizabeth M. Crone
2008

Table of Contents

List of Figures

List of Tables

Acknowledgements

Firstly I would like to thank my supervisor Dr Steven Gieseg for his direction and support throughout the research. To all the past and present members of the FRB laboratory a big thank you, especially Liz Flavall, Tina Yang, Zunika Amit and Hanadi Katouah for teaching techniques, the know how of methods and answering my relentless questions.

Thanks to Liz Flavall for being patient when first teaching me all the need to know on plaques and plaque assays, your contributions to the plaque research and the tricks and trade of the laboratory especially HPLC troubleshooting. Also to Hanadi Katouah for your contributions to the LDL experiments.

Thanks to all involved in the plaque study at the Christchurch Hospital especially Prof Justin Roake and to the registrars, surgical teams and plaque donors. Also thanks to Mr Lewis for the opportunity to observe a carotid endarterectomy. It was fascinating to get an insight into how these plaques where removed.

Thank you to Dr Jenny Willis for bleeding the volunteers and to all the blood donors. This extends to the Canterbury Health Laboratory haematology team for when fresh blood was required.

Finally thanks to my family and friends. To my mum, dad, grandparents and Jenny and Peter Rayne for all their support throughout the years. And to Daniel and my friends, for attempting to maintain the sanity and understand my ramblings when talking about my research.

Abstract

Five atherosclerotic carotid and femoral plaques were sliced longitudinally. Each section was analysed for the concentrations of neopterin, α-tocopherol, TBARS, DOPA, dityrosine, protein carbonyl, protein and cholesterol. The spatial concentrations of the oxidative and inflammatory markers were diverse across and between the individual plaques suggested by the lack of consistent correlations and trends. The only correlation that occurred twice within the individual plaques was a positive correlation between α-tocopherol and cholesterol levels. In the combined plaque analysis which included data from eight previously studied plaques, neopterin, protein carbonyl and protein concentrations all had significant positive correlations and α-tocopherol concentrations positively correlated to cholesterol and negatively to TBARS. Thus overall the level of protein may influence protein carbonyl concentration and α-tocopherol may provide an antioxidant effect towards lipid peroxidation. Furthermore, the plaques were divided into three zones, pre-bifurcation, bifurcation and post-bifurcation, associated with shear stress levels. The neopterin concentrations were significantly high within the pre- and post-bifurcation region and the opposite trend occurred with the to peroxyl radical driven TBARS levels. The protein and cholesterol content in the post-bifurcation was high, possibly due to the low and/or oscillatory shear stress occurring at these sites. The overall composition of the plaque, either thrombosed, heavily calcified or neither, also identified significant trends in marker concentrations between the plaques. The calcified plaques had significantly low levels of protein, cholesterol, α-tocopherol, DOPA and dityrosine whereas the thrombosed plaques had significantly high protein, α-tocopherol and dityrosine concentrations. The medication and symptoms presented by the patient had no major influence of the overall concentration of the markers within the plaques. Therefore even though individually the plaques have varied biochemical compositions, common influences were dictate the spatial and overall concentration of the markers within and across the plaques. Further potential markers were investigated for detection within plaque. AAS and GGS for replacement of the protein carbonyl assay as a more specific marker for protein oxidation, as well as the oxysterol 7-ketocholesterol detected simultaneously during α-tocopherol analysis. The 7-ketocholesterol would increase the information on lipid oxidation occurring in the plaque without increasing the volume of the limited homogenate required for the analysis. Investigation was also carried out on the mechanism of protein oxidation in human plasma that may provide mechanisms and interactions to protein oxidation within plaques.

Abbreviations

AAPH	2,2-azobis (2-aminopropane) dihydrochoride
AAS	α-Aminoapidic semialdehyde
ABA	4-Aminobenzoic acid
ACN	Acetonitrile
AF	Amaurosis fugax
ANOVA	Analysis of variance
apoB	Apolipoprotein B_{100}
BCA	Bicinchoninic acid
BHT	Butylated hydroxytoulene
BSA	Bovine serum albumin
CAD	Coronary artery disease
DFO	Deferoxamine (Deferoxamin methansulfonic)
Cu^{2+} /Cu^{+}	Cupric/copper ion
DNPH	Dinitrophenylhydrazine
DNA	Deoxyribonucleic acid
DOPA	3,4-Dihydroxyphenylalanine
e^{-}	Electron
EDTA	Ethylenediaminetetraacetic acid
ELISA	Enzyme-linked immunosorbent assay
ESS	Endothelial shear stress
Fe^{3+} /Fe^{2+}	Ferric/ferrous ion
FOX	Ferric-xylenol orange
GGS	γ-Glutamic semialdehyde
H^{+}	Hydrogen ion
HCl	Hydrochloric acid
H_2O_2	Hydrogen peroxide
HOCl	Hypochlorous acid
HPLC	High performance liquid chromatography
HSA	Human serum albumin
HUVEC	Human umbilical vein endothelial cells

I_2	Iodide
ICAM-1	Intracellular adhesion molecule-1
7-KC	7-Ketocholesterol
KBr	Potassium bromide
KI	Potassium iodide
$L^{\bullet}$	Lipid carbon centred radical
LD_{50}	Lethal dose which induces 50 % of mortality
LDL	Low density lipoprotein
LH	Lipid
LS	Least square (mean)
$LO^{\bullet}$	Lipid alkoxyl radical
$LOO^{\bullet}$	Lipid peroxyl radical
LOOH	Lipid hydroperoxide
MDA	Malonaldehyde
MES	2-(N-Morpholino)ethanesulfonic acid
MPO	Myelopeoxidase
NADPH	Nicotinamide adenine dinucleotide phosphate
NaH_2PO_4	Sodium dihydrogen orthophosphate
$NaHCO_3$	Sodium hydrogen carbonate
NF-κβ	Nuclear factor- κβ
7,8-NP	7,8-Dihydroneopterin
O_2	Oxygen
$O_2^{\bullet -}$	Superoxide
OH^-	Hydroxyl ion
$^{\bullet}OH$	Hydroxyl radical
$^{\bullet}OOH$	Peroxyl radical
oxLDL	Oxidised low density lipoprotein
PBS	Phosphate buffered saline
$Pr^{\bullet}$	Protein carbon centred radical
PrH	Protein
$PrO^{\bullet}$	Protein alkoxyl radical
$PrOO^{\bullet}$	Protein peroxyl radical

PrOOH	Protein hydroperoxide
PUFA	Polyunsaturated fatty acids
$R^{\bullet}$	Radical
RH	Radical in unreactive state
SD	Standard deviation
SDS	Sodium dodecyl sulphate
SEM	Standard error of the mean
SMC	Smooth muscle cells
TBA	2-Thiobarbituric acid
TBARS	Thiobarbituric acid reactive substances
TCA	Trichloroacetic acid
TFA	Trifluroacetic acid
TIA	Transient ischemic attack
TMP	α-Tocopherol mediated peroxidation
$\alpha\text{-Toc}^{\bullet}$	α-Tocopheroxyl radical
α-TocH	α-Tocopherol
VCAM-1	Vascular cell adhesion molecule-1

Introduction

1.1 Atherosclerosis

Cardiovascular disease is the number one cause of mortality, accounting for 40% of deaths (Hay, 2004), and hospital admissions within New Zealand (Wells et al., 2006). Atherosclerosis, a cardiovascular disease, literally means ‘gruel hardening’, that is a mass accumulation of cellular and lipid material within the arterial wall that eventually leads to hardening and occlusion of the artery. It is now fully acknowledged as a chronic inflammatory multi-factorial disease (Gieseg et al., 2008a; Libby et al., 2002; Stadler et al., 2004) and this reflects in its complexity. It is a disease that develops over time spanning many decades, where clinical events generally occur later in life. Risk factors associated with this disease includes hypertension, smoking, hypercholesteromia, obsesity, insulin resistance and dyslipidemia and of these factors many occur in conjugation with one another (Libby et al., 2002; Scott, 2004; Wilson et al., 1999). Although this disease has long been studied, it is still not completely understood and theories to its genesis continue to be debated. By revealing processes involved in plaque initiation, progression and events leading to clinical outcomes, subsequent intervention may be able to reduce what ultimately makes this disease the leading cause of mortality and morbidity within the developed world (Danilevicius et al., 2007; Helderman et al., 2007; Stocker and Keaney, 2004).

1.1.1 Plaque development from early lesion to complex atherosclerotic plaque

Arteries are made up of three defined layers the intima, media and adventitia (Figure 1.1). The intimal layer begins with a continuous monolayer of endothelial cells. These cells provide a permeable barrier between the blood flow and the arterial components. The endothelial cells synthesize and secrete extracellular materials like collagen, proteoglycans and fibronectin and under normal conditions are thromoboresistant. Endothelial cells are also involved in the regulation of vascular tone and contraction through various factors like the endothelial derived relaxation factor, involving nitric oxide and the activation of cyclic GMP production via smooth muscle cells (SMC) resulting in a cellular contractibility response (Stary et al., 1992). Endothelial cells are able to detect differences in shear stress by the distortion of cytoskeletal components. This mechantransduction

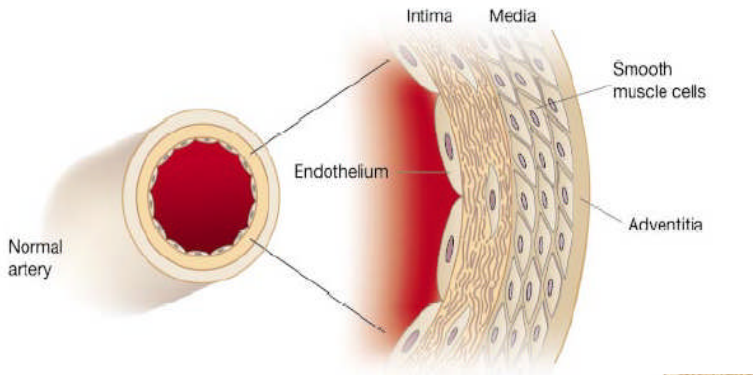

Figure 1.1 Defined layers of the arterial vessel wall

A single layer of endothelial cells provides the barrier between tissue and flowing blood. The intima, site of plaque formation, and the media consists mostly of smooth muscle cells. The adventitia and the basement membrane form the outer layers of the artery. Adapted from Libby (2002a).

triggers different physiological responses by the activation of cellular membrane proteins for example integrins and activating intracellular signallers like the GTPase (Helderman et al., 2007). Endothelial cells are also involved in the inflammatory and immune responses (Stary et al., 1992). Oxidised LDL induces the expression of growth factors like the macrophage colony stimulating factor (Rakjavashisth et al., 1990) and for leukocyte recruitment the expression of adhesion molecules for example the endothelial-leukocyte adhesion molecule-1 (Bevilacqua et al., 1987). The endothelial cells are underlayed with a region rich in connective tissue, SMC generally as single cells and isolated macrophages, followed by a third region of layered SMC, elastic fibres and a high concentration of collagen. It is this region that borders the medial layer. The intimal SMC are involved in the maintenance of the structure of the vessel through synthesis and secretion of connective tissue components such as collagen, proteoglycans and elastin. Like endothelial cells they help regulate the contractibility and vascular tone of the artery. SMC have been identified to phagocytose lipoproteins therefore are involved in lipid metabolism. The isolated macrophages present in healthy arteries function to remove antigens including dead cells and bacteria and can also mediate the inflammatory and immune response. The macrophages are also involved in remodelling of the artery through the production of growth factors (Stary et al., 1992) for example type β transforming growth factor and platelet derived growth factor (Assoian et al., 1987), and lipid metabolism by the uptake of native and modified lipoproteins (Goldstein et al., 1979; Stary et al., 1992). The underlying medial layer is primarily SMC bound together with collagen and elastin

(Stocker and Keaney, 2004). The third layer, the adventita, is predominantly connective tissue and functions to provide elasticity and dynamic rigidity to the artery.

The process of plaque formation can be briefly described by the accumulation of lipids overtime within the intimal layer via low density lipoproteins (LDL). LDL and monocytes permeate across the endothelial layer and it is at this site that oxidation of LDL can occur (Ross and Glomset, 1973), and monocytes differentiate into macrophages. The migration of monocytes and T cells through the endothelial layer is mediated by adhesion molecules. Vascular cell adhesion molecule-1 (VCAM-1) is present within early atheromas and are able to binds these leukocytes. Nuclear factor-κB (NF-κB), an inflammatory mediator, can upregulation gene expression of VCAM-1 in the endothelial cells. The cytokines interleukin 1-β and tumor necrosis factor as well as disturbed shear stress can also induce the expression of VCAM-1 in endothelial cells (Libby, 2002a). Within the intimal layer these macrophages can rapidly take up oxidise LDL (oxLDL) via scavenger receptor A and CD36 receptors resulting in the formation of the macrophage foam cells (Libby, 2002a). There are three main hypotheses to the of initiation of plaque formation (discussed below), however regardless of genesis all lesions at the beginning have similar characteristic features. The growth and progression of the plaque occur in defined stages which have been characterised into a progression of types.

Type 1 has a thickening of the wall, attributed to the formation and accumulation of macrophage foam cells. Type 1 lesions can start to form as early as at birth. The foam cells are situated in small microlocations as discrete droplets at sites within the arterial wall prone to lesion formation. The initial lesion progresses into a type II lesion by the continual accumulation of the lipid laden foam cells (Stary et al., 1994), and due to the death of these cells, by apoptotic and necrotic mechanisms, the precursor of the acellular lipid core starts to form (Ball et al., 1995; Hegyi et al., 1996). The ‘fatty streak’ a lesion that provides the first visible sign by the naked eye of plaque growth is defined as a type II lesion. The major cell type in these lesions are macrophages and this is where the majority of the lipids are localised, however native intimal SMC can also contain a high level of these lipids. The macrophages are stratified with the cells located at the bottom of the proteoglycan layer within the intima containing higher concentration of lipids compared to the macrophages closest to the endothelial layer containing fewer to no lipids. Also localised within these lesions are T cells. Type III lesions have only recently been acknowledged as an intermediate between the Type II fatty streaks and Type IV atheromas. They are defined by an increased number of

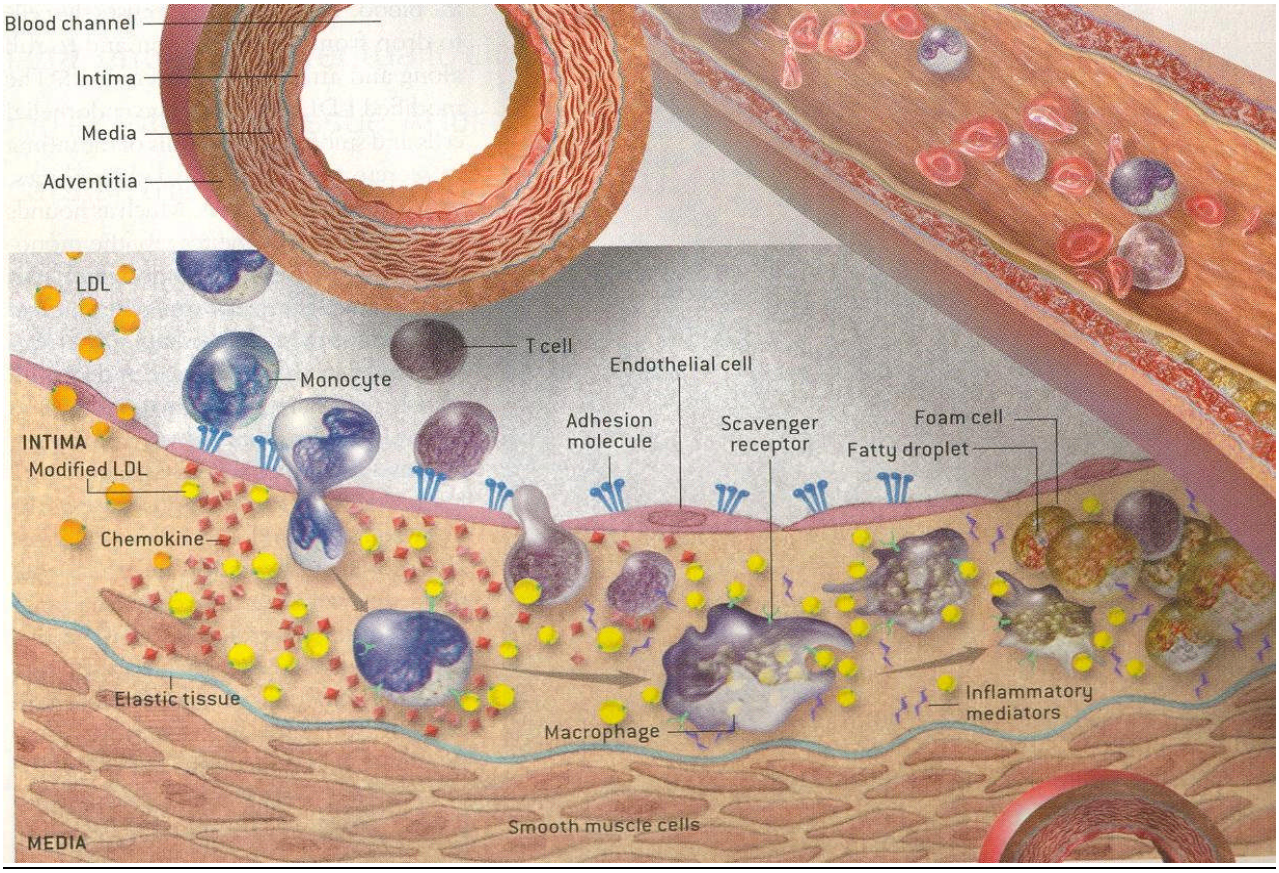

Figure 1.2 Processes involved in the formation and progression of atherosclerotic plaques
LDL and monocytes from the blood channel migrate into the intimal layer of the artery. The LDL becomes oxidised and the monocytes differentiate into macrophages. The macrophages accumulate cholesterol by the uncontrollable uptake of oxLDL leading to the formation of foam cells. Continuation of this process leads to the formation of the complex plaque. Symptoms can occur through occlusion of blood flow and/or plaque rupture. Adapted from Libby (2002b).

extracellular lipid droplets underneath the layers of macrophage and macrophage foam cells. The lipid droplets begin to replace the proteoglycan intercellular matrix and these droplets also cause the separation of SMC from other SMC (Stary et al., 1994).

Type IV, an atheroma lesion, enters the definition of an advanced plaque having a greater proportion of extracellular lipids in between layers of SMC, resulting in the deformation of the arterial lumen and disordered environment of intimal components (Stary et al., 1994). The intimal SMC proliferate and are involved in developing the abundant extracellular matrix (Libby, 2002a). Continual death of the macrophage foam cells and coalescence of the lipid pools contributes to the enlargement of the acellular lipid core, sourced from the dead macrophages which had taken up the

LDL (Jang et al., 1993; Stary et al., 1995). Type IV plaques are associated with compensatory expansive remodelling, where the artery intrudes into the outer layers of the wall maintaining the lumen structure and size (Chatzizisis et al., 2007; Stary et al., 1995). The macrophages and SMC are predominantly located on the peripheral of the lipid core where the SMC and matrix have a scattered arrangement. Microvessels within the plaque can start to form along with the process of calcification. The fibrous cap consisting of connective tissue and collagen starts to appear, and when this cap becomes significant in size the plaque is classified as Type V (Stary et al., 1995).

1.1.2 Plaque progression from the advanced plaque to clinical events

After the progression from the type IV to the more complex type V lesion, plaques are more diverse, creating many different compositional and morphological types (Stary et al., 1995) which maybe responsible for the variable clinical outcomes. Within this type are subtypes classified based on the degree of fibrous material, number and size of the lipid cores and calcification. These subtypes are formed through remodelling and repeated cycles of thrombus formation and lipid accumulation. Type V plaques contain a fibrous cap which are a distinct structure overlaying the lipid core and is rich in collagen and SMC. Fractures within the cap can result in exposure of plaque components to circulating blood which can induce events such as the thrombotic cascade event (Stary et al., 1995). Within these plaques the SMC now occupy the fibrous cap, media and outer regions of the intima (Ball et al., 1995). The plaques can continue onto a type VI classification termed complicated lesions based on the presence of hematomas or thrombi (Stary et al., 1995).

The strength of the fibrous cap is dependent on the balance between SMC maintenance and matrix degradation. The fibrous cap consists predominantly of collagen, but also SMC, proteoglycans, elastin and glycoproteins and provides a barricade between the acellular lipid core and blood. The cap of the shoulder region is thinner and more prone to rupture as it is also abundant in macrophages, foam cells and SMC (Chapman, 2007; Jang et al., 1993; Stary et al., 1995). Macrophages can secrete proteases like elastase and collagenase which digest the extracellular matrix (Jang et al. 1993), contributing to the weakening of the cap. Thrombosis is a prevalent event in determining the clinical outcome of patients. Disturbed haemodynamic forces can cause fracture of the fibrous cap and subsequent exposure of pro-thrombotic materials such as tissue factor and collagen inducing the adhesion of circulating platelets and co-augulation resulting in a thrombus

(Chapman, 2007; Libby, 2002a). Thrombus formation may also be triggered by superficial disruption to the overlying endothelial cells. Another common pathway involves the foam cells where it is thought they release proteolytic enzymes that may contribute to the disintegration of the fibrous cap (Jang et al., 1993; Stary et al., 1995). One study identified that with an increasing mass volume of the extracellular lipid core correlated with the presence of thrombotic events within aortic plaques. These plaques also had a greater proportion of macrophage cells within the cap and shoulder region of the plaque relative to SMC (Davies et al., 1993). The occurrence of a thrombotic event is responsible for the majority of the mortality and mobility rates associated with atherosclerosis (Stary et al., 1995). These clinical events when triggered from a carotid plaque can result in stokes or transient ischemic attacks, the temporary blockage within the blood flow leading to lack of oxygen to the brain and/or face. If a blockage occurs due to a femoral plaque significant tissue death can occur which can lead to the development of gangrene.

The process of calcification in plaques, likened to osteoporosis, involves the production of bone like material by the mineralisation of tissue. It is estimated that over 90% of plaques have some form of calcification (Danilevicius et al., 2007). It is now know that this process within the artery is not passive but occurs through a regulatory pathway (Abedin et al., 2004; Demer et al., 1994; Tanimura et al., 1983). A primary mineral in bone is hydroxyapaptite and has been identified within carotid and aortic plaques (Guo et al., 2000; Li et al., 2006). Osteogenic differentiation factor and bone morphogenetic protein 2a which are bone related proteins involved in bone matrix formation (Bostrom et al., 1993) as well as numerous other proteins have also been identified in plaques (Demer and Tintut, 2003). Therefore within plaques, bone morphogenetic protein along with other proteins stimulates the differentiation (Demer et al., 1994) of multipotent vascular cells into osteogenic cells (Abedin et al., 2004) and the laying down of a bone like matrix including hydroxyapaptite (Demer et al., 1994).

Plaques can undergo numerous types of remodelling depending on the type of plaque and the response of the artery. As plaques grow the arterial vessel can undergo expansive remodelling as the system tries to compensate for the increased thickness associated with the plaque. In expansive remodelling the plaque encroaches into the medial layer to maintain lumen structure and physiological endothelial shear stress. Excessive expansive remodelling refers to an over compensation of the vessel where it ultimately over enlarges the lumen of the artery compared to

the normal artery. A lowered endothelial shear stress (ESS) can increase inflammation and oxidative stress which can lead to the degradation of the extracellular matrix. Constrictive remodelling in which the plaque intrudes into the lumen hampering the flow of blood may be induced by continual rupture/healing cycles resulting in protrusion of the plaque into the lumen and stenosis (Chatzizisis et al., 2007). Stenosis is defined by the percentage of the blood flow loss within the plaque narrowed artery compared to the what it would be in a normal healthy artery (Stary et al., 1995).

1.1.3 The main hypotheses to the genesis of atherosclerotic plaques

One of the hypotheses for initiation is the 'oxidative modification hypothesis'. It is based upon the formation of cytotoxic oxLDL by oxidation of LDL lipids within the intima with subsequent modification of the apolipoprotein B_{100} (apoB) the only protein in LDL. This oxLDL is taken up by scavenger receptors, expressed on the surface of macrophage cells. This process is not regulated by the level of free cholesterol within the cell so could be described as unregulated. The scavenger receptors have a high binding affinity towards oxLDL, but do not bind native LDL (Goldstein et al., 1979). The internalisation of oxLDL into the macrophages has many consequences, including the formation of the foam cells, macrophage cell death and the triggering of the inflammatory response. Endothelial cells (Dayuan et al., 1998) and SMC (Nishio et al., 1996) also take up oxLDL which is cytotoxic to these cells at high levels.

Another hypothesis outlined by Ross and Glomset (1973) termed the 'response-to-injury' hypothesis is based upon the injury or dysfunction of the overlying endothelial cells. This allows increased permeability of the LDL and plasma proteins into the intima triggering the migration and proliferation of SMC from the medial layer. The accumulation of lipids and formation of macrophage foam cells along with the dysfunctional endothelial cells trigger an inflammatory response which re-enforces the recruitment of macrophages. This inflammatory response will generate oxidants which contribute to the formation of oxLDL. Continual proliferation of the SMC and accumulation of the macrophage foam cells leads to the formation of the complex plaque.

Response-to-retention' hypothesis implies that the retention of the LDL within the artery is the initialisation event to lesion formation (Williams and Tabas, 1995). The retention is mediated by the

apoB moiety interaction with the arterial extracellular martix, and once bound at these locations oxidation of the LDL occurs. It is well established that oxLDL is formed within the intimal layer, absent of the protective mechanism within plasma (Williams and Tabas, 1995). The presence of the oxLDL and macrophages within the intimal layer contribute to the process of lesion formation.

1.1.4 Localisation of plaques and the role of shear stress

It is well known that atherosclerotic plaques form predominantly at branch points and points of high blood turbulence (Chatzizisis et al., 2007; Helderman et al., 2007; Libby et al., 2002; Stary et al., 1995). At these points the flow of blood is non-linear due to the change in the arterial structure. Endothelial shear stress (ESS) is defined and determined by the blood viscosity and shear rate (spatial gradient of blood velocity) of the blood across the endothelial cells. Pusatile ESS on the endothelial cells occurs in relation to cardiac output, where this type of stress occurs before the branch points. When the artery is non-linear the pulsatile ESS can give rise to low and oscillatory ESS. Low ESS typically occurs around and upstream of the bifurcation, whereas oscillatory occurs typically downstream (Chatzizisis et al., 2007). However, low ESS may also occur downstream (Tricot et al., 2000) and high shear stress may also occur upstream (Helderman et al., 2007).

Shear stress is a mechano-transducer influencing the function of endothelial cells. Normal shear stress induces the expression of anti-atherogenic, anti-inflammatory and anti-apoptotic genes including superoxide dismutase and endothelial nitric oxide synthase producing nitric oxide which can inhibit VCAM-1 expression (Libby, 2002a). When this shear stress is disturbed, different genes are activated including atherogenic and inflammatory genes (Gimbrone, 1999; Resnick et al., 2003). This makes these regions prone to inflammation due to the constitutive activation of inflammatory mediators NF-κβ (Helderman et al., 2007) which activates monocyte chemoattractant protein-1 and γ-interferon (Chatzizisis et al., 2007). In the downstream area of carotid plaques associated with low ESS, endothelial cells had an increased rate of cell death via apoptotic mechanisms, relative to the upstream region (Tricot et al., 2000). One study found that the VCAM-1 receptor, expressed on endothelial cells is upregulated by low ESS compared to high ESS. A higher proportion of monocytes were co-localised with the increased level of VCAM-1 under the low ESS. This indicates that shear stress is involved in the increased permeability of LDL through the endothelial layer (Walpola et al., 1995). Also the low ESS is associated with an increase in SMC proteoglycans

synthesis therefore increasing the ability to retain and oxidise LDL (Libby et al., 2002). Other properties of low ESS include an increase of oxidative stress by increasing the NADPH oxidase within endothelial cells and downregulating superoxide dismutase and glutathione (Chatzizisis et al., 2007). In a hypercholesteremic mouse model low shear stress increased the size of the intima relative to oscillatory shear stress. The low shear stress plaques also had an increased proportion of lipid, where the oscillatory shear stress plaques had a higher proportion of vascular SMC and collagen. Furthermore in another mouse model, regions of high shear stress contained more macrophages, SMC, lipid and metalloproteinase activity. This indicates that the level and type of shear stress induced by the plaque may influence the plaque composition (Helderman et al. 2007).

1.2 Free radicals and oxidants are mediators of oxidative stress in biological systems

Free radicals are defined by any species which has one or more unpaired electrons and is able to independently exist (Halliwell and Gutteridge, 1999). Radicals can either react with each other to form a non-radical product, or it can ‘steal’ an electron from easily extractable molecules effectively neutralising the unpaired electron. These reactions are in part dependent on the mobility and reactivity of the radical. Radicals are not only produced as a metabolic product but also intentionally under controlled situations and locations (Cheeseman and Slater, 1993). The immune system is a classic example of this, where activated macrophages and neutrophils release superoxide which can be processed to the oxidants hydrogen peroxide and hypochlorous acid as an anti-bacterial and anti-fungal response (Halliwell and Gutteridge, 1999). Oxidative stress occurs when the rate of clearance of free radicals and oxidants is exceeded by their formation (Aldini et al., 2007). Oxidative stress and therefore oxidative damage is associated with many diseases including atherosclerosis and neurodegenerative diseases such as alzheimers and parkinsons disease (Beal, 2002) to name a few. The macrophages and monocytes within the plaque can release oxidants and oxygen derived radicals contributing to the source of oxidative stress (Jang et al., 1993). Aortic plaque gruel was shown to stimulate lipid peroxidation in microsomes and deoxyribose degradation due to the presence of free iron and copper (Smith et al., 1992). This indicates that within the plaque oxidative damage can occur. Supporting this, numerous studies have identified oxidative damage associated with radical attack within plaques (Figure 1.3) (Fu et al., 1998; Leeuwenburgh et al., 1997; Martinet et al., 2002; Prunet et al., 2006; Smith et al., 1992; Stanley et al., 2006). Theses

oxidative products may contribute to the persistence of plaques due to their cytotoxcity to immune cells. The gruel of carotid and aortic plaques phagocytosed by macrophage like cells and human monocyte derived macrophage induced apoptosis attributed to the presence of aldehydes, carbonyls and hydroperoxides within the gruel (Li et al., 2006).

Superoxide ($O_2^{\bullet -}$) is the primary free radical generated within a biological system (Dean et al., 1997). It is formed by the reaction between oxygen and an electron (reaction 1). The electron transport chains within the mitochondria and endoplasmic reticulum are the major source for superoxide (Halliwell and Gutteridge, 1999). Superoxide can be removed from the system by dismutation to hydrogen peroxide via the enzyme superoxide dismutase (reaction 2). Because superoxide is a relatively unreactive radical (Dean et al., 1997), its main fate is the precursor to hydrogen peroxide and the reduction of transition metals (Cheeseman and Slater, 1993). These transition metals can cause the formation of hydroxyl, peroxyl and alkoxyl radicals (Dean et al., 1997). In the presence of the most biologically relevant transition metals, iron and copper, hydrogen peroxide and superoxide can reduce the ions to a redox active state (reaction 3). The reduced metal ion can undergo Fenton reactions by reacting with hydrogen peroxide catalysing the formation of hydroxyl radicals ($OH^{\bullet}$) (reaction 4). These reactions constitute the main fate of hydrogen peroxide within the system. Hydroxyl radicals can also be formed by a non-catalysed reaction between superoxide and hydrogen peroxide, however *in vivo* this reaction is slow (Cheeseman and Slater, 1993). Reaction 4 is also dependent on the oxidative state and concentration of the iron and copper present (Berlett and Stadtman, 1997). Using a minimally invasive technique Stadler et al. (2004) identified high non-ferritin non-heme iron levels concentrated within the intimal layer of plaques, along with copper ions, that may represent a redox active pool capable of undergoing these reactions.

(1) $O_2 + e^- \rightarrow O_2^{\bullet -}$

(2) $2O_2^{\bullet -} + 2H^+ \rightarrow H_2O_2 + O_2$

(3) $Fe^{3+}/Cu^{2+} + O_2^{\bullet -} \rightarrow Fe^{2+}/Cu^{+} + O_2$

(4) $H_2O_2 + Fe^{2+}/Cu^{+} \rightarrow {}^{\bullet}OH + OH^- + Fe^{3+}/Cu^{2+}$

The hydroxyl radical is the most reactive radical with a reaction rate of 10^{-9} seconds at 37ºC, therefore is considered the most prominent inducer of biomolecular damage (Gebicki, 1997). This damage can be induced on a range of molecules including protein, lipids and nucleic acids.

1.2.1 Protein oxidation

The hydroxyl radical is non-discriminative towards biomolecules. Protein is the most abundant component within the cell therefore the hydroxyl radical will most likely react with and induce protein damage (Gebicki, 1997). The damage caused to proteins by radicals and oxidants range from protein carbonyls, protein hydroperoxides, DOPA, dityrosine, 3-chlorotyrosine and 5-hydroxy leucine (Aldini et al., 2007; Davies et al., 1999; Dean et al., 1997; Gebicki, 1997; Gieseg et al., 1993) to name a few. Many of these changes can alter the structure at either the primary, secondary, tertiary and if applicable quaternary structure contributing to full or partial inactivation (Aldini et al., 2007). Metal-dependent oxidation of proteins is facilitated by the ability of proteins to bind metals and to their abundance within the system (Gebicki, 1997). This results in a localised level of damage. Many of the protein oxidation markers mentioned above have previously been identified within atherosclerotic plaques (Davies et al., 1999).

1.2.1.1 Protein carbonyls formation

Protein carbonyls are the most studied form of protein damage (Dalle-Donne et al., 2003). Protein carbonyl formation can be induced by numerous radicals (Halliwell and Gutteridge 1998). Because of this the primary radical that induced the formation of the protein carbonyls within a biological system cannot be identified therefore protein carbonyls are a general marker of oxidation (Dalle-Donne et al., 2003; Halliwell and Gutteridge, 1999). Protein carbonylation is irreversible (Aldini et al., 2007), indicative of large degree of oxidative stress (Dalle-Donne et al., 2003) and associated with aging and numerous diseases (Berlett and Stadtman, 1997).

There are many pathways for protein carbonyl formation including direct derivatisation of amino acid residues particularly on lysine, arginine, proline and threonine. More complex mechanisms include, a secondary reaction involving the lipid oxidation breakdown products, reactive aldehydes (malondialdehyde and 4-hydroxy-2-nonenal) reacting with nucleophilic residues like lysine, histidine and cysteine. The reaction of protein with reducing sugars (glyoxal and methylglyoxal) and their corresponding breakdown products (ketoaldehydes and ketoamines) with lysine residues via glycation and glycoxidation reactions also leads to carbonyl formation. By oxidative cleavage of the protein backbone occurring through the α-amidation pathway or the abstract of the γ-carbon on

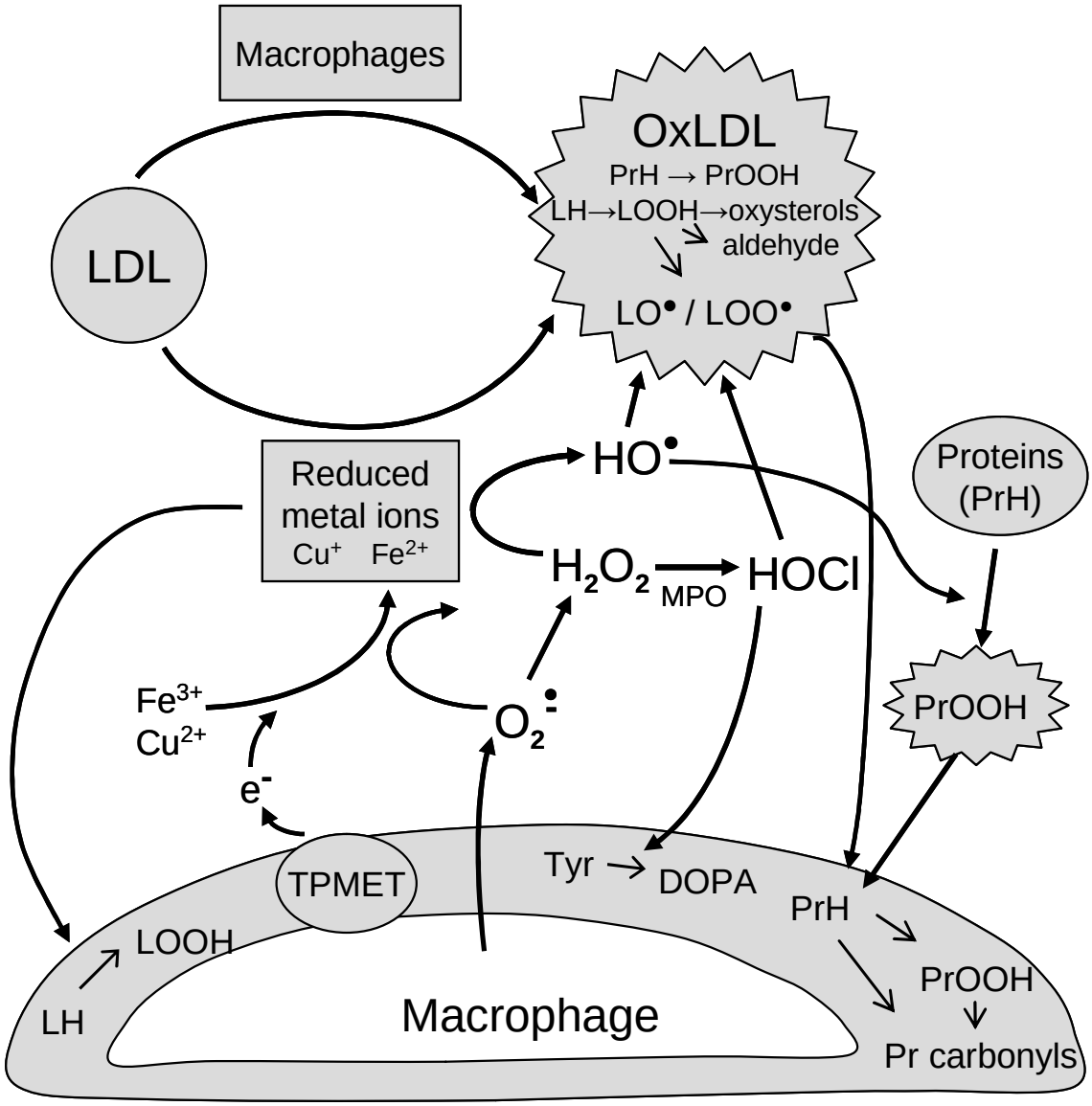

Figure 1.3 Overview of the free radicals, oxidants and oxidative damage identified within atherosclerotic plaques

Within the intima LDL can become oxidised via cell or metal mediated oxidation. The oxLDL contains protein hydroperoxides (PrOOH) and lipid hydroperoxides (LOOH), where the LOOH can break down forming oxysterols and reactive aldehydes. The peroxyl radicals ($LOO^{\bullet}$) and aldehydes can mediate the formation of protein carbonyls (Pr carbonyls) and PrOOH. The PrOOH can themselves mediate oxidative damage including the formation of protein carbonyls. The macrophage releases superoxide ($O_2^{\bullet -}$) which can mediate the formation of hydrogen peroxide (H_2O_2), as well as reduce iron and copper maintaining the pool of redox active ions. Electrons from the trans plasma membrane electron transport (TPMET) within macrophages can also maintain this pool. Via myeloperoxidase (MPO) the H_2O_2 is converted to hypochlorous acid (HOCl) which along with the hydroxyl radical ($^{\bullet}OH$) can induce PrOOH and LOOH formation contributing to the oxidative damage on the oxLDL and cellular damage. The tyrosine residues are also prone to modification to DOPA and dityrosine. Modified from Gieseg et al. (2008b).

the glutamic residue along with subsequent reactions can result in cleavage of the peptide and a N-terminus block via a α-ketoacyl derivative forming protein carbonyls (Aldini et al., 2007; Berlett and Stadtman, 1997; Dalle-Donne et al., 2003). Protein carbonyls are also formed from the breakdown of protein hydroperoxides by the formation of an alkoxyl radical on the α-carbon mediated by transition metals. Rearrangement of the one electron results in the cleave of the peptide bond and the formation of the protein carbonyl (Davies, 1996). It has been proposed that protein hydroperoxide formation and degradation is the main reaction pathway leading to carbonyl formation.

1.2.1.2 Protein hydroperoxidation

Protein hydroperoxides (PrOOH) are the most abundant form of protein oxidation (Firth et al., 2008). In the presence of radicals ($R^{\bullet}$) a hydrogen can be abstracted from a protein carbon (PrH) to form a carbon centred radical ($Pr^{\bullet}$) (reaction 5). This radical is stable enough to remain and react with oxygen forming the protein peroxyl radical ($PrOO^{\bullet}$) (reaction 6), which propagates a chain reaction by abstracting a hydrogen from another carbon forming a second carbon centred radical (reaction 7). The chain reaction is terminated when either the carbon centred radical or protein peroxyl radical reacts forming non-radical products (reaction 8).

(5) $PrH + R^{\bullet} \rightarrow Pr^{\bullet} + RH$

(6) $Pr^{\bullet} + O_2 \rightarrow PrOO^{\bullet}$

(7) $PrOO^{\bullet} + R'H \rightarrow PrOOH + R'^{\bullet}$

(8) $Pr^{\bullet}/PrOO^{\bullet} + e^{-} + H^{+} \rightarrow PrH/PrOOH$

There are six amino acids which are highly susceptible to PrOOH formation isoleucine, leucine, valine, glutamate, proline and lysine. These six amino acids either have a tertiary or secondary carbon on the side chain providing sufficient stability of the carbon centred radical long enough for its reaction with oxygen (Gebicki, 1997; Simpson et al., 1992). Not only are the side chains modified, the α-carbon on residues is also a site for PrOOH formation (Dean et al., 1997). PrOOH is an oxidising agent capable of oxidising antioxidants like ascorbate and glutathione, thereby propagating oxidative stress (Simpson et al., 1992). As previously mentioned PrOOH breakdown products can also induce the formation of protein carbonyls (Firth et al., 2008). PrOOH are further

involved in oxidative stress as PrOOH can form strong intermolecular bonds with DNA on non-specific sites at relatively slow rates (Gebicki and Gebicki, 1999) thus inducing DNA damage.

1.2.1.3 DOPA and dityrosine formation

Protein bound 3,4-dihydroxyphenylalanine (DOPA) formation can occur via a radical mechanism by the addition of hydroxyl radicals onto the ortho-position of the tyrosine aromatic ring (Gieseg et al., 1993; Rodgers and Dean, 2000). Its formation can also be mediated by HOCl (Sutherland et al., 2003) and peroxyl radicals (Davies et al., 1999). DOPA is also intentionally formed by enzymatic activity of tyrosinase as DOPA is a naturally occurring pigment associated with melanin. It has been found in the active site of some amine oxidases and shown that DOPA can extensively cross link increasing its resistance to proteolysis. Protein-bound DOPA is also formed by incorporation of free DOPA into proteins. Whereas degradation by detoxification, tyrosinase, proteolysis and auto-oxidant to dopaquinone can remove it from the system (Rodgers and Dean, 2000).

DOPA is a strong reducing agent able to reduce metalloprotein and transition metals which can then undergo Fenton reactions (reaction 4) (Dean et al., 1997; Exner et al., 2003; Fu et al., 1998; Gieseg et al., 1993). Morin et al. (1998) found that DOPA in the presence of Cu^{+} and oxygen induces damage to DNA putatively via a hydroxyl radical intermediate. The effects of DOPA can be far reached as it is able to diffuse from its point of origin due to is relatively high stability (Gieseg et al., 1993). Because of this it is hypothesised that DOPA may be involved in the progression of plaque development (Rodgers and Dean, 2000). Peptide bound-DOPA has also been reported to inhibit Cu^{2+} mediated LDL oxidation by the sequestering of the ion preventing its interaction with apoB on LDL. When the LDL oxidation was already in progress the role of DOPA convert to a pro-oxidant effect, thus the DOPA was involved in mediating the oxidation of LDL (Exner et al., 2003).

Dityrosine is another prominent stable protein oxidation marker, where the concentration of this marker is dependent on the radical flux determined by the degree of oxidative stress and radical formation rate (Davies et al., 1999). Redox active metal mediated hydroxyl radicals (reaction 4) can abstract the hydrogen from the hydroxyl group of the tyrosine residue. The lone electron can resonate from the oxygen to the ortho position (Figure 1.3) (Giulivi and Davies, 1994) producing the long lived tyrosyl radical (Heinecke et al., 1993). The dityrosine is formed by the reaction

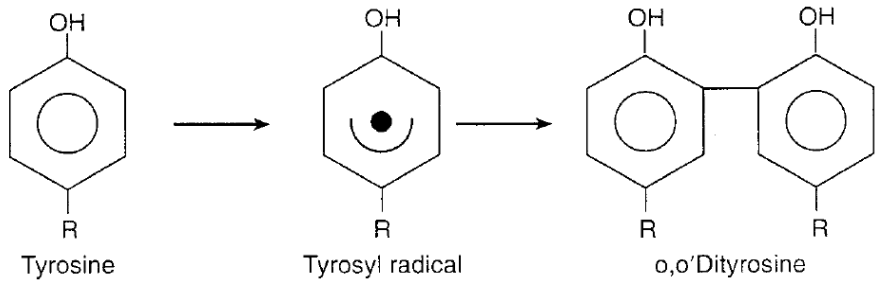

Figure 1.4 Dityrosine formation
A hydrogen from the tyrosine residue is abstract via hydroxyl radicals, forming the tyrosyl radical where the unpaired electron can resonate around the aromatic ring increasing its stability. Two tyrosyl radicals can neutralise creating a carbon-carbon bond across the ortho position of the ring and the production of dityrosine. Adapted from Heinecke (1999)

between two tyrosyl radicals across the ortho position. Dityrosine is also formed via metal-independent pathways associated with activated phagocyte secreted myeloperoxidase (MPO). The MPO-H_2O_2 system mediated by hydrogen peroxide results in the tyrosyl radical (Heinecke et al., 1993; Leeuwenburgh et al., 1997). Further supporting this system Heinecke et al. (1993) treated neutrophils and macrophages with heme poisons, knocking out the MPO, which inhibited the formation of dityrosine. DOPA and dityrosine have both been identified within atherosclerotic plaques (Fu et al., 1998), acting as a marker of oxidative and free radical damage respectively (Davies et al., 1999).

1.2.2 Lipid oxidation and the formation of oxidised low density lipoprotein

Lipid oxidation occurs on polyunsaturated fatty acids (PUFAs) which are highly susceptible to free radical attack. Cellular membranes have a high proportion of PUFAs where alterations can lead to modification in structure and possibly function making it a destructive component of oxidative stress. LDL has a high proportion of cholesterol and PUFA substrates for lipid oxidation and the ε-amino groups of lysine residues are highly susceptible to modified by lipid peroxidation products (Esterbauer et al., 1993). PUFAs have easily extractable hydrogens which radicals can rapidly abstract forming carbon centred radicals ($L^{\bullet}$) (reaction 9). This carbon centred radical readily reacts with oxygen to form the peroxyl radical ($LOO^{\bullet}$) (reaction 10), which propagates the radical damage by abstracting an electron from a hydrogen of another PUFA (reaction 11), effectively creating a

chain reaction. The products formed are the lipid peroxide (LOOH) and a second carbon centred radical. This chain reaction will continue until it is neutralised forming a non-radical product (reaction 12) (Cheeseman and Slater, 1993). The chain reaction can also be terminated by antioxidants primarily α-tocopherol. In the presence of transition metals LOOH can decompose forming alkoxyl ($LO^{\bullet}$) and peroxyl radicals resulting in the formation of a large range of products including reactive aldehydes, isoprostanes and oxysterols (reaction 13) (Cheeseman and Slater, 1993). The lipid hydroperoxide breakdown products of isoprostanes and reactive aldehydes 4-hydroxy-2-nonenal and malondialdehyde have been identified within plaques (Gniwotta et al., 1997).

(9) $LH + R^{\bullet} \rightarrow L^{\bullet} + R^{\bullet}$

(10) $L^{\bullet} + O_2 \rightarrow LOO^{\bullet}$

(11) $LOO^{\bullet} + L'H \rightarrow LOOH + L'^{\bullet}$

(12) $LOO^{\bullet} + LOO^{\bullet} \rightarrow$ non-radical product

(13) $LOOH \rightarrow LO^{\bullet}$ or $LOO^{\bullet}$ or aldehydes or oxysterols

It is well established that the lipid peroxides and/or lipid oxidation products can mediate protein oxidation (see section 1.2.1.1). LDL oxidation is a prime example of this where on LDL's only protein, apoB, modification can be mediated by the more complex lipid peroxidation breakdown products (Gieseg et al., 2003; Steinbrecher et al., 1989). Roubal and Tappel (1966) identified that lipid peroxyl radicals can mediate protein crosslinking. Furthermore the formation of protein hydroperoxides on copper and peroxyl radical mediated LDL oxidation was induced by the lipid peroxyl radicals formed from the lipid hydroperoxides (Gieseg et al., 2003).

1.2.3 Properties of oxidised low density lipoprotein

LDL is the main free and ester cholesterol carrying particle in the blood. It consists of 42% cholesteryl esters, 22% phospholipids, 22% of the protein, apoB, 10% free cholesterol and 6% triglycerides (Esterbauer et al., 1992). It is well established that one of the risk factors for atherosclerosis is high plasma LDL (Steinberg et al., 1989), as it is this LDL that is retained and oxidised within the arterial wall (Upston et al., 2002a). The high content of PUFA within the LDL makes it highly susceptible to lipid oxidation and indeed when the composition of LDL was

compared to LDL collected from plaques the fatty acid content was greatly decreased (Esterbauer et al., 1992).

There are three phases to LDL oxidation, the lag phase where all the antioxidants predominantly α-tocopherol are consumed. The propagation phase, where cholesterol dienes and lipid peroxide concentrations rapidly increase along with a slower rate of TBARS formation. Followed by the decomposition stage where the level of lipid hydroperoxide breakdown products such as malondialdehyde, 4-hydroxynonenal increase. As discussed above the apoB can be modified by the lipid peroxyl and alkoxyl radicals produced by the propagation phase (Esterbauer et al., 1992). Additionally the apoB protein can be oxidised via reaction of reactive aldehydes to the ϵ-amino groups on lysine (Esterbauer et al., 1992). This leads to fragmentation of the apoB and increased substrate for the scavenger receptors (Steinberg et al., 1989) scavenger receptor A and CD36 presented by the macrophages (Goldstein et al., 1979; Libby, 2002a).

LDL modified into a state which is recognisable by the scavenger receptor has been reported to be mediated by the main cells types within the vascular wall (Steinberg et al., 1989); monocytes, macrophages (Hiramatsu et al., 1987), SMC (Heinecke et al., 1986) and endothelial cells (Steinbrecher, 1988). The mechanism of cell mediated LDL oxidation requires redox active metal ions (Garner and Jessup, 1996; Kritharides et al., 1995). Copper is able to strongly bind to specific binding sites on the apoB protein, and in the presence of preformed lipid peroxides the redox active ions can initiate further lipid oxidation chain events (reaction 14 and 15) (Esterbauer et al., 1992; Patterson et al., 2003).

$$(14)\quad LOOH + Cu^{+} \rightarrow LO^{\bullet} + OH^{-} + Cu^{2+}$$

$$(15)\quad LOOH + Cu^{2+} \rightarrow LOO^{\bullet} + H^{+} + Cu^{+}$$

Even though many cells may mediate the oxidation of LDL, the oxLDL is itself cytotoxic towards the cells. Studies have identified that it induces apoptosis in SMC (Nishio et al., 1996), endothelial cells, macrophages (Dayuan et al., 1998) and T cells (Alcouffe et al., 1999). In terms of the macrophage when the oxLDL is taken up it causes the loss of pH homeostasis within the lysosome, affecting the activity of lysosomal lipase, an enzyme responsible for the hydrolysis of the cholesterol esters. By loss of its activity the lipids cannot be processed and therefore accumulate

within the macrophage (Cox et al., 2007). Also lysosomal leakage results in macrophage foam cell death (Yuan et al., 2000), contributing to the formation of the acellular lipid core. Another toxicity property of oxLDL is that it is a chemoattractant for circulating monocytes (Quinn et al., 1987). It is also chemotactic to SMC and T-cells (Williams and Tabas, 1995), cells all involved in the inflammatory component of atherosclerosis. There are numerous other properties including encouraging adhesion of monocytes to endothelial cells, the formation of the macrophage foam cells, migration and proliferation of SMC, and inducement of necrosis as well as apoptosis of various cells (Chisolm and Steinberg, 2000; Esterbauer et al., 1992).

1.2.4 Oxysterols

Oxidation of cholesterol produces oxysterol by either enzymatic (sterol 27-hydroxylase, cholesterol 7 α-hydroxylase) or non-enzymatic auto-oxidation (Jessup and Brown, 2005; van Reyk et al., 2006). Oxysterols levels are maintained at low concentrations, however in disease states they can accumulate. They have been identified within plaques, where 27-hydroxylcholesterol, 7-ketocholesterol (7-KC) (Jessup and Brown, 2005) and 7-β-hydroxylcholesterol are the most abundant oxysterols (Larsson et al., 2006). Within macrophage foam cells 7-KC accounted for 0.1-9.9% of oxysterol as a percentage of cholesterol (van Reyk et al., 2006). Cholesterol oxidation most likely begins from the radicals produced by PUFA oxidation. An increase in α/β-expoide, 7-α/β-hydroxylcholesterol and 7-KC, with a concomitant decrease in α-tocopherol was observed within LDL after copper oxidation (Chang et al., 1997).

Chang et al. (1997) propose that the non-enzymatic formation of 7-KC begins by the auto-oxidation of cholesterol in the presence of lipid alkoxyl or peroxyl radicals and a redox active metal. The reactive allylic hydrogen at the 7 position is abstracted (Figure 1.5 (2)), creating a carbon centred radical which reacts with oxygen to form a peroxyl radical (Figure 1.5 (3)). The abstraction of hydrogen from a lipid results in a peroxide on the 7-position (Figure 1.5 (4)). Thermal or transition metal induction of homolysis of the peroxide bond yields an alkoxyl radical (Figure 1.5 (5)) and the formation of the 7-KC (Figure 1.5 (6)). Alternatively the rearrangement of the peroxyl radical (Figure 1.5 (4)) to the keto functionality may also produce 7-KC (Figure 1.5 (6)).

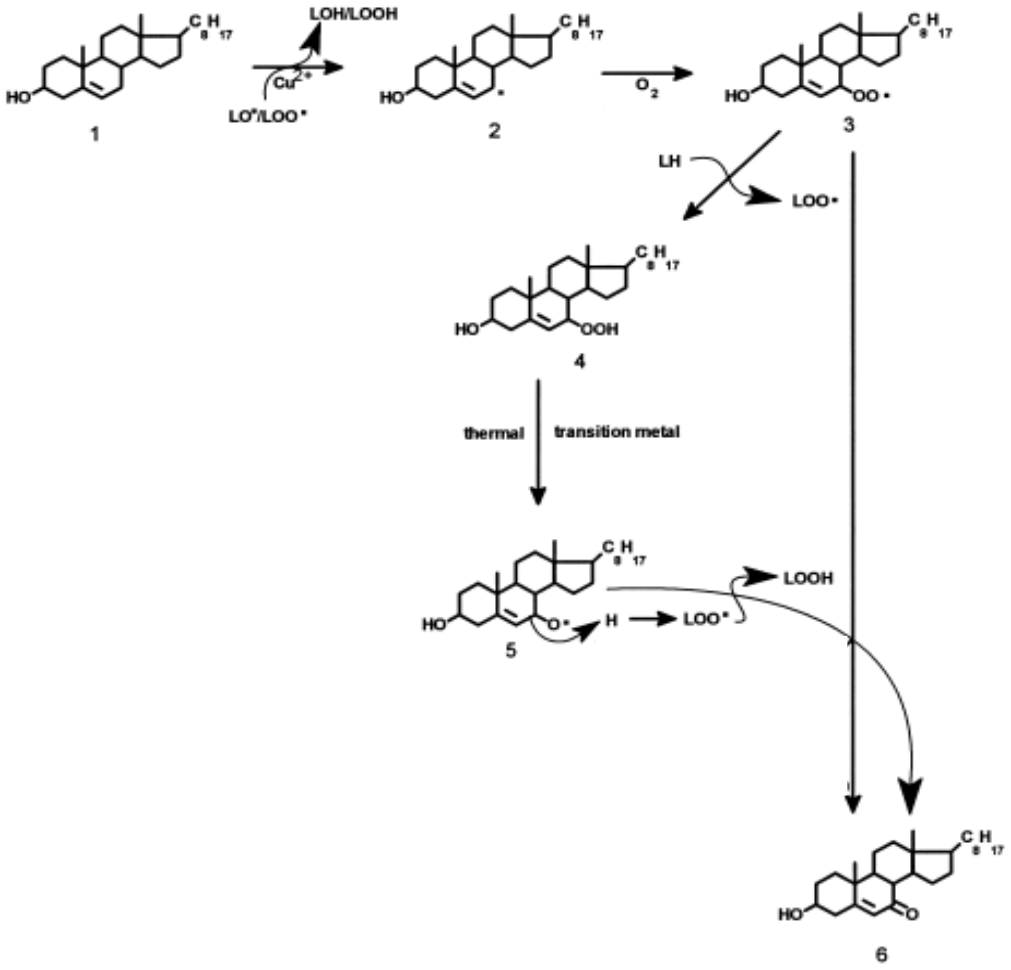

Figure 1.5 Putative reaction scheme for the formation of 7-ketocholesterol
In the presence of redox active metal lipid peroxyl or alkoxyl radicals can abstract the hydrogen from the 7 position on cholesterol (1), forming 3β-hydroxycholes-5-en-7-yl a carbon centred radical (2). In the presence of oxygen forms 3β-hydroxycholes-5-en-7-peroxyl (3) radical and can propergate by abstraction of hydrogen from lipid to form 3β-hydroxycholes-5-ene-7-hydroperoxide (4), and dervises 3β-hydroxycholes-5-en 7-oxyl (5) radical before forming 7-ketocholesterol (6). Alternatively 7-ketocholesterol can be directly produced from 3β-hydroxycholes-5-en-7-peroxyl (3). Adapted from Chang et al. (1997).

Oxysterols may contribute to plaque growth. It is hypothesised the plaques are able to maintain and grow because this material cannot be detoxified and removed due to the cytotoxic effects towards various cells including macrophages (Larsson et al., 2007). In a study which exposed 7-β-hydroxycholesterol and 7-KC in proportions reported within lesions to the human monocyte line U-937, the oxysterols induced apoptosis and necrosis along with increased lysosome and mitochondria membrane permeability, a decrease in cellular thiol content and increased in oxidants. The 25- and

27-hydroxylcholesterol displayed protective effects towards the 7-β-hydroxycholesterol and 7-KC induced cytotoxicity towards the cells. However when all four oxysterols where present in atheroma relevant proportions the cytotoxic effect prevailed (Larsson et al., 2006). When HUVEC and human artery SMC where exposed to 7-KC and 7-β-hydroxycholesterol, apoptotic like features were observed and with fibroblast cells the oxysterols induced necrosis like features, further supporting the cytotoxic role of these oxysterols on vascular cells (Lizard et al., 1999). One of the cytotoxic components of death inducing oxLDL towards porcine aortic SMC was identified as 7-KC (Hughes et al., 1994). Furthermore, within copper mediated oxidation of LDL the concentration of 7-KC increased with exposure of copper and it was the high 7-KC containing oxLDL which showed the most toxicity towards human retinal pigment epithelial cells. Exposure of these cells to 7-KC alone had the most pronounced effect compared to other 7-modified cholesterols supporting its cytotoxic role towards the cells (Rodriguez et al., 2004). Steffen et al. (2006) argued that 7-β-hydroxycholesterol exerts the proapototic effect on endothelial cells and the 7-KC counteracts this. That the proportion of 7-ketocholesterol and 7-β-hydroxycholesterol present within the site and not the total concentration of oxysterols will dictate the pro-apopototic effects on the cells (Steffen et al., 2006).

1.3 Inflammation and atherosclerosis

Inflammation is closely associated and plays a crucial role in atherosclerosis (Libby, 2002a). The migration and presence of inflammatory cells within the plaque such as macrophages and T cells (Chatzizisis et al., 2007), and a large array of inflammatory mediators supports this (Lassila, 1993). For example cytokines released within the plaque include growth factor-β and γ-interferon which stimulate and inhibit collagen synthesis by the SMC respectively (Libby, 2002a; Stocker and Keaney, 2004), platelet-derived growth factor released from endothelial cells, macrophages, SMC and platelets induces the proliferation and migration of SMC (Lassila, 1993). Furthermore, low shear stress can upregulate the expression of γ-interferon along with VCAM-1 and ICAM-1 (Chatzizisis et al., 2007). Interleukins and tumour necrosis factor-α released by macrophages can further recruit monocytes into the intima (Jang et al., 1993), and regulate metalloproteinase (Lassila, 1993), where interleukins and lymphokines from activated T cells are involved in lipid uptake of macrophages. SMC migration and proliferation may be mediated by the macrophage-derived

growth factor (Jang et al., 1993). Thus the inflammatory components within the plaque qualitatively and quantitatively can alter the extracellular matrix within plaques (Lassila, 1993). Further supporting the role of inflammation with atherosclerosis is the presence of the inflammatory marker neopterin (Firth et al., 2008; Gieseg et al., 2008a).

1.3.1 Neopterin and 7,8-dihydroneopterin

Activated T cells release γ-interferon stimulating the synthesis and secretion of 7,8-dihydroneopterin (7,8-NP) by macrophages. Based on literature it is suggested that 7,8-NP may act to protect macrophages and other cells from oxidants released during inflammation, including the macrophages own oxidants (Gieseg et al., 2008a). The concentration of neopterin, the oxidation product of 7,8-NP, within plasma of cardiovascular diseased patients are elevated (Tatzber et al., 1991), and correlate to the severity of the disease (Weiss et al., 1994). Because neopterin is relatively stable and highly fluorescent it is a marker of immune cell activation (Widner et al., 2000). Hence it has been used in numerous clinical settings to monitor HIV (Wirleitner et al., 2005), bacterial and viral infections (Denz et al., 1990), predictor of long term renal graft outcome (Grebe et al., 2004), and cancer (Reibnegger et al., 1991). Neopterin has been identified within plaques and is most likely the source of the high levels of neopterin in the plasma of the cardiovascular diseased patients (Gieseg et al., 2008a).

The synthesis of 7,8-NP and neopterin begins with an enzyme unregulated by γ-interferon, guanosine triphosphate (GTP)-cyclohydrolase which converts GTP to dihydroneopterin triphosphate. In the presence of 6-pyruvoyl tetrahydropterin synthase and sepiapterin reductase the dihydroneopterin triphosphate is converted to 5,6,7,8-tetrahydrobiopterin. 5,6,7,8-Tetrahydrobiopterin is a co-factor for many enzymes like the aromatic acid hydroxylases and inducible nitric oxide synthase. However, within primate macrophages there is little to no significant 6-pyruvoyl tetrahydropterin synthase activity allowing the buildup of dihydroneopterin triphosphate. Via unspecific intracellular proteases the phosphates are cleaved to yield 7,8-dihydroneopterin (Figure 1.6) (Hoffmann et al., 2003; Schoedon et al., 1987).

7,8-NP has been reported to have antioxidant (Firth et al., 2008; Gieseg et al., 1995; Herpfer et al., 2002; Weiss et al., 1993) and pro-oxidant activity (Herpfer et al., 2002; Wirleitner et al., 2003).

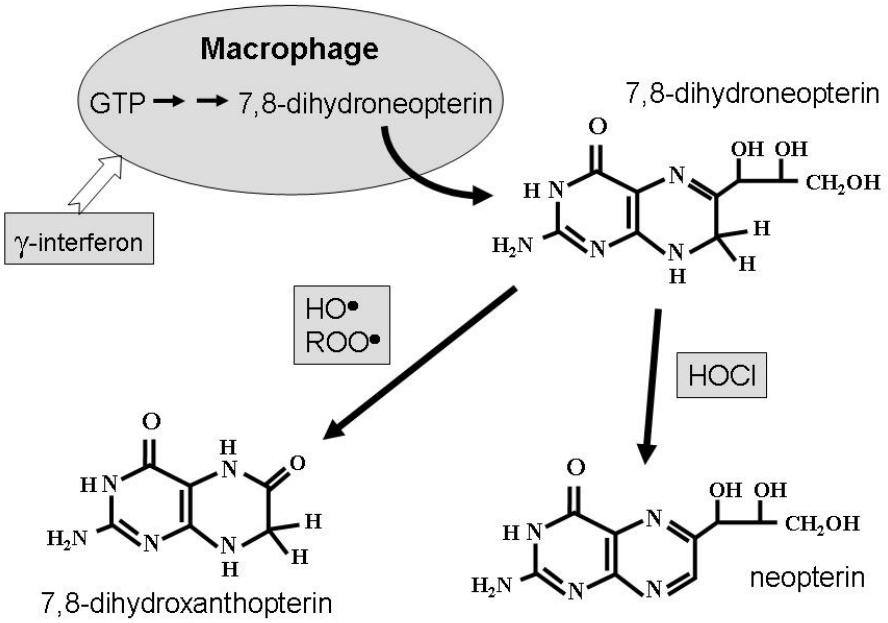

Figure 1.6 Overview of the synthesis of 7,8-dihydroneopterin and neopterin
T cell released γ-interferon stimulates the synthesis and secretion of 7,8-dihydroneopterin from macrophages. In the presence of hypochlorous acid (HOCl), 7,8-dihyroneopterin is oxidised to neopterin, and in the presence of hydroxyl ($HO^{\bullet}$) or peroxyl radicals ($ROO^{\bullet}$) 7,8-dihydroxanthopterin is formed. Adapted from Gieseg et al. (2008b).

Evidence suggests 7,8-NP is an effective peroxyl radical scavenger (Baird et al., 2005; Firth et al., 2008; Gieseg et al., 2003). Measurement of spin trapping of superoxide and peroxyl radicals in the presence of 7,8-NP indicated that it was a potent scavenger of these radical with rate constants of 10^3 and 10^7 moles per second respectively. This scavenging ability was not seen with neopterin (Oettl et al., 1997). THP-1 and human monocyte derived macrophages have been reported to mediate LDL oxidation by the formation of lipid and protein hydroperoxides. As a result of the lipid peroxyl radical scavenging ability of 7,8-NP, micromolar concentrations inhibited the protein and lipid hydroperoxidation formation on the LDL (Firth et al., 2008). 7,8-NP also protected the viability of U937 cells from Fe^{2+} and hypochlorous acid mediated oxidation (Gieseg et al., 2001), as well as protein hydroperoxidation formation and peroxyl radical mediated thiol cell loss (Duggan et al., 2002). 7,8-NP was able to protect U937 cells from oxLDL mediated cell death. It was also able to protect both THP-1 and U937 cells from AAPH derived peroxyl radicals (Baird et al., 2005). However, 7,8-NP failed to protect THP-1 from oxLDL mediated death (Baird et al. 2005) and

human monocyte derived macrophages from peroxyl mediated death (Firth et al., 2007). Thus the mechanism of 7,8-NP antioxidant activity is not fully understood.

7,8-NP is a reducing agent and thereby under specific conditions can help maintain a pool of redox active copper (Herpfer et al., 2002) and iron (Oettl et al., 1999). At high concentrations 7,8-NP may induce apoptosis within Jurkat T cells by an interruption to the balance of the redox status of the cells (Baier-Bitterlich et al., 1996). In conjugation with tumour necrosis factor-α, higher concentrations can induce oxidative stress mediated death of U-937 cells (Baier-Bitterlich et al., 1995). Within peripheral T cells 7,8-NP induced apoptosis at concentrations as low as 200 micromolar. When co-incubated with superoxide dismutase, catalase and a metal chelator the cytotoxic effect of 7,8-NP was significantly reduced putatively due to the removal of the hydrogen peroxide supporting the oxidative stress mediated mechanism of 7,8-NP (Wirleitner et al., 2003).

In vivo the only know pathway to neopterin is the oxidation of 7,8-NP by hypohalous acids such as hypochlorous acid (HOCl) sourced from the MPO/H_2O_2 system (Gieseg et al., 2000; Widner et al., 2000). The expression of MPO which has been identified within plaques associated with macrophages rich regions (Daugherty et al., 1994), is also secreted from activated neutrophils providing a source for HOCl within the plaque (Chisolm et al., 1999; Libby, 2002a). Further evidence for the activation of MPO and subsequent HOCl production within plaques is the presence of the HOCl mediated protein oxidation product chlorotyrosine (Upston et al., 2002a).

As with 7,8-NP, the *in vivo* function if any of neopterin is not fully understood (Gieseg et al., 2008a), Neopterin has been reported as pro-oxidant (Hoffmann et al., 1998), which suggests that one of the main functions of neopterin is to enhance the cytotoxic effect of oxidants during inflammation (Hoffmann et al., 2003). Neopterin in the presence of hydrogen peroxide or chloramines enhanced the killing effect of the oxidants towards *E.coli* compared to 7,8-NP which displayed the opposite effect via a scavenging mechanism. This relationship towards hydrogen peroxide supports the balancing role between neopterin and 7,8-NP, by either a protective effect or a enhanced oxidative stress effect (Weiss et al., 1993). Neopterin, tumour necrosis factor-α and γ-interferon exposed to vascular SMC *in vitro* induced apoptosis potentially mediated by the interruption of nitric oxide synthesis and inducible nitric oxide synthase gene expression (Hoffmann et al., 1998). Nanomolar concentrations of neopterin and 7,8-NP transiently increase the calcium

concentration within THP-1 cells via an extracellular source. This increase in calcium may have a role in activation of the macrophages (Woll et al., 1993). In the presence of phorbol myristate acetate stimulated macrophages, neopterin decreased the release of superoxide thus thought to be exerting a scavenging effect. However, neopterin failed to reduce the concentration of superoxide in a xanthine/xanthine oxidase system therefore its mode of action against the reduction of superoxides produced by the macrophages was thought to be due to interaction within the cells itself (Kojima et al., 1992).

1.3.2 Antioxidants in biological systems

Antioxidants are capable of removing or converting free radicals and/or oxidants into a less reactive state. The mechanism of antioxidant activity includes enzymatic removal for example the enzymes superoxide dismutase and catalase which remove superoxide and hydrogen peroxide respectively. Also compounds which scavenge free radicals for example α-tocopherol and ascorbic acid and proteins which sequester redox active metals (Halliwell and Gutteridge, 1999). Plasma contains a number of antioxidants including ascorbic acid, uric acid, α-tocopherol, albumin and bilirubin (Frei et al., 1988), making blood a highly protected environment against oxidative stresses. Within atherosclerotic plaques α/γ-tocopherol, ascorbic acid, ubiquinol-10, uric acid, glutahione peroxidise, glutahione reductase and the three isoforms of superoxide dismutase have been identified (Stocker and Keaney, 2004). However, despite this extensive list, oxidative damage still occurs within plaques.

1.3.2.1 α-Tocopherol and ascorbic acid

α-Tocopherol, the biologically active form of vitamin E, is an important lipid soluble antioxidant in blood and tissue. It is localised within membranes and lipoproteins (Stocker and Keaney, 2004; Upston et al., 2002b) and is present at approximately 6-7 molecules per LDL particle (Esterbauer et al., 1992). α-Tocopherol is an effective scavenger of peroxyl radicals by donation of an electron forming a relatively nonreactive intermediate, the α-tocopheroxyl radical (α-Toc$^{\bullet}$) (reaction 16) at a rate of ~10^6 moles per second. Under a high radical flux the α-tocopheroxyl radical can neutralise another lipid peroxide radical to a non radical product (reaction 17), thereby breaking the chain reaction. Therefore α-tocopherol potentially removes two radicals from the system (Bowry and

Stocker, 1993; Stocker and Keaney, 2004). In the presence of endogenous co-antioxidants, aqueous ascorbic acid or lipid soluble ubiqinol-10, the α-tocopheroxyl radical can be scavenged recycling it back to α-tocopherol (reaction 18) and in the case of ascorbic acid effectively exporting the radical into the aqueous media (Bowry and Stocker, 1993; Neuzil et al., 1996).

(16) α-TocH + $LOO^{\bullet}$ → α-$Toc^{\bullet}$ + LOOH

(17) α-$Toc^{\bullet}$ + $LOO^{\bullet}$ → non radical product + LOOH

(18) α-$Toc^{\bullet}$ + ascorbic acid → α-TocH + ascorbyl radical

(19) α-$Toc^{\bullet}$ + LH → $L^{\bullet}$ + α-TocH

Despite the presence of α-tocopherol within the atherosclerotic plaque (Niu et al., 1999; Suarna et al., 1995), lipid oxidation still occurs evident by the high level of lipid oxidation products identified within plaques (Upston et al., 2002b). Via a temporal factor, transitory depletion of α-tocopherol may allow the occurrence of lipid peroxidation with subsequent recycling of the α-tocopherol pool via co-antioxidants (Upston et al., 2002b). This may give explanation to how α-tocopherol and lipid oxidation products both exist at relatively high proportions within the plaque. Alternatively of α-tocopherol maybe involved in the oxidation of lipids by a mechanism of tocopherol mediated peroxidation (TMP).

Under a low radical flux, the α-tocopheroxyl radical can mediate radical formation by abstracting a hydrogen from a susceptible site on the lipid forming a carbon centred radical (reaction 19) (Neuzil et al., 1996). The rate of reaction of TMP is relatively slow at a rate of ~10^{-1} - 10^{-2} moles per second (Bowry and Stocker, 1993; Halliwell and Gutteridge, 1999). Therefore, for TMP to occur the radical flux is low which increases the probability of interacting with a lipid rather than a radical. Suarna et al. (1995) reported relatively high concentrations of α-tocopherol and its co-antioxidant ascorbic acid within human plaques, in coexistence with oxidised cholesterol esters, indicating that the ascorbic acid may also have a temporal depletion and restoration. Another pro-oxidant feature of α-tocopherol is its ability to reduce free Cu^{2+} to Cu^{+} potentially contributing to a pool of redox active metals within the system (Yoshida et al., 1994).

Ascorbic acid is the main water soluble antioxidant within the system (Halliwell and Gutteridge, 1999), and predominantly occurs in its redox active state (Suarna et al., 1995). As a reducing agent

it is able to reduce metals, hydroxyl radical and superoxide, thus can exert both anti- and pro-oxidant properties. Upon the addition of an electron it forms ascorbyl radical which like the α-tocopheroxyl radical is relatively inert. This antioxidant is effectively recycled via the disproportional reaction between two ascorbyl radicals (Halliwell and Gutteridge, 1999). Ascorbic acid has been localised within femoral and carotid plaques at concentrations higher that that detected within normal arterial tissue and similar to that within healthy plasma (Suarna et al., 1995).

1.4 Objective of this study

Many studies have identified antioxidant and oxidative products within atherosclerotic plaques (Davies et al., 1999; Fu et al., 1998; Leeuwenburgh et al., 1997; Stanley et al., 2006; Suarna et al., 1995), but none have investigated the spatial localisation of these markers within the plaques in relation to one another. Within the published literature only studies from our laboratory have measured the concentration of neopterin within carotid and femoral plaques (Firth et al., 2008; Gieseg et al., 2008a). By identifying relationships within and between the markers within the plaques in a spatial context, mechanisms driving the process of advance plaque formation maybe hypothesised on. By understanding these processes and the potential relationships between the markers, the important and more informative conclusions may provide a base for elucidating the mechanisms of plaque growth. Knowledge of these processes is vital for providing preventative measures towards this disease.

Within our laboratory, to date, eight plaques have been fully analysed, however due to the complexity and differences of these plaques at the advance disease stage, it is difficult to obtain significant trends or correlations between the plaques due to the small sample size. Therefore I have analysed a further six plaques. In addition the mechanism of plasma protein oxidation was examined to gain further understanding of the processes likely to be occurring within the plaques.

Materials and Methods

2.1 Materials

2.1.1 Chemicals

All solutions were prepared using de-ionised and ultrafiltrated water from a NANOpure ultra-filtration system supplied by Barnstead/Thermolyne (IA, USA). All reagents used are of analytical grade or better, unless otherwise stated.

Acetic acid (glacial)	JT Baker, Mallinckrodt Baker Inc.
Acetone	Merck
Acetonitrile	JT Baker, Mallinckrodt Baker Inc.
	Riedel-de Haen, Honeywell International Inc.
	BDH Chemicals Ltd
Argon gas	BOC gasses, N.Z.
4-Aminobenzoic acid (ABA)	Sigma Chemical Co.
Ammonium phosphate dibasic minimum 98%	Sigma Chemical Co.
Ammonium ferrous sulphate	Hopkins and Williams Ltd
2,2-azobis (2-aminopropane) dihydrochloride (AAPH)	Arcos, N.J., U.S.A.
Bicinchoninic acid (BCA) protein determination kit	Pierce, U.S.A.
Bovine serum albumin (BSA)	Sigma Chemical Co.
Bromophenol blue	
Butylated hydroxytoulene (BHT)	Sigma Chemical Co.
Chelex 100 resin	Bio-Rad Laboratories, USA
Cholesterol reagent	Roche Diagnostics, USA
Chloroform	Merck
Coumassie brilliant blue	Scharlau Chemie S.A.
Deferoxamin methansulfonic (Desferal)	Ciba-Gergy Ltd, Switzerland
Diethyl ether	Merck
Diethylenetriaminepentaacetic acid (DTPA)	Sigma Chemical Co.
7,8-Dihydroneopterin (7,8-NP)	Schiricks Laboratory
2,4-Dinitrophenylhydrazine (DNPH)	Aldrich
Ethanol	Scharlau Chemie S.A.
	BDH Chemical Ltd
Ethyl acetate	BDH Chemical Ltd

Ethylenediaminetetraacetic acid (EDTA)	BDH Chemical Ltd
Guanidine hydrochloride	Sigma Chemical Co.
Glycerol	Sigma Chemical Co.
n-Hexane	Unichrom, ARS
Hydrochloric acid (HCl)	Merck
Iodine	BDH Chemicals Ltd
L-3,4-Dihydroxyphenylalanine	Sigma Chemical Co.
L-Ascorbic acid	Sigma Chemical Co.
	BDH Chemicals Ltd
Mercaptoacetic acid	Sigma Chemical Ltd
2-Mercaptoethanol	Sigma Chemical Co.
Methanol	Scharlau Chemie S.A.
	Merck
2-(N-Morpholino)ethanesulfonic acid (MES)	Sigma Chemical Co.
3-(N-Morpholino)propanesulfonic acid (MOPS)	Sigma Chemical Co.
Neopterin	Schiricks Laboratory
Nitrogen gas	Boc Gasses, N.Z.
Nitrogen liquid	Cryogenics, Department of Chemistry, University of Canterbury
Orthophosphoric acid (85%)	BDH Chemicals Ltd
Phenol	Sigma-Aldrich
Potassium Bromide	Merck
Potassium Iodide	Merck
Prestained Protein Molecular Weight Marker	Fermentas, Life Sciences
2-Propanol (isopropanol)	Merck
Sigma Marker Wide Range	Sigma Chemical Co.
Sodium acetate	Merck
Sodium chloride	Merck
Sodium carbonate ($NaHCO_3$)	BDH Chemicals Ltd
Sodium cyanoborohydride ($NaCNBH_3$)	Fluka
Sodium dihydrogen phosphate monohydrate	Scharlau Chemie S.A.
Sodium dodecyl sulphate (SDS)	Sigma-Aldrich
Sulfuric acid	BDH Chemicals Ltd
1,1,3,3-Tetramethoxypropane	Sigma Chemical Co.
2-Thiobarbituric acid, minimum 98% (TBA)	Sigma Chemical Co.
α-Tocopherol	Sigma Chemical Co.
Trichloricacetic acid (TCA)	Merck
Trifluroacetic acid (TFA) anahydrous	Sigma Chemical Co.
Xylenol orange	Riedel-de Haen, Honeywell International Inc.

2.1.2 HPLC system

The HPLC system (Shimadzu Corporation, Japan) consists of the controller SCL-10Avp, a fluorescence detector RF-10AXL, UV-Vis detector SPD-10A, SIL-10A autosamplier and on-line degasser. Peak areas were determined using Class-VP software.

2.1.3 General solutions and buffers

A) HPLC mobile phases

Salt based HPLC mobile phases were filtered through a 45 μm filter and all mobile phases were sonicated for 10 minutes before loading onto the HPLC.

B) Phosphate buffered saline (PBS)

Phosphate buffered saline with a final concentration of 150 mM sodium chloride and 10 mM sodium dihydrogen orthophosphate pH 7.4 was stirred with water washed chelex 100 for at least 12 hours prior to use.

C) Reagents for the FOX assay

5 mM xylenol orange (MW 760.59 g/mol) and 5 mM ammonium ferrous sulphate (MW 392.16 g/mol) were freshly prepared daily in 25 mM sulphuric acid for both the sulphuric acid and acetic acid FOX assays.

D) Gel electrophoresis solutions

Cracker buffer

A solution 0.5M Tris-HCl was adjusted to a pH of 6.8 with concentrated HCl. To obtain the correct conductivity care was taken not to overshoot the pH value. A cracker buffer stock was then prepared consisting of 0.125 M Tris-HCl pH 6.8, 10% SDS, 20% glycerol and 0.1% bromophenol blue in water and stored at room temperature. The final cracker buffer solution was freshly prepared

by mixing 1 mL of stock cracker buffer with 20 μL of mercaptoethanol and 2 μL of 100 mg/mL EDTA.

MOPS transfer buffer

A 10 times concentrated stock was prepared and stored at 4ºC. When required it was diluted with water to give a final concentration of 50 mM MOPS, 50 mM Tris base, 0.1% SDS and 1 mM EDTA at pH 7.7.

Cousmassie Brilliant Blue Stain

0.1% cousmassie brilliant blue, 10% $^{v}/_{v}$ acetic acid and 50% $^{v}/_{v}$ methanol in water.

Destain

10% $^{v}/_{v}$ glacial acetic acid and 5% $^{v}/_{v}$ methanol in water.

2.2 Methods

2.2.1 Plaque Homogenisation

Plaques were surgically removed at the Christchurch Hospital and immediately transported to the Free Radical Biochemistry Laboratory on ice before storing at -80ºC. When ready the plaques were sectioned into 3-5 mm segments down their longitudinal axis while still frozen. Numbering of the sections began at the end prior to the bifurcation and were photographed before homogenising under liquid nitrogen. To each homogenised plaque section 4 mL of water, 50 μL of 100 mg/mL EDTA and 50 μL of 20mg/mL BHT (in methanol) was added and further homogenised by the Tissumizer 3000 (Takmar Company, USA). The Tissumizer was rinsed with 1 mL of water and added to the homogenate to minimise loss of sample. Total mass and final volume of each section was noted.

2.2.2 Cholesterol Determination

This spectrophotometric assay is based on a series of reactions involving the enzymes cholesterol esterase, cholesterol oxidase and peroxidase ultimately resulting in the development of a red dye. The intensity of the dye is directly proportional to the concentration of total cholesterol within the sample. To 10 μL of plaque homogenate, 1 mL of cholesterol reagent (CHOL, Roche Chemicals) was added and incubated in the dark for 10 minutes at room temperature. The absorbance was read at 500 nm against a cholesterol reagent blank.

2.2.3 Protein determination

In the presence of bicinchoninic acid (BCA), the concentration of protein dictates the intensity of a purple dye development forming the basis of the BCA protein determination kit (Pierce, Illinois, USA). Optimally, the protein concentration within the sample is required to be between 25 and 250 μg/mL therefore plaque homogenate was diluted with water by a factor of 10, and plasma diluted by a factor between 100 and 500. 1 mL of the freshly prepared working reagent (Reagent A sodium carbonate, sodium bicarbonate, BCA and sodium tartrate in 0.1 M sodium hydroxide and reagent B 4% hydrated copper sulphate in a 50:1 ratio of reagent A:B) was added to 50 μL of diluted sample and placed on a heated block at 60ºC with gentle shaking for 30 minutes. The reaction was stopped by incubating the samples on ice before reading the absorbance at 562 nm against a water blank. Concentrations were determined from a BSA standard curve analysed by Prism (version 4.0; GraphPad Software, USA).

2.2.4 Antioxidant detection

2.2.4.1 Pterin Assay

The pterin assay takes advantage of neopterin's natural fluorescence allowing the detection and determination of neopterin and 7,8-dihydroneopterin (7,8-NP). To determined the 7,8NP concentration it is oxidised to neopterin giving a total neopterin value, therefore subtracting the neopterin from the total neopterin gives the 7,8NP concentration. Using reverse phase HPLC the accuracy of the assay is dependent on the removal of protein from the sample, as it has been shown

to interact with proteins leading to an underestimation of its concentration (Flavall et al., 2008). Due to the lability of 7,8-NP the pterin assay was performed on the same day as the homogenisation of the plaque.

For neopterin quantification the protein precipitation was induced by mixing 100 µL of ACN with 100 µL of plaque homogenate/plasma followed by vortexing and centrifugation at 10,300 g for 10 minutes at 4ºC. For the total neopterin samples 100 µL of ACN was added to 100 µL plaque homogenate/plasma, vortexed and centrifuged as described above for 5 minutes. For the oxidation of 7,8-NP to neopterin 10 µL of acidic iodide (5.4% I_2/10.8% KI in 1 M HCl) was added, vortexed and incubated in the dark for 15 minutes. This was followed by 10 µL of 0.6 M ascorbic acid to neutralise excess acidic iodide, and centrifuged as before for 10 minutes.

From the neopterin and total neopterin supernatants, 10 µL was injected onto a reverse phase Develosil C18, 250 x 4.6 mm, 5 µm column (Phenomenex) maintained at 35ºC. The 20 mM ammonium phosphate pH 6.0 with 5% methanol mobile phase was pumped at a flow rate of 1 mL/minute and the neopterin detected at an excitation of 353 nm and emission 438 nm.

A standard neopterin stock stored at -20ºC was prepared in 10 mM phosphoric acid and sonicated for 2 minutes. When required an aliquot was thawed and diluted to 1 µM with mobile phase. The 7,8-NP standard was prepared fresh in mobile phase and kept on ice and in the dark to minimise loss. Where spiking of 7,8-NP was required a known concentration was added to samples and allowed to equilibrate on ice for 5 minutes before beginning sample preparation.

2.2.4.2 α-Tocopherol assay

α-Tocopherol is a lipid soluble antioxidant due to its long hydrocarbon chain and efficient peroxyl radical scavenging properties. It has a cyclic structure which is important for its antioxidant activity and also allows its detection at 292 nm.

Within a 10 mL glass culture tube with screw top 100 µL of plaque homogenate was diluted with 400 µL of water. To prevent additional oxidation occurring 10 µL of 100 mg/mL EDTA and 25 µL of 20 mg/mL BHT (in methanol) was added. Protein precipitation was induced with 500 µL of ice

cold ethanol and vortexed for 10 seconds. The α-tocopherol was extracted by adding 2 mL of ice cold hexane and further vortexing for 30 seconds. At this point the samples can be stored at -80ºC. Once thawed the samples are re-vortexed for 60 seconds before centrifuging at 1,600 g for 5 minutes at 4ºC to maximise phase separation. Into glass tapered 10 mL centrifuge tubes 70% of the hexane layer was transferred before it was evaporated in a hot water bath under nitrogen gas. The remaining residue was dissolved in 100 μL ice cold methanol and transferred to the HPLC.

With a mobile phase of 100% methanol, 20 μL of the sample was injected onto a reverse phase Econosphere C18, 4 x 125 mm, 5 μm column (Alltech Associates Inc.) maintained at 35ºC, and detected at an extinction and emission of 292 and 353 nm respectively. The α-tocopherol standard was prepared by diluting approximately 1 mg/mL α-tocopherol in methanol and the concentration determined spectrophotometrically using an extinction coefficient of 3086 $cm^{-1}M^{-1}$ at a wavelength of 294 nm. The α-tocopherol standard stock was stored at -20ºC under argon gas and when required was diluted to 3 μM concentration with 100% methanol.

2.2.5 Lipid oxidation detection

2.2.5.1 TBARS assay

The TBARS assay provides a general measurement of fatty acid oxidation occurring within biological systems. One of the breakdown products of lipid oxidation is malondialdehyde (MDA). The well established 2-thiobarbitutic (TBA) reaction with MDA yields a pink colour that is detectable around 553 nm.

After combining 100 μL of plaque homogenate, 50 μL of 150 mM of phosphoric acid to increase the acidity and precipitate the protein and 10 μL of 20 mg/mL BHT (in methanol) to prevent further oxidation, the samples are stored at -80ºC. When ready for analysis 50 μL of freshly prepared 42 mM TBA was added to the thawed samples and placed on a heated block at 95ºC with gently shaking for 30 minutes allowing the formation of the TBA-MDA adduct. The samples were immediately cooled on ice and centrifuged at 10,300 g at 4ºC for 10 minutes. In the original method (Plaques A-C,F) 100 μL of the supernatant was combined with 300 μL of ice cold methanol, vortexed and left on ice for 5 minutes. The samples were re-spun at 21,000 g for 5 minutes before

loading onto the HPLC. Modifications were made to the original method to improve within and between run measurements. The new method (Plaques D-E) involved adding 800 μL of ice cold methanol to the cooled sample immediately after the incubation step. Samples were then left on ice for 5 minutes followed by centrifugation at 21,000 g for 10 minutes at 4ºC. To equilibrate the sample to the mobile phase 100 μL of the supernatant was added to 100 μL of 50 mM NaH_2PO_4 pH 6.8 and injected onto the HPLC.

The HPLC pumped 50 mM NaH_2PO_4 pH 6.8 with 45% methanol at a flow rate of 1 mL/min through a reverse phase Phenosphere C-18, 4.6 x 150 mm, 5 μm column (Phenomenex) heated to 35ºC. The TBA-MDA was detected at an excitation of 525 nm and emission of 550 nm. Both blank and 1 μM TBA-MDA standards are required to determine the concentration of TBARS within the samples.

MDA is very labile, therefore the standard was prepared fresh with every sample block by incubating a known concentration of the MDA precursor 1,1,3,3-tetramethoxypropane with TBA. 1,1,3,3-Tetramethoxypropane hydrolyses to MDA during the heated incubation step forming a known concentration of TBA-MDA. During preparation of the standard the first dilution step of 1,1,3,3-tetramethoxypropane was in a solution of ethanol:water at 2:3, where further dilutions were made in water.

2.2.5.2 7-ketocholesterol and α-tocopherol assay

The LDL and oxLDL was diluted with PBS to a concentration of 1 mg/mL in 500 μL and with plaque 100 μL of homogenate was added to 400 uL of water. To prevent additional oxidation 10 μL of 20 mg/mL BHT (in methanol) and 20 μL of 100 mg/mL EDTA were added. Protein precipitation was induced by 1 mL ice cold methanol and vortexed briefly. The 7-ketocholesterol and α-tocopherol was extracted by the addition of 5 mL of ice cold hexane and a 60 second vortex. To ensure phase separation the samples were centrifuged at 200 g for 5 minutes at 4ºC. Of the top hexane layer 80% was transferred to glass tapered 10 mL centrifuge tubes and dried under nitrogen gas, before re-solubilising in 100 μL of mobile phase.

Onto an Phenosphere-NEXT C18, 250 x 4.6 mm, 5μm (Phenomenex, NZ) maintained at 35ºC pumping a mobile phase of 54 isopropanol:44 acetonitrile:2 water at 1 mL/min, 20 μL of the sample was injected. The sample first runs through the UV-Vis detector set at a wavelength of 234 nm for the detection of 7-ketocholesterol, and continues through to the fluorescence detector set at an excitation of 292 nm and emission of 335 nm for the detection of α-tocopherol.

The 7-ketocholesterol standard was freshly prepared in and diluted with mobile phase, and the α-tocopherol stock stored in the -20ºC under argon gas was diluted with mobile phase. (Preparation of the α-tocopherol stock is described in section 2.2.4B.)

2.2.6 Protein oxidation detection

2.2.6.1 DOPA and dityrosine assay

DOPA and dityrosine are oxidative products derived from the tyrosine residue. Because HPLC analysis is able to separate the products after release from the protein this allows the detection of both protein oxidative products within the one assay.

To 7.5 mm glass durham tubes 10 μL of 100 mg/mL EDTA and 10 μL 20 mg/mL BHT was added to 10 μL of plaque homogenate. The protein was precipitated by the addition of 900 μL acetone (stored at -20ºC) and incubated on ice for 10 minutes followed by centrifugation at 7000 g at 4ºC for 15 minutes. The supernatant was removed and the pellet washed with 500 μL of ice cold diethyl ether and centrifuged as before. After removal of the supernatant the pellets were dried under vacuum for 1 hour and then placed into Pico-Tag vials (Millipore, USA) with 1 mL of 6 M HCl with 1% ($^{w}/_{v}$) phenol and 50 μL mercaptoacetic acid in each vial. Argon gas was flushed through the Pico-Tag vials for 5 minutes and the vials were evacuated by connecting to the vacuum line of a solvent Speed Vac for 2 seconds (ensuring that the Vac. gauge pressure was below 200 mm Torr) creating an anaerobic environment. For the acid hydrolysis of the proteins the vials were incubated in a 110ºC oven for 16 hours. After cooling, the samples were centrifuged under vacuum (Speed Vac) for 2 hours before re-solubilising the pellet with 200 μL of 0.1% TFA. To enable the samples to be spun at 21,000 g for 5 minutes at 4ºC, the samples were transferred to eppendorf tubes before loading onto the HPLC.

Onto a reverse phase Aqua C18, 250 x 4.6 mm, 5 μm column (Phenomenex) 10 μL of supernatant was injected with a gradient mobile phase pumping at 1 mL/minute. The gradient began at 100% 0.1% TFA pH 2.5 with 1% ACN where the ACN linearly increased to 5% by the 10th minute, 10% by the 14th minute and 50% by the 16th minute. This was maintained for 5 minutes to clean the column, after which the ACN concentration was returned and maintain at 1% until the 30th minute. Because DOPA elutes first the fluorescence detector began at an excitation of 280 nm and an emission of 320 nm. At the 11th minute the emission was changed to 410 nm for the detection of dityrosine. The DOPA standard was prepared fresh and a dityrosine stock stored at -20ºC were diluted to 1 μM with mobile phase.

2.2.6.2 Protein carbonyls spectrophotometric assay

Protein carbonyls are a general protein oxidation marker that detects the formation of carbonyls on amino acid side chains. The dye reagent dinitrophenylhydrazine (DNPH) interacts with these moieties allowing the quantification of the protein carbonyls.

Within the black top glass tubes 1 mL of DNPH in 2 M HCl was added to 200 μL of plaque homogenate alongside blanks prepared by mixing 1 mL 2 M HCl to 200 μL of plaque homogenate, and then stored at -80ºC. After the samples were thawed in the dark they were incubated at 37ºC for 90 minutes with shaking at 80 rpm permitting the reaction between the carbonyls and DNPH. The samples were cooled on ice and the protein precipitated with of 1 mL of 28% TCA and left on ice for 10 minutes followed by centrifugation at 4,100 g at 4ºC for 10 minutes. The supernatant was decanted and the pellet re-suspended in 5 mL of 1:1 ethanol:ethyl acetate to remove excess DNPH. After the samples were vortexed and centrifuged as before, the ethanol:ethyl acetate wash was repeated followed by a third centrifugation. The remaining protein pellet was dissolved in 1 mL of 6 M guandine hydrochloride (in 2 M HCl), incubated in the dark for 30 minutes and the absorbance read at 560 nm against a water blank. To calculate the concentration within the sample the average absorbance of the blank was subtracted from each DNPH treated sample and the concentration determined using the extinction coefficient of 21,000 $cm^{-1}M^{-1}$ (Quinlan et al., 1994).

2.2.6.3 Protein carbonyls AAS and GGS HPLC assay

This method detects the two main protein carbonyl products α-aminoadipic semialdehyde (AAS) and γ-glutamic semialdehyde (GGS). AAS and GGS accounts for 23% of the total carbonyls within native BSA (Akagawa et al., 2006).

The samples were prepared in glass durham tubes with either 200 µL of BSA, 40 µL of plasma or plaque homogenate made up to 200 µL with water. For the prevention of further oxidative events 50 µL of 20 mM DTPA and 50 µL of 20 mg/mL BHT (in methanol) was added followed by protein precipitation with 200 µL of 72% TCA. The samples were kept on ice for 10 minutes then centrifuged at 1,500 g at 4ºC for 10 minutes. The supernatant was removed and using a sealed pasteur pipette the protein pellet re-suspended in 250 µL of MES buffer pH 6.5 with 0.5% SDS. To the mixture 500 µL of 150 mM aminobenzoic acid (in MES buffer pH 6.5) and 125 µL of 250 mM sodium cyanoborohydride (in MES buffer pH 6.5) was added and the tubes inverted before incubating at 37ºC at 80 rpm for 90 minutes, allowing the condensation of ABA to AAS and GGS. After the samples were cooled on ice the protein was precipitated with 500 µL of ACN and centrifuged at 1,500 g at 4ºC for 15 minutes. To ensure the protein was precipitated the protein pellet was washed with 200 µL of 28% of TCA and centrifuged as before. Once the supernatant was removed the pellets were re-suspended using a sealed pasteur pipette in 500 µL ice cold ethanol and spun as before. For the final time the supernatant was removed and residual ethanol drained off by inverting the tubes for 5 minutes. The pellets were dried under vacuum for 1 hour before placing them into Pico-Tag vials with 1.5 mL 6 M HCl for acid hydrolysis. Air was flushed out using argon gas for 5 minutes before the vials were evacuated by connecting to the vacuum line of a solvent Speed Vac for 2 seconds (ensuring that the Vac. gauge pressure was below 200 mm Torr). Acid hydrolysis began once the vials were placed into the 110ºC oven and left for 24 hours. After the vials had cooled the vacuum was released from the Pico-Tag vials and the durham tubes were spun under vacuum for 2 hours (Speed Vac, Solvant) before re-solubilsing in 200 µL of 50 mM sodium acetate pH 5.4. For the samples to be centrifuged at a high g force the samples were transferred to an eppendorf tube and centrifuged for 5 minutes at 21,000g.

Onto a reverse phase Synergi Fusion 250 x 4.6 mm, 4 µm column (Phenomenex) with a gradient mobile phase pumping at 1 mL/minute, 20 µL of the sample was injected. The mobile phase began

at 95% of 50 mM sodium acetate pH 5.4 and 5% ACN and was maintained until the 30th minute. The ACN concentration linearly increased reaching 50% by the 35th minute. This was maintained for 5 minutes to clean the column, after which the ACN concentration returned to and was maintained at 5% until the end of the run (50 minutes). The AAS-ABA and GGS-ABA compounds were detected at an excitation of 283 nm and an emission of 350 nm. For the standard, ABA was prepared in mobile phase, sonicated for 2 minutes and injected at a concentration of 1 μM.

2.2.7 Plasma oxidation methods

2.2.7.1 Blood collection and plasma preparation

Blood was collected from healthy volunteers by venipuncture and approximately 50 mL immediately added to 500 μL of 100 mg/mL EDTA to prevent clotting. The blood was separated by centrifugation at 4,100 g at 4ºC for 20 minutes with slow stop. The plasma was transferred and centrifuged on a fixed angled rotor at 12,400 g for 20 minutes at 4ºC with soft start and stop to further remove remaining red blood cells. The resulting plasma was stored at -80ºC until use.

2.2.7.2 Oxidation of BSA and plasma

All BSA solutions were prepared using PBS. Immediately after the addition of 10 mM AAPH the plasma or BSA solutions were incubated at 37ºC at 80 rpm for the required time period.

2.2.7.3 Dialysis of human plasma

The 14 kDal dialysis tubing (Medicell International Ltd) was prepared by boiling in 5% ($^{w}/_{v}$) $NaHCO_3$ and 1 mM EDTA, washed with water before boiling in water and stored at 4ºC in 50% ethanol. Immediately before use the dialysis tube was extensively washed with double distilled water. Pre-cooled PBS in 1 litre bottles was degassed with nitrogen for 10 minutes. Plasma was transferred into the dialysis tube and flushed with argon gas for 5 minutes, before placing into PBS, overlaying the PBS with argon gas for a further 5 minutes and sealing the bottle. The plasma was dialysed with constant stirring in the dark at 4ºC, with a PBS change every 3 hours. The third change of PBS was left to stir overnight.

2.2.7.4 Protein hydroperoxide determination via the FOX assay

The FOX assay determines the concentration of protein hydroperoxides by the hydroperoxides reacting with ferrous ions oxidising them to ferric ions. The ferric ions react with xylenol orange providing a colour intensity that is detected spectrophotometrically.

a) Sulphuric Acid FOX assay

This version optimally determines the protein hydroperoxide concentrations within a pure protein system and therefore was used on BSA samples. The protein was precipitated on ice with the addition of 40 μL of 72% TCA to 1 mL of BSA, followed by a 5 minute incubation and a 7 minute centrifugation at 10,300 g and 4ºC. After the supernatant was decanted the pellet was washed twice by re-solublising in 1 mL of 5% TCA using a sealed pasteur pipette and centrifuged as before, effectively removing the AAPH. The supernatant was removed and the pellet was re-dissolved in 900 μL of 25 mM sulphuric acid using a sealed pasteur pipette, before the addition of 50 μL of 5 mM xylenol orange (in 25 mM sulphuric acid) and 50 μL 5 mM ammonium ferrous sulphate (in 25 mM sulphuric acid). Blanks were prepared alongside consisting of 900 μL of 25 mM sulphuric acid, 50 μL 5 mM xylenol orange (in 25 mM H_2SO_4) and 50 μL 5 mM ammonium ferrous sulphate (in 25 mM H_2SO_4). The colour was allowed to develop by a 30 minute incubation in the dark at room temperature followed by an absorbance reading at 560 nm against a water blank. The protein hydroperoxide concentration was calculated using the extinction coefficient of 32,500 $cm^{-1}M^{-1}$ (Gay et al., 1999).

b) Acetic Acid FOX assay

This FOX assay version modified by Pearson (2002) is used for plasma because plasma requires the removal of lipid hydroperoxides as it interferes with the detection of protein hydroperoxides. The resulting plasma pellets also have an increased solubility in the 50% acetic acid compared to the 25 mM H_2SO_4 therefore increasing the accuracy of the assay.

To 200 μL of plasma, 800 μL of water was added and the protein precipitated with 140 μL of 72% TCA. The samples were incubated on ice for 5 minutes before centrifugation at 10,300 g at 4ºC for 7 minutes. After the supernatant was decanted 1 mL of 1:1 chloroform:ethanol was added for the removal of lipid peroxides and centrifuged as before. The pellet was dissolved in 900 μL of 50%

acetic acid before the addition of 50 μL 5 mM xylenol orange (in 25 mM H_2SO_4) and 50 μL 5 mM ammonium ferrous sulphate (in 25 mM H_2SO_4). Blanks were prepared alongside consisting of 900 μL of 50% acetic acid, 50 μL 5 mM xylenol orange (in 25 mM H_2SO_4) and 50 μL 5 mM ammonium ferrous sulphate (in 25 mM H_2SO_4). The colour was allowed to develop by incubating the blanks and samples in the dark at room temperature for 30 minutes. The absorbance was read at 560 nm and concentration calculated using the extinction coefficient of 32,500 $cm^{-1}M^{-1}$ (Gay et al., 1999).

2.2.7.5 Gel electrophoresis

This technique allows the accurate separation of proteins due to their mass. To be able to compare band intensity between lanes the protein loading per well needs to be equivalent. Protein concentration was determined by the BCA method (section 2.2.3). To the required volume of sample 100 μL of cracker buffer was added before placing on a heated block at 95ºC for 3 minutes with rigorous shaking inducing the denaturation of the proteins. The samples are spun at 23,100 g for 5 minutes at 4ºC. Onto a NuPAGE 4-12% Bis-Tris Gel (Invitrogen), 10 μL of sample was loaded per well and 5 to 10 μL of protein marker in either the first or last well. The gel was run in MOPS transfer buffer and a voltage applied at 50 volts until the front line had entered the gel before increasing the voltage to 120 volts until the end of the run. The gel was stained with coumassie brilliant blue stain for 30 minutes with gentle rocking, and excess stain removed by washing in destain. The destain was changed three times every 15 minutes, where the last change was left overnight. The gel was photographed on Syngene Chemigenius-2 bioimaging system using Genesnap software (Global, NZ).

2.2.8 LDL preparation and oxidation

2.2.8.1 LDL preparation

After defrosting a tube of plasma (section 2.2.7A), it was centrifuged at 4700 rpm for 10 minutes at 4ºC to remove precipitated fibrinogen. The plasma was transferred to a beaker placed on ice and 0.3816 grams of potassium bromide (KBr) was added per mL of plasma creating a plasma density of 1.24. The mixture was gently stirred to avoid denaturation of LDL which can interfere with later

separation techniques. A solution of 1 mg/mL EDTA pH 7.4 was deoxygenated with nitrogen gas for 15 minutes before adding 8 mL into an OptiSeal^{TM} centrifuge tube (Beckman, USA). This was underlayed with 4 mL of the plasma containing KBr using a long luer-fitting needle attached to a 5 mL syringe. Ensuring there are no bubbles the tubes were capped, placed into the NVT-65 rotor (Beckman, USA) and centrifuge at 60,000 rpm for 120 minutes at 10ºC allowing the lipoproteins to migrate along their density gradient.

The LDL was isolated by first discarding the top colourless layer by pipette, followed by the removal of the yellow LDL band using a right angled needle attached to a 20 mL syringe. The LDL was transferred into treated dialysis tubing (section 2.2.7C) and layered with argon gas. To remove the EDTA the LDL was dialysed at 4ºC in nitrogen degassed PBS. Every four hours the PBS was changed for up three times with the last change left overnight.

2.2.8.2 Determination of the LDL concentration

The cholesterol concentration of the LDL was measured as before (section 2.2.2). Based on an estimate of the mass of cholesterol in LDL particle as 31.69% and using the molecular weight of 2.5 MDa LDL (Gieseg and Esterbauer, 1994) the concentration of LDL was calculated.

Calculations

Ab_{500nm} x 14.9 (extinction coefficient) = Cholesterol concentration (mole/L)

Cholesterol concentration (mole/L) x cholesterol molecular weight (386.64 g/mol) = Cholesterol concentration (g/L)

Cholesterol concentration (g/L) x 100/31.69 = LDL concentration (g/L)

LDL concentration (g/L) / LDL molecular weight (2.5×10^{-6} g/mol) = LDL concentration (mole/L)

2.2.8.3 Copper mediated oxidation of LDL

To produce oxidised LDL (oxLDL) the LDL at a concentration of 3-4 mg/mL was incubated with copper chloride ($CuCl_2$) at 37ºC for 24 hours. The $CuCl_2$ was added from a 50 mM stock solution to a final concentration of 300-400 μM. The Cu^{2+} ions were removed by mixing the oxLDL with chelex-100 for two hours at 4ºC on a rotating turntable at 8 rpm. For the removal of the chelex the

oxLDL was centrifuge at 500 g for 2 minutes. The LDL and oxLDL were concentrated using a Vivapore membrane concentrator (Millipore, U.S.A.) and stored under argon gas at 4ºC for up to 2 weeks.

2.3 Statistical Analysis

Unless otherwise stated, data shown represents the mean ± standard error of the mean (SEM) of triplicates for each section/treatment. The SEM is represented on each bar or data point within the graphs. Except for the combined plaque analysis (section 3.1.7), comparison between treatments were analysed by the Tukey's test, performed on Prism (version 4.0, GraphPad Software, USA). The combined plaque analysis involving the Cochran C, Hartley and Bartlett test, Tukey's test, one way- ANOVA, factorial-ANOVA and correlations were performed using Statistica (version 7.1, StatSoft, Inc. USA). Statistical significance are represented by * ($P<0.05$), ** ($P<0.01$) and *** ($P<0.001$).

The purpose of the combined plaque analysis (section 3.1.8) was to determine if any significant variation in the marker concentrations existed between the different zones of the plaque, different overall composition and overall morphology of the plaque along with the external factors, medication and symptoms presented by the patient. To do this analysis the plaques were independent and assumed to be homogenous. For the zoning analysis (section 3.1.8.2) the data from the sections classified as a pre-bifurcation zone from all 12 plaques (excludes plaque B and F) was pooled. The data for the bifurcation and post-bifurcation zones were also prepared in the same way. One way-ANOVA and Tukey's test were performed to determine if any significant variation occurred between the zones. This provided information on the general trends that occur across all plaques, to identify, if any, common trends and mechanism that may occur across all the plaques. For the remaining analysis (sections 3.1.8.3-3.1.8.6) the plaques were classified into categories and if applicable subcategories associated with the factor investigated. For example thrombosed, calcified or neither categories and further subcategorised into Y shaped, small secondary branch or linear morphology. The data across all sections of the plaques for each subcategory were pooled and differences between the categories assessed via factorial-ANOVA and Tukey's test. This

provided information on the general trends associated with the marker concentrations between the plaques and the factors that maybe contributing to the variation.

2.4 Ethics Approval

Ethics approval for access to patient information and analysis of atherosclerotic plaques was granted from the Upper South A Regional Ethics Committee, ethics number CTY/01/04/036. Under this agreement consent from the donor was obtained and the plaques remained anonymous from the donor labelled by a laboratory based code.

Results

3.1 Atherosclerotic Plaques

All atherosclerotic plaques were received from patients undergoing carotid or femoral endarterectomy and were in an advanced stage of the disease. The plaques were cut into 3-5 mm sections beginning at the proximal end in relation to the direction of blood flow and the bifurcation point (section 2.2.1). During homogenisation, the plaques were qualitatively assessed on their morphology and overall composition, including the degree of calcification and the presence of an obvious thrombus. Sections described as 'gruelly' refers to the sections with a relatively high proportion of the lipid core.

Because the level of shear stress may play a role in the formation, progression and rupture of these plaques (Chatzizisis et al., 2007; Helderman et al., 2007; Tricot et al., 2000), each plaque section was classified into zones based on its location along the plaque. These zones represent the pre-bifurcation, bifurcation and post-bifurcation regions. The zones may be under different levels of shear stress and therefore represent potentially different oxidative environments. The zoning also allows for standardisation of each plaque for a combined plaque analysis.

Within each plaque the inflammatory marker neopterin, lipid soluble antioxidant α-tocopherol, the general lipid oxidation marker TBARS, general protein oxidation markers DOPA and protein carbonyls, a specific protein oxidation marker dityrosine along with protein and total cholesterol were measured within each section of six atherosclerotic plaques. Within the plaque graphs the dotted filled bars represent the section/s from the pre-bifurcation zone, solid filled the bifurcation zone and the stripped bars represent the section/s from the post-bifurcation zone.

Common medication for CAD patients are aspirin, a known anti-thrombotic and anti-inflammatory drug (Cyrus et al., 2002), primarily involved in the attenuation of platelet aggregation by the inhibition of cyclo-oxygenase-1 (Chapman, 2007), and statins a lipid lowering drug which also has anti-atherosclerotic properties (Chapman, 2007; Danilevicius et al., 2007). The main mechanism attributed to statins is associated with the increased uptake of LDL by the liver via the up-regulation

of LDL receptor leading to a decrease in cholesterol accumulation within the plaque which may contribute to increased plaque stability. Both aspirin and statins also have anti-inflammatory properties (Chapman, 2007). Within the six plaques analysed two were exposed to statins alone, one to aspirin alone, two to both statins and aspirin and one exposed to neither. All but one of the patients was being treated for hypertension and all were on additional medication for other aliments and/or conditions.

3.1.1 Plaque A (RB040407a)

Plaque A was removed from the right femoral artery. It was characterised with over 75% stenosis, 33 mm in length and a total mass of 1.156 grams. In overall composition, this plaque had a high degree of calcification occurring predominantly around the bifurcation region (Figure 3.1.1). Plaque A was cut into 8 sections where section 1 was the pre-bifurcation section, 2-4 were the bifurcation and sections 5-8 were the post-bifurcation. The plaque lacked a definitive secondary branch but the opening was clearly seen in sections 2-4 corresponding to the bifurcation region.

Table 3.1.1. Plaque A patient and clinical information

Location	Left femoral artery	**Stenosis**	>75%
Symptoms	Not stated	**Gender**	M
Smoking status	Non-smoker	**Age**	75

Medication - Generic Name	**Purpose/Function**
Simvastatin	Reduction cholesterol and lipids
Frusemide	Hypertension
Prednisolone	Steroid anti-inflammatory drug
Digoxin	Congestive heart failure

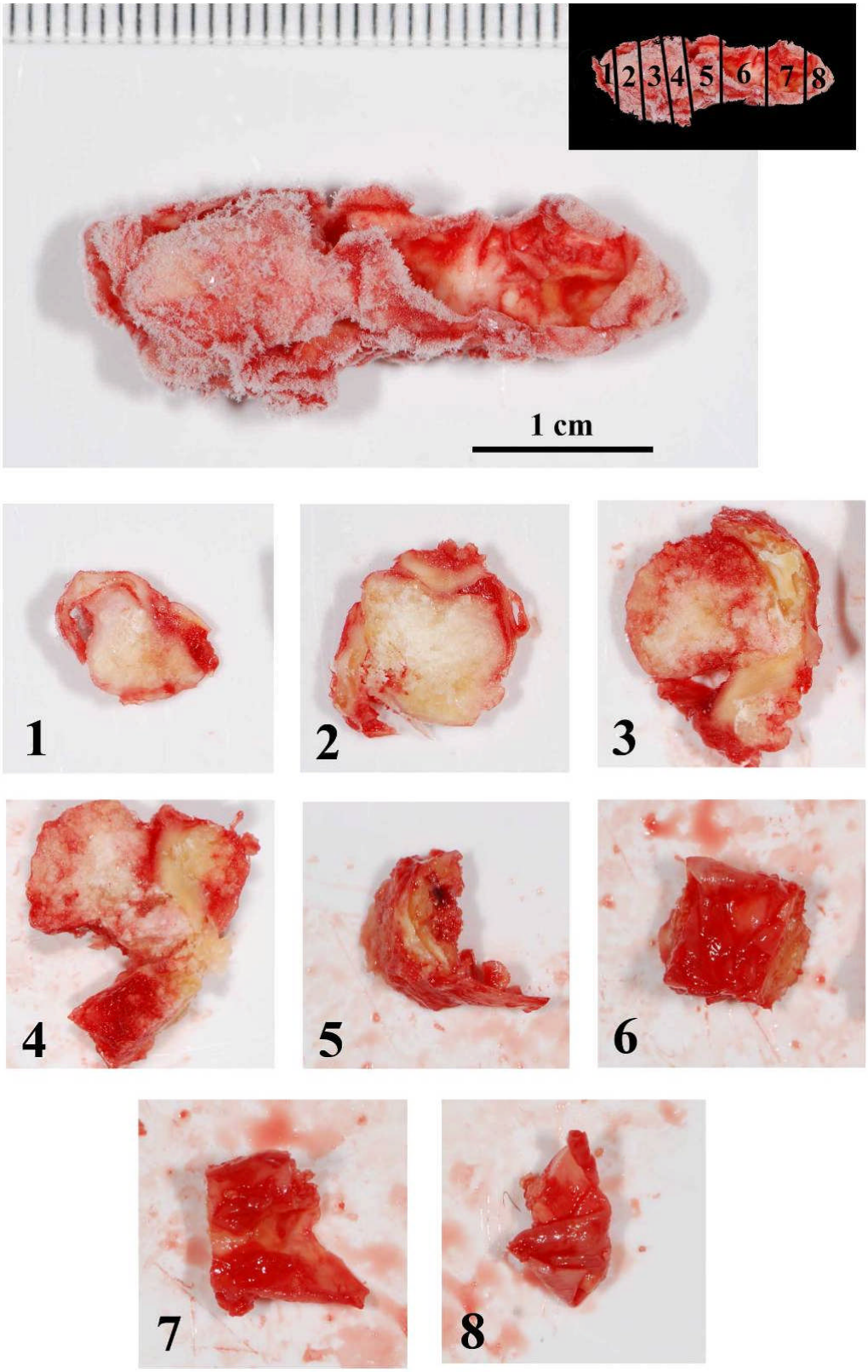

Figure 3.1.1 Sectioning and zones of plaque A
Plaque A was removed from the left femoral artery and homogenised into 8 sections. Section 1 was the pre-bifurcation zone, sections 2-4 were the bifurcation zone and sections 5-8 were the post-bifurcation zone. Top right hand insert not to scale.

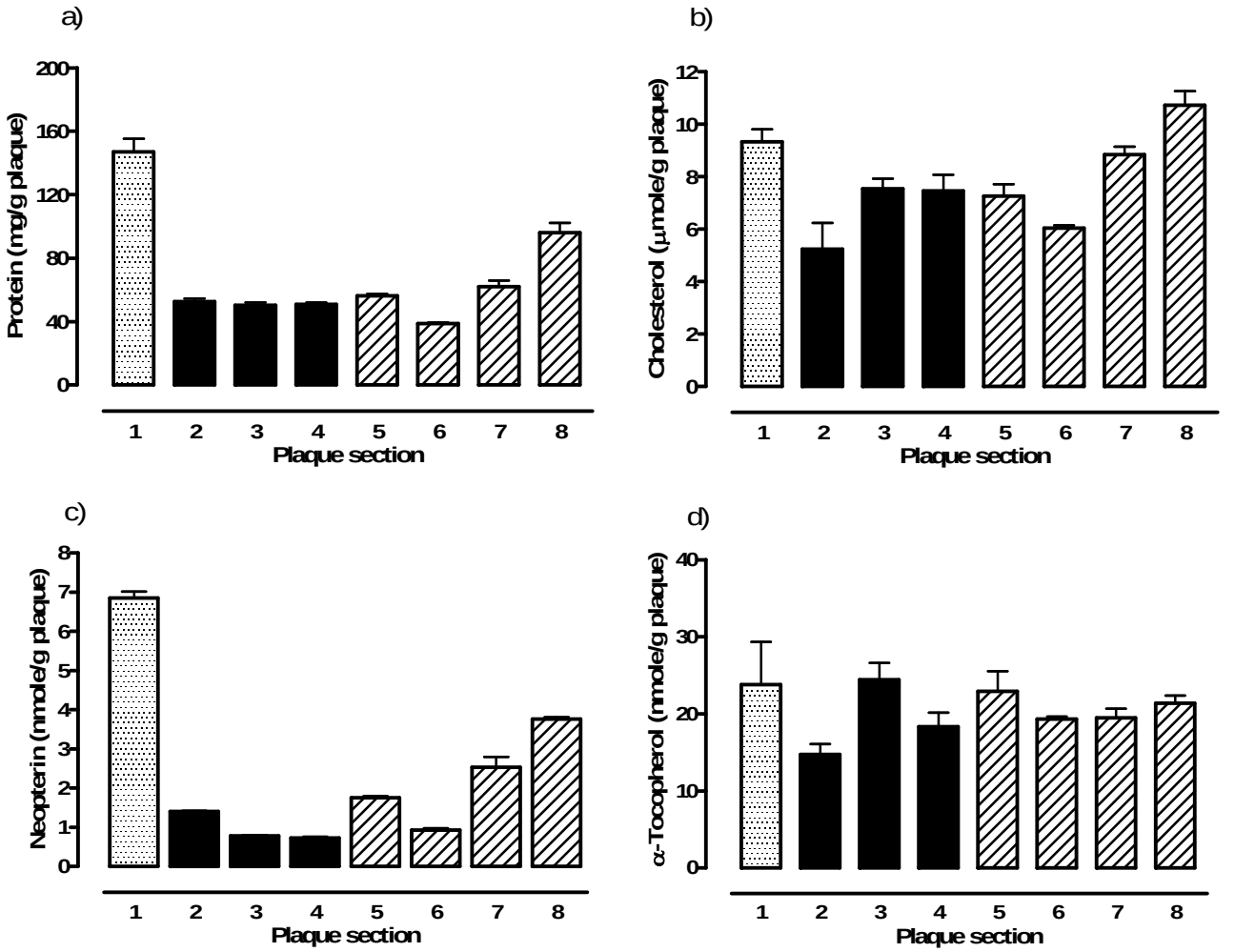

Figure 3.1.2 Protein, cholesterol, neopterin and α-tocopherol content within plaque A
Protein (a) and cholesterol (b) concentrations were determined spectrophotometrically where the neopterin (c) and α-tocopherol were quantified by reverse phase HPLC. Dotted filled bar represents the pre-bifurcation zone, solid filled bars the bifurcation and stripped filled bars the post-bifurcation. Each bar represents the mean ± SEM of triplicate samples.

The protein content within plaque A had statistically high levels in the two peripheral sections, section 1 and section 8, and a low in section 6. Therefore the protein in the pre-bifurcation zone was significantly high compared to the subsequent zones ($P<0.001$) (Figure 3.1.2a). The cholesterol concentration was the highest in the most distal section; section 8 ($P<0.05$) along with section 1 and 7 and due to these high levels, sections 2 and 6 were significantly low (Figure 3.1.2b). Like protein, the concentration of neopterin was the highest in the most proximal and distal sections of plaque A with 6.65 ± 0.16 and 3.76 ± 0.05 nmole/g of plaque respectively (Figure 3.1.2c). Consequently the bifurcation zone had significantly low neopterin levels compared to the pre- and post-bifurcation

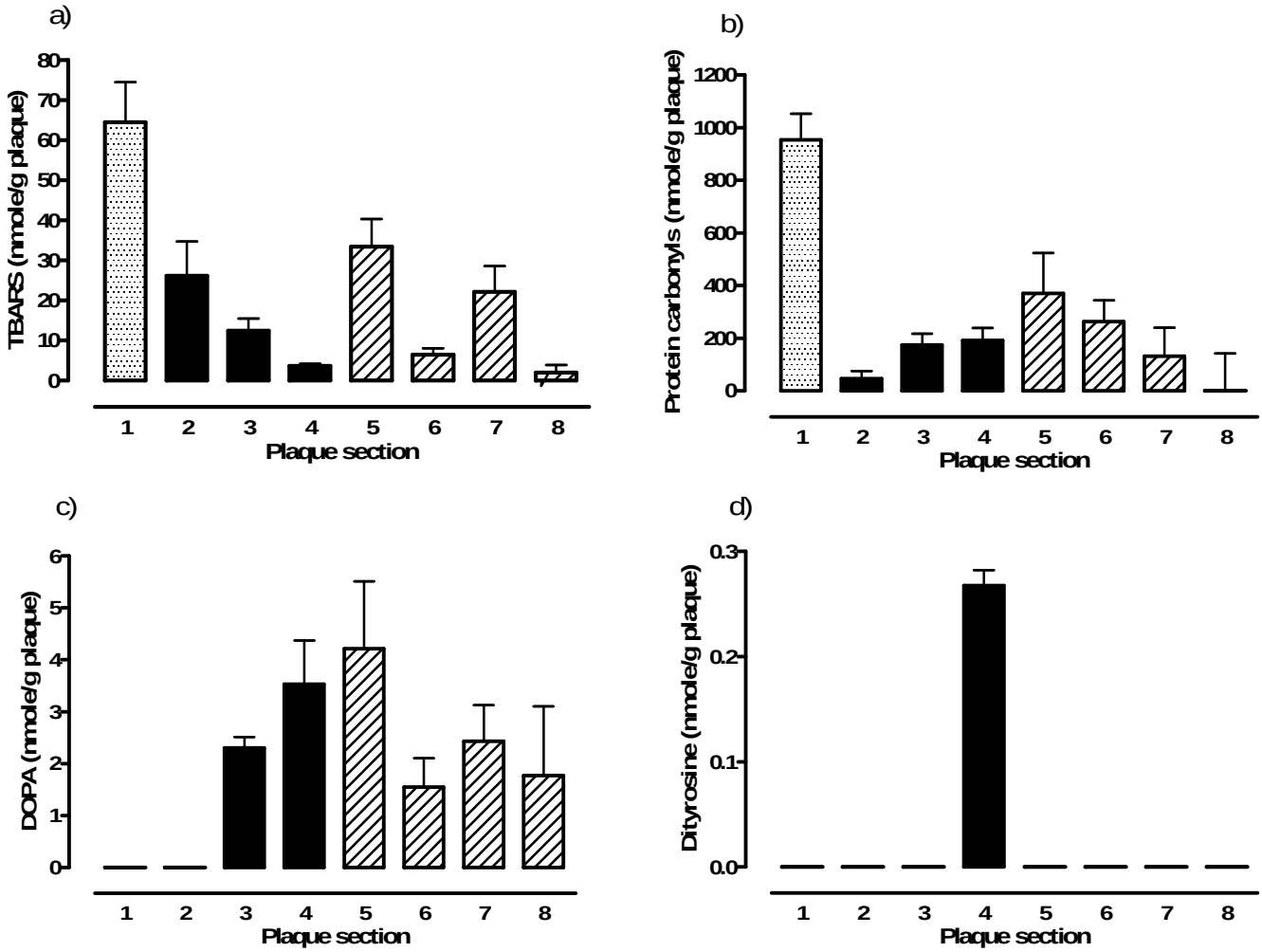

Figure 3.1.3 Lipid and protein oxidative product markers within plaque A
TBARS (a), protein carbonyls (b), DOPA (c) and dityrosine (d) were either quantified via reverse phase HPLC or spectrophotometry. Dotted filled bar represents the pre-bifurcation zone, solid filled bars the bifurcation and stripped filled bars the post-bifurcation zone. Each bar represents the mean ± SEM of triplicate samples.

zones ($P<0.001$). The average concentration of α-tocopherol was 21.84 ± 1.66 nmole/g plaque with no significant variation occurring across the length of plaque A (Figure 3.1.2d). Both TBARS and protein carbonyl concentrations were at maximum levels within the pre-bifurcation zone with concentrations of 64.48 ± 10.0 and 954.57 ± 97.8 nmole/g of plaque respectively ($P<0.01$) (Figure 3.1.3a,b). As with α-tocopherol, DOPA had no significant variation across the plaque while dityrosine was only detected within the post-bifurcation section 4 at a concentration of 0.267 ± 0.015 nmole/g of plaque (Figure 3.1.3c,d).

Overall, neopterin, α-tocopherol and protein concentrations had a significant positive correlation towards each other across the length of plaque A (Table 3.1.17), correlations not seen within any other plaque. With the oxidative markers, neopterin levels had a positive correlation with TBARS levels ($P<0.05$), and α-tocopherol with protein carbonyl concentrations ($P<0.01$). In turn TBARS and protein carbonyl levels had a positive correlation ($P<0.01$). Compared to the pre- and post-bifurcation zones neopterin levels were significantly low in the bifurcation which is where the dityrosine was detected.

3.1.2 Plaque B (RB040407b)

Plaque B was removed from the right femoral artery from the same patient as plaque A. In comparison to plaque A this plaque was considerably smaller at a length of 13 mm and mass of 0.474 grams making the directionality of the plaque difficult to determine based on its morphology. Therefore the plaque sections can only be classified as a bifurcation section flanked by two peripheral sections. Plaque B had two distinct openings on either end and like plaque A was highly calcified.

Table 3.1.2 Plaque B patient and clinical information

Location	Right femoral artery	**Stenosis**	Not stated
Symptoms	Not stated	**Gender**	M
Smoking status	Non-smoker	**Age**	75

Medication - Generic Name	**Purpose/Function**
Simvastatin	Reduction of cholesterol and lipids
Frusemide	Hypertension
Prednisolone	Steroid anti-inflammatory drug
Digoxin	Congestive heart failure

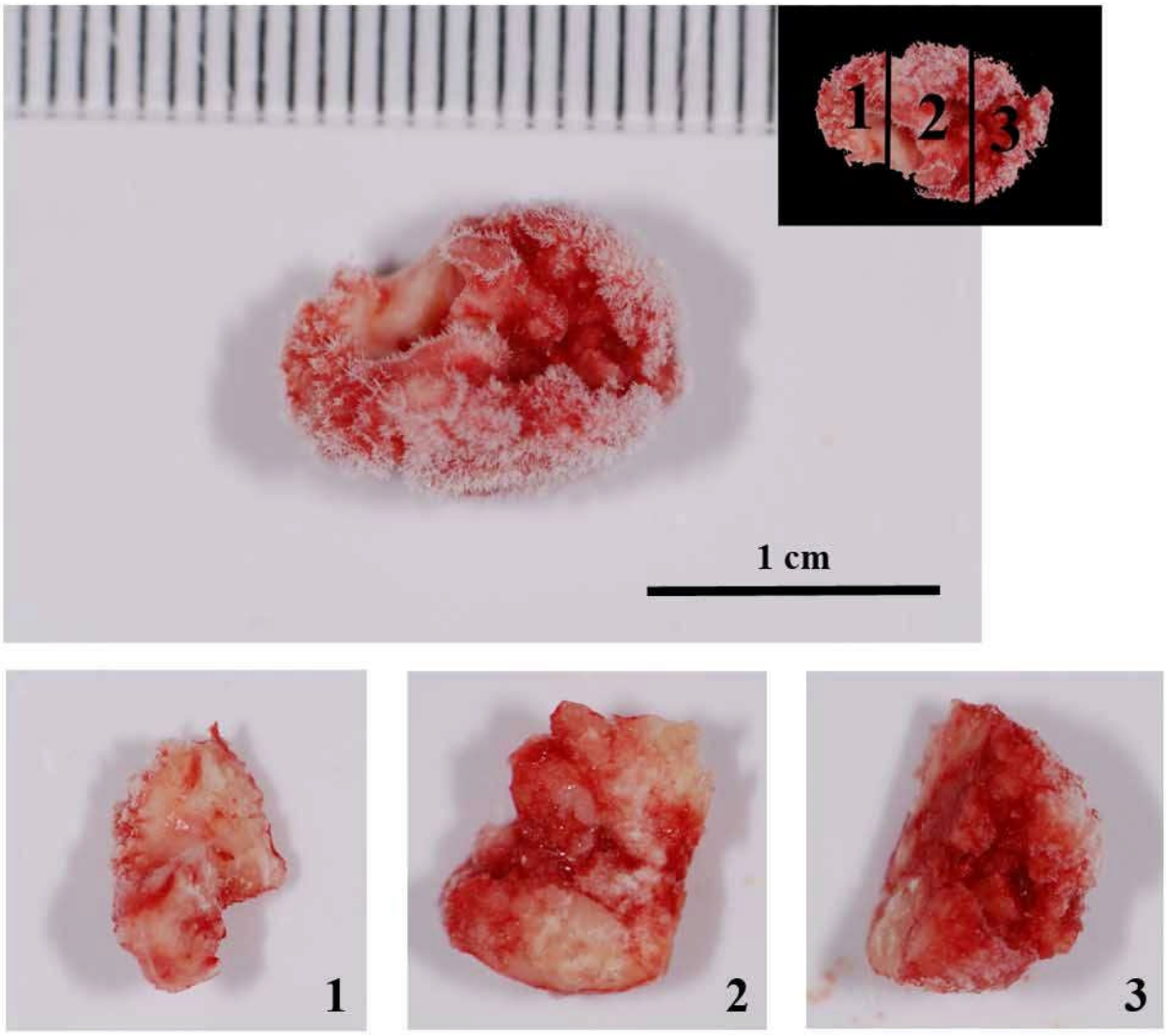

Figure 3.1.4 Sectioning and zones of plaque B
Plaque B was removed from the right femoral artery from the same patient as plaque A and homogenised into three sections. Sections 1 and 3 represent the peripheral sections and section 2 the bifurcation region. Top right hand insert not to scale.

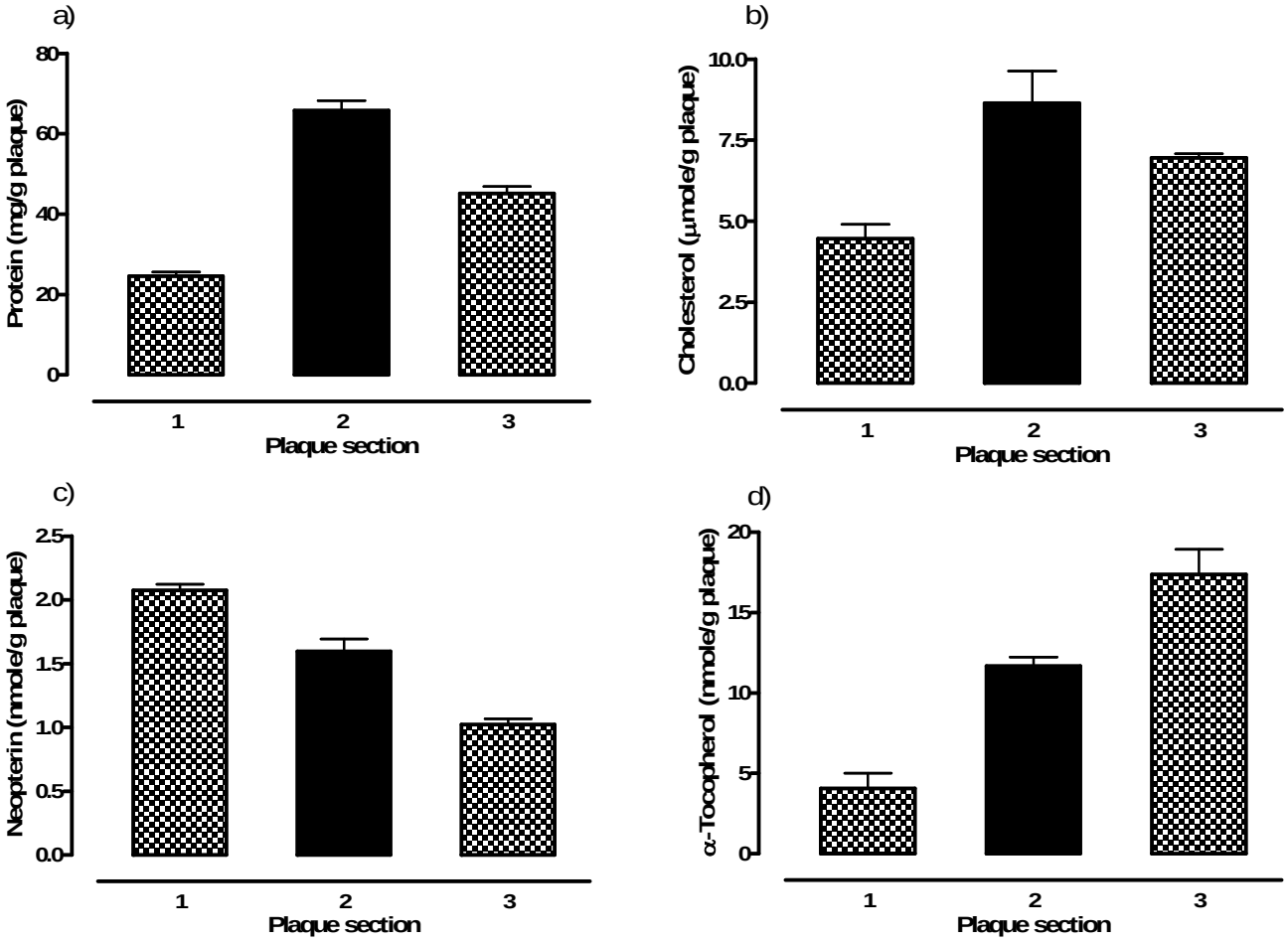

Figure 3.1.5 Protein, cholesterol, neopterin and α-tocopherol content within plaque B
The protein (a) and cholesterol (b) content were determined spectrophotometrically and the neopterin (c) and α-tocopherol (d) concentration via reverse phase HPLC. The chequered bars represent the peripheral sections and the solid bar the bifurcation section. Each bar represents the mean ± SEM of triplicate samples.

The concentration of protein differs within all three sections across plaque B with a maximum concentration in section 2, the bifurcation zone ($p<0.001$) (Figure 3.1.5a). Like that of protein, the cholesterol concentration was also significantly lower within the first peripheral section ($P<0.01$) (Figure 3.1.5b). The neopterin levels significantly decreased along the plaque with a maximum concentration of 2.08 ± 0.05 nmole/g of plaque in section 1 (Figure 3.1.5c). The α-tocopherol concentration mirrored this by increasing along the length of the plaque with a significant difference between the two peripheral sections ($P<0.05$) (Figure 3.1.6d). Opposite of α-tocopherol and like neopterin, the TBARS concentration was maximum within the peripheral section 1 ($P<0.05$) (Figure 3.1.6a). Along with protein, the DOPA and protein carbonyl concentration had

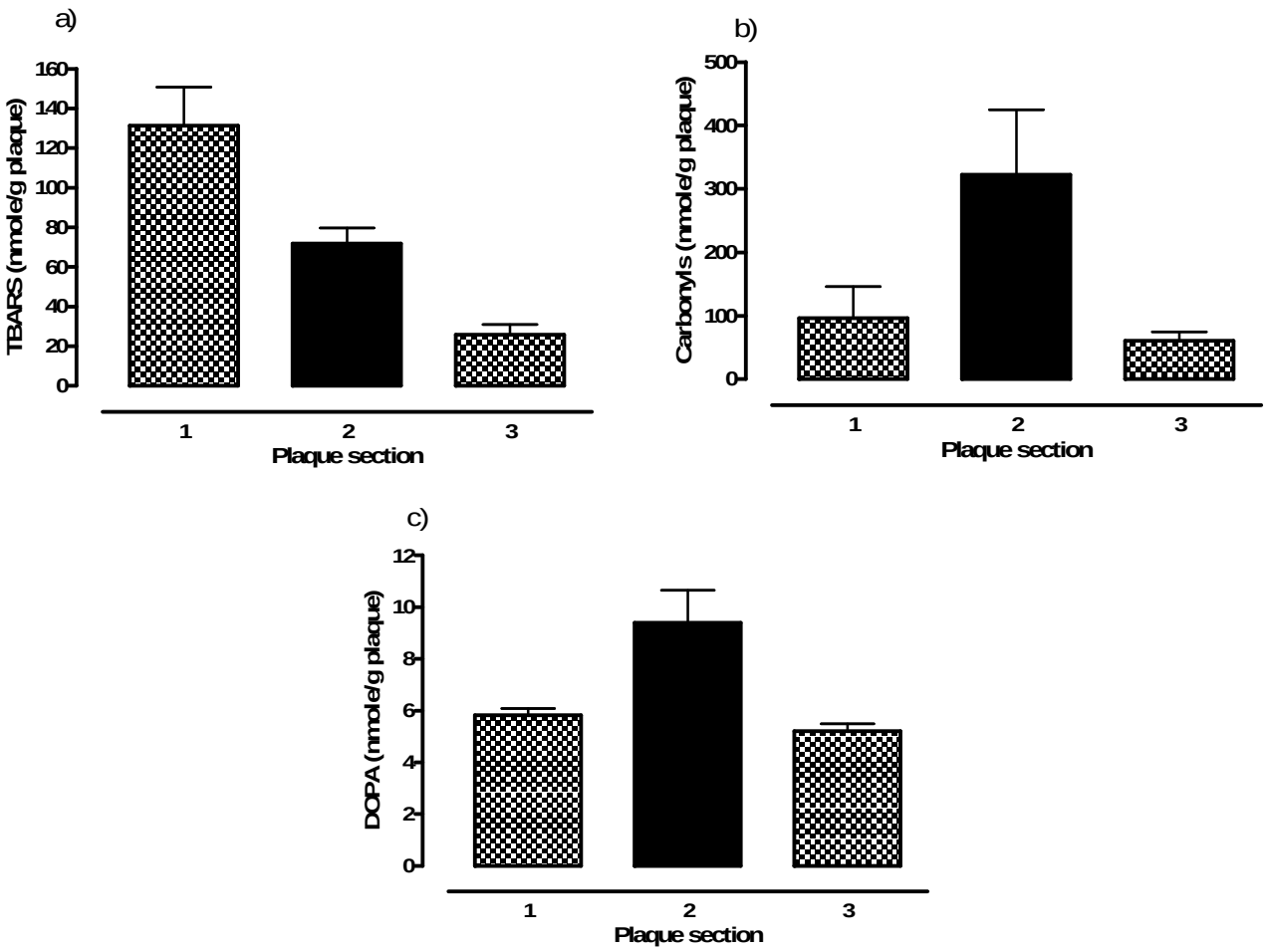

Figure 3.1.6 Lipid and protein oxidative product markers in plaque B
TBARS (a), protein carbonyls (b) DOPA (c) were measure via either reverse phase HPLC or spectrophotometry. The chequered bars represent the peripheral sections and the solid bar the bifurcation section. Each bar represents the mean ± SEM of triplicate samples.

significantly high levels in the bifurcation section. This is reflected in the positive correlation between protein carbonyls and DOPA ($P<0.05$) (Table 3.1.7). No dityrosine was detected within this plaque.

3.1.3 Plaque C (MD260407)

Plaque C was removed from the left common carotid artery and was 28-29 mm long with a total mass of 0.834 grams. Morphologically it had the characteristic Y shape with the primary branch from the internal carotid artery and the smaller secondary branch from the external carotid artery. The lipid core was located predominately in the bifurcation sections and along the primary branch. Qualitatively the solid mass was a red white marble colour with relatively little calcification and no visible thrombus.

Table 3.1.3 Plaque C patient and clinical information

Location	Left common carotid artery	**Stenosis**	85%
Symptoms	Transient ischemic attack	**Gender**	F
Smoking status	Non-smoker	**Age**	84

Medication - Generic Name	**Purpose/Function**
Aspirin	Anti-inflammatory and anti-thrombotic
Tenoxicam	Non-steroid anti-inflammatory drug
Omeprazole	Reduction of gastric acid
Alendronate	Osteoporosis
Calcium	Osteoporosis
Calciferol	Vitamin D/Osteoporosis

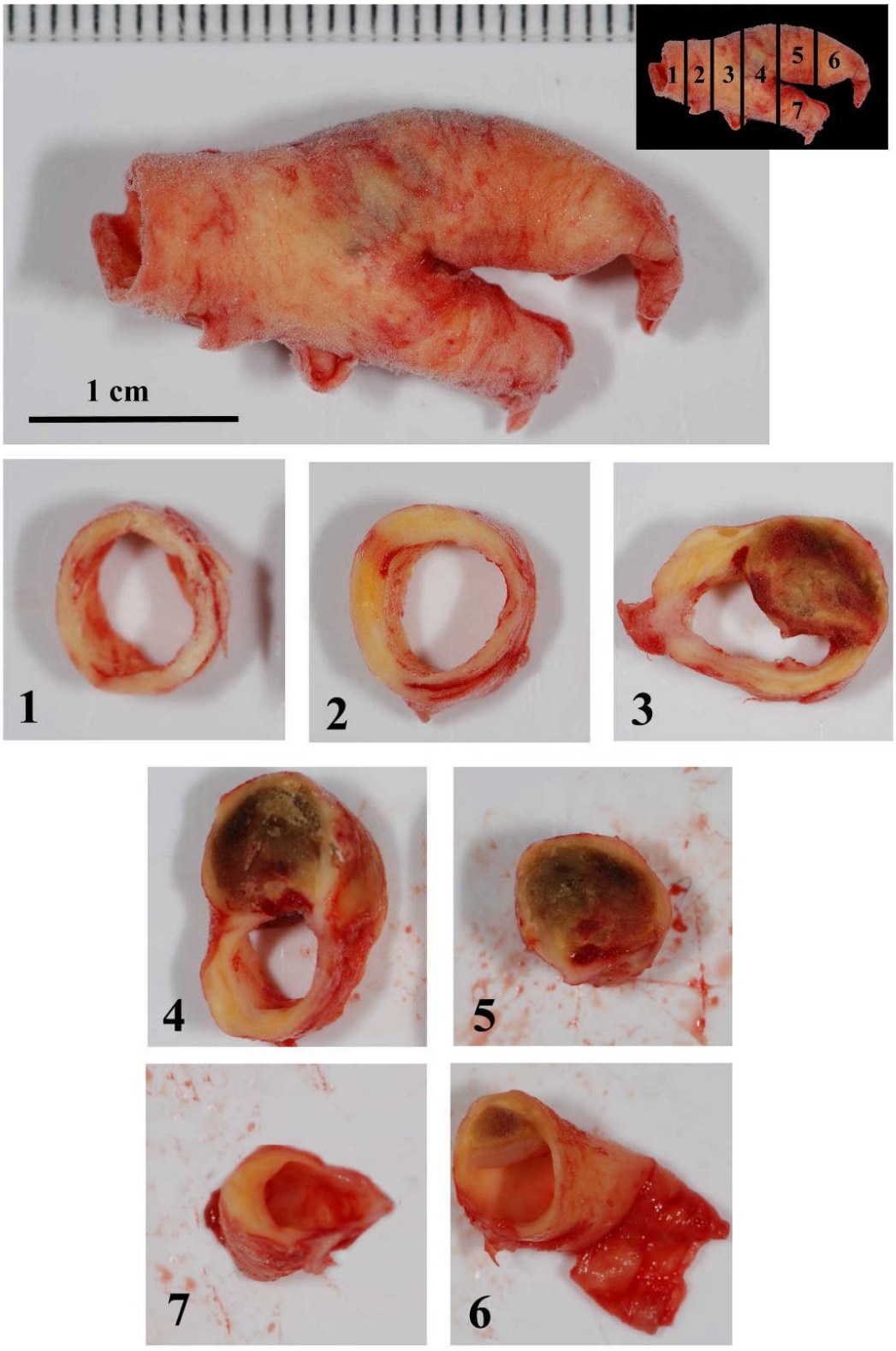

Figure 3.1.7 Sectioning and zones of plaque C
Plaque C was removed from the right carotid artery and homogenised into seven sections. Sections 1, 2 and 3 represent the pre-bifurcation zone, sections 4 and 5 the bifurcation zone, section 6 the post-bifurcation zone and section 7 was classified as the secondary branch and a sub-region of the bifurcation zone. Top right hand insert not to scale.

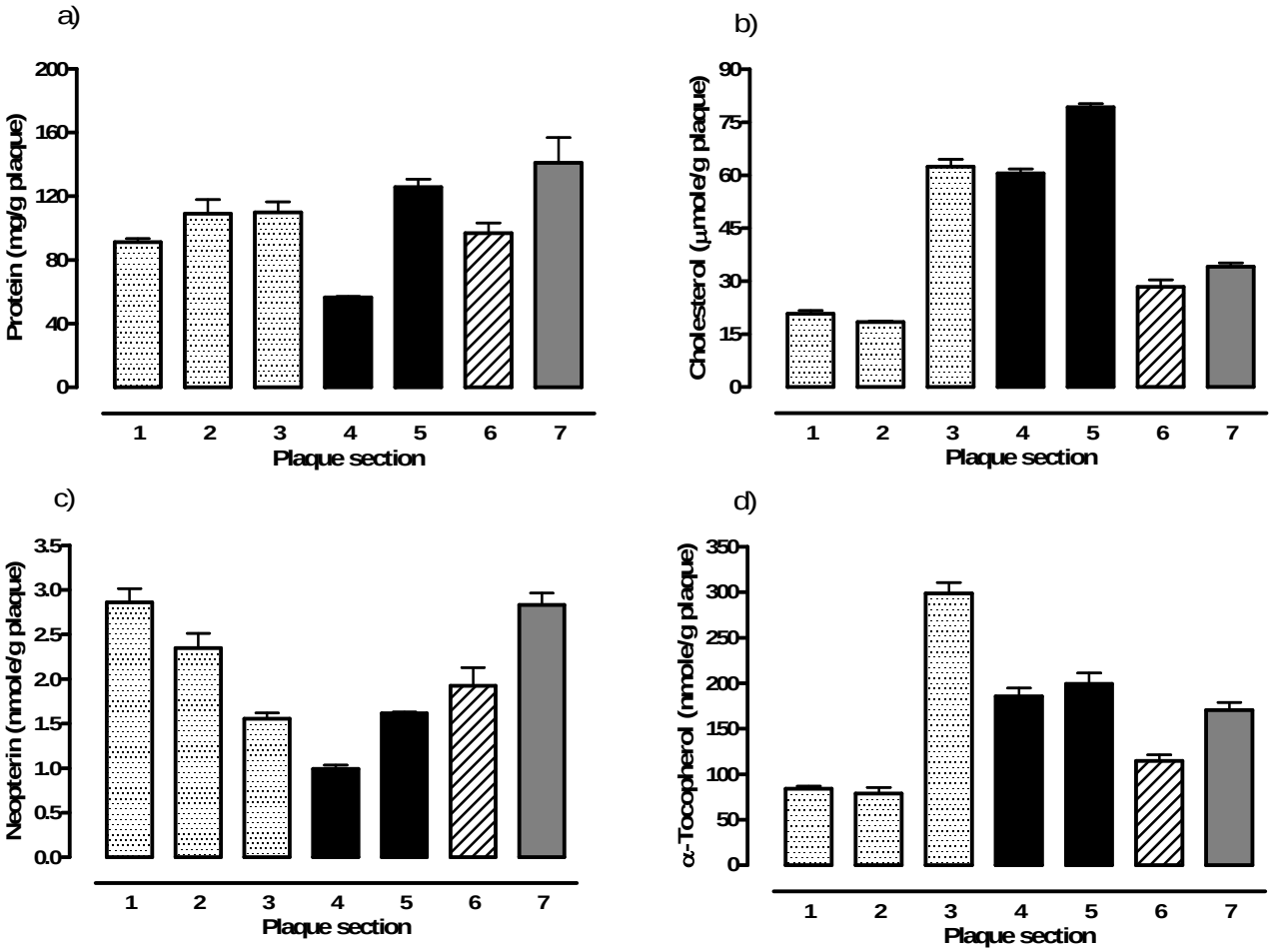

Figure 3.1.8 Protein, cholesterol, neopterin and α-tocopherol content within plaque C
Protein (a) and cholesterol (b) were measured by spectrophotometry and neopterin (c) and α-tocopherol (d) were measured by reverse phase HPLC. The dotted bars represent the pre-bifurcation sections, black solid bars the bifurcation sections, the stripped bar the post-bifurcation section and the grey solid bar represents the secondary branch a sub-region of the bifurcation zone. Each bar represents the mean ± SEM of triplicate samples.

The protein concentration was significantly low in section 4 compared to all but the two peripheral sections 1 and 6 (Figure 3.1.8a). The majority of the cholesterol concentration was within sections 3, 4 and 5 with a maximum level within section 5 (Figure 3.1.8b). There was significantly high neopterin (maximum concentration of 2.86 ± 0.13 nmole/g of plaque in section 1) in the peripheral sections compared to the 'gruelly' sections 3, 4 and 6 ($P<0.001$). This was reflected in the significantly low concentration of neopterin in the bifurcation zone compared to the pre-bifurcation and secondary branch ($P<0.01$) (Figure 3.1.8c). The α-tocopherol had the opposite trend to neopterin with high levels in the 'grueller' sections 3, 4 and 5 ($P<0.001$), with a maximum

concentration of 298.77 ± 12.18 nmole/g of plaque in the pre-bifurcation section 3 (Figure 3.1.8d). The TBARS concentration was maximum in the proximal section 1 and lowered in the distal section 6, therefore the pre-bifurcation had significantly high levels ($P<0.05$) compared to the post-bifurcation zone (Figure 3.1.9a). Protein carbonyl levels were maximum within the pre-bifurcation section 2 with 603.08 ± 94.81 nmole/g of plaque and were significantly high within the 'non-gruelly' sections compared to the 'gruelly' central sections ($P<0.01$) (Figure 3.1.9b). The dityrosine concentration was significantly high within the bifurcation sections 4 and 6 ($P<0.001$) (Figure 3.1.9d), therefore the 'gruelly' sections also contained the maximum dityrosine concentration within the plaque. DOPA had the opposite trend with high concentrations within the 'non-gruelly' sections ($P<0.001$) (Figure 3.1.9c).

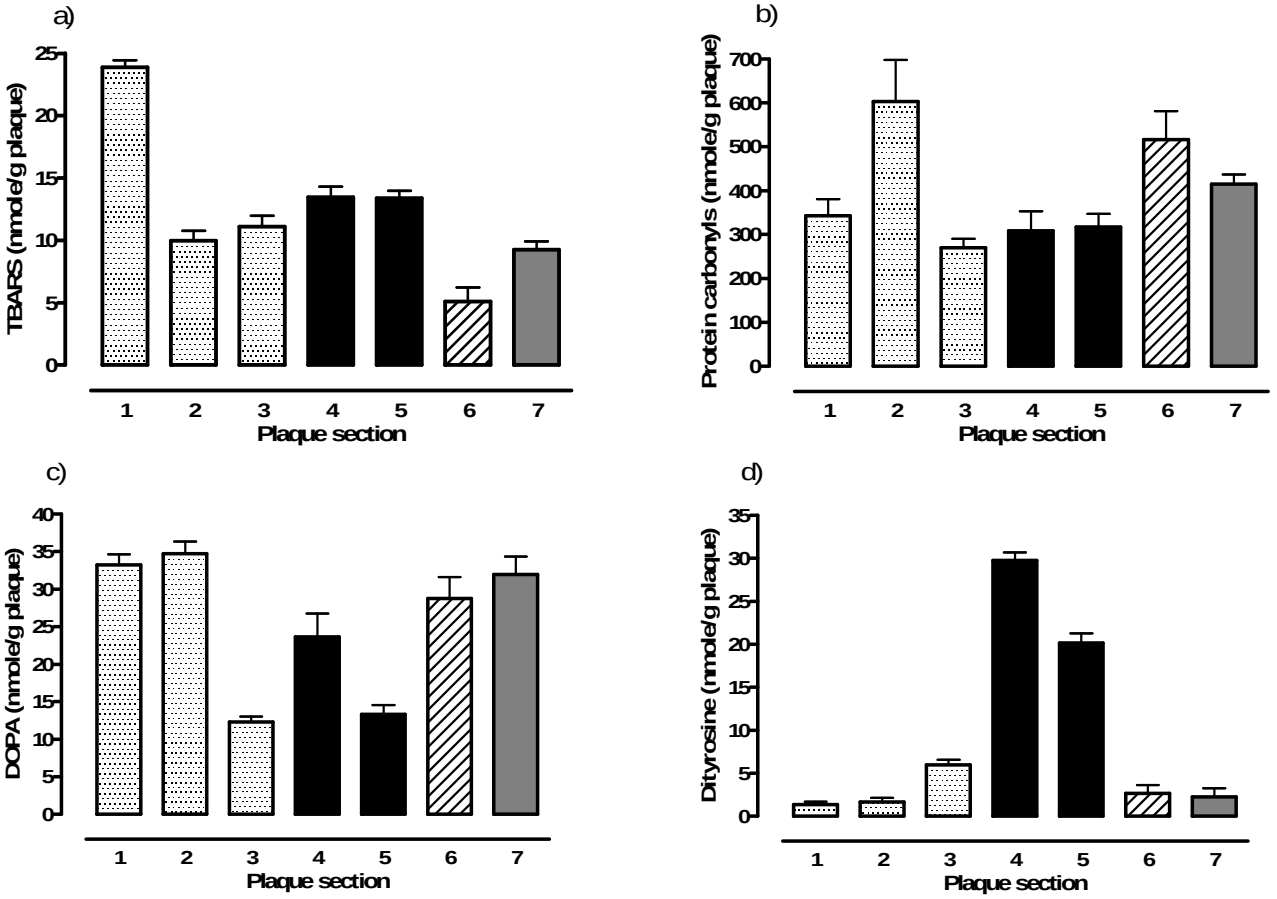

Figure 3.1.9 Lipid and protein oxidative product markers in plaque C
TBARS (a), protein carbonyls (b), DOPA (c) and dityrosine (d) were measured by either reverse phase HPLC or spectrophotometry. The dotted bars represent the pre-bifurcation sections, solid bars the bifurcation sections and the stripped bar the post-bifurcation section. The solid grey bar represents the secondary branch a sub-region of the bifurcation section. Each bar represents the mean ± SEM of triplicate samples.

Cholesterol and α-tocopherol concentrations displayed a significant positive correlation ($P<0.05$) towards each other and both also showed a negative correlation towards DOPA (Table 3.1.17). The dityrosine concentration across the plaque mirrored that of DOPA levels therefore the dityrosine had a positive correlation towards cholesterol concentrations ($P<0.05$). Neopterin the inflammatory marker had the negative relationship towards the dityrosine levels ($P<0.05$). As for the 'gruelly' sections there were higher concentrations of α-tocopherol and dityrosine compared to the low levels of DOPA, neopterin and protein carbonyls within these sections.

3.1.4 Plaque D (MLA130607)

Plaque D was removed from the right carotid artery. It was 30 mm in length with a total mass of 1.238 grams. It had a relatively small degree of calcification observed predominantly within the first two sections identified within the outer rings (Figure 3.1.10). The 'gruel' was primarily a red and white solid mass. Plaque D was cut into 7 sections where the pre-bifurcation zone was represented by section 1, the bifurcation zone by section 2 and includes the small secondary branch from the external carotid artery, and sections 4-7 the post-bifurcation zone. Unlike previous plaques much of the mass was located in the post-bifurcation region.

Table 3.1.4 Plaque D patient and clinical information

Location	Right carotid artery	**Stenosis**	98%
Symptoms	Stroke	**Gender**	M
Smoking status	Non-smoker	**Age**	82

Medication - Generic Name	**Purpose/Function**
Aspirin	Anti-inflammatory and anti-thrombotic
Simvastatin	Reduction cholesterol and lipids
Doxazosin	Hypertension
Cilazapril	Hypertension
Metaprolol	Hypertension
Paracetamol	Analgesic

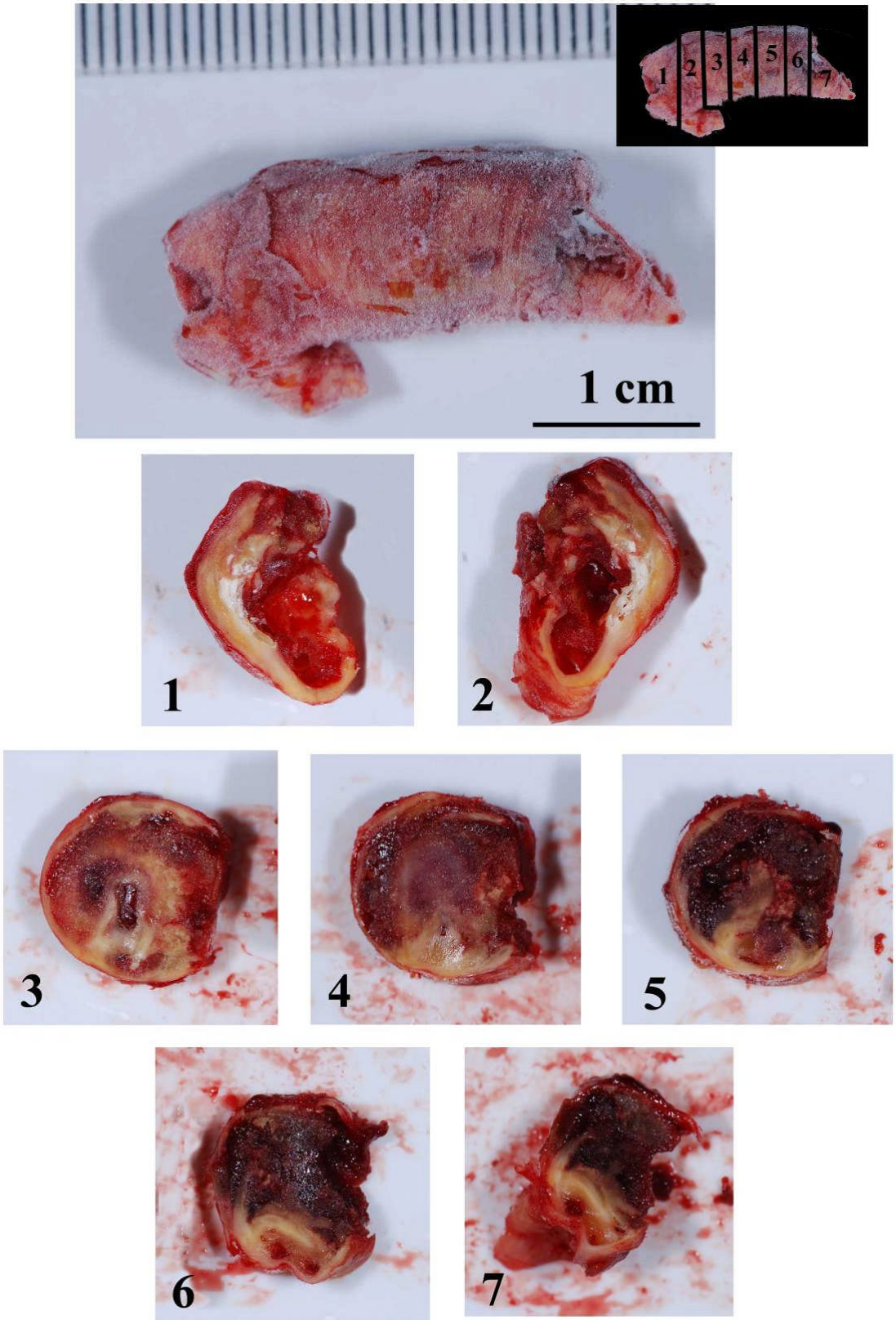

Figure 3.1.10 Sectioning and zones of plaque D
Plaque D was removed from the right carotid artery and homogenised into seven sections. Section 1 represents the pre-bifurcation zone, section 2 the bifurcation zone, and sections 3-7 the post-bifurcation zone. Top right hand insert not to scale.

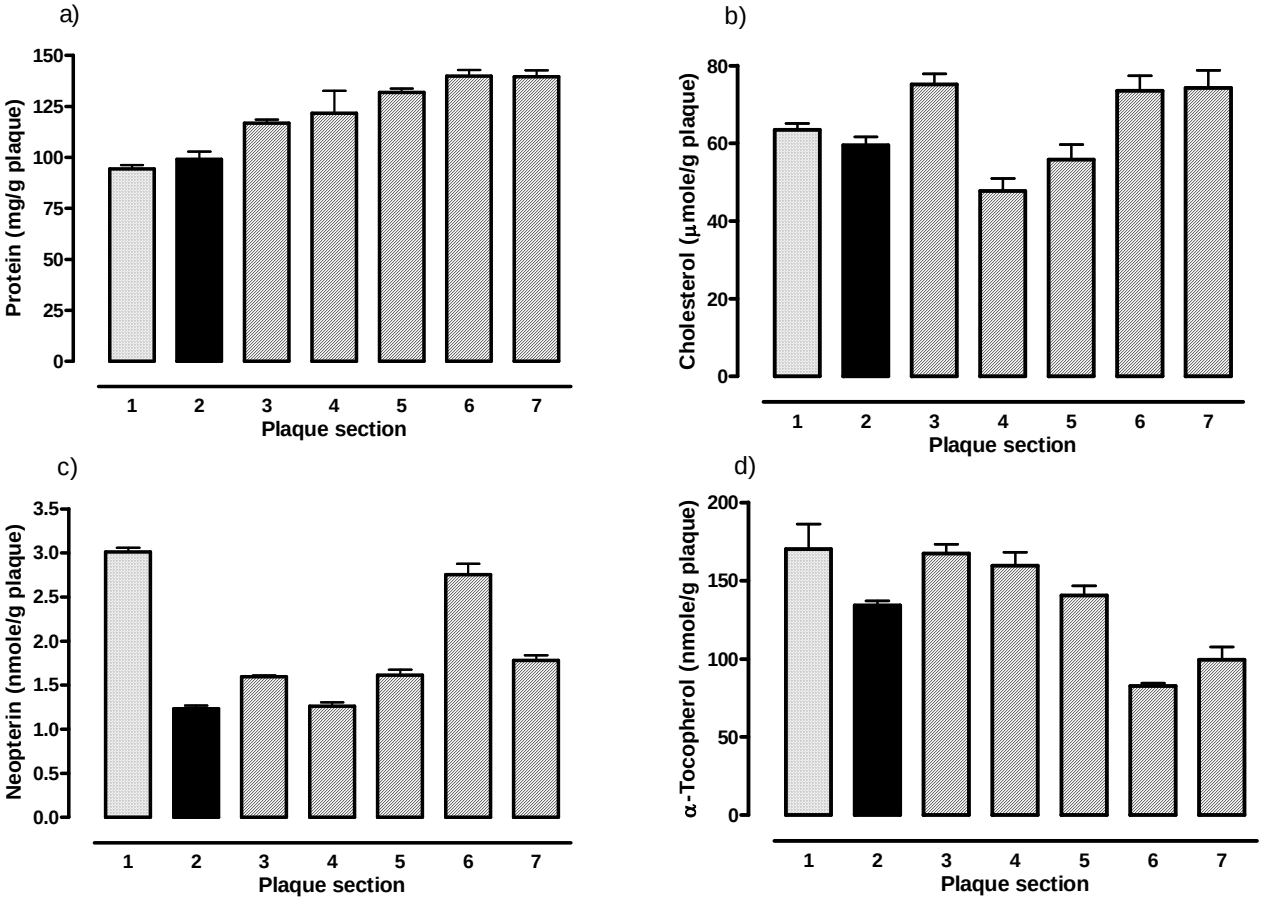

Figure 3.1.11 Protein, cholesterol, neopterin and α-tocopherol content in Plaque D
Protein (a) and cholesterol (b) were determined by spectrophotometric analysis and neopterin (c) and α-tocopherol (d) via reverse phase HPLC. The dotted filled bar represents the pre-bifurcation section, solid bar the bifurcation section and the stripped bars the post-bifurcation sections. Each bar represents the mean ± SEM of triplicate samples.

The pre-bifurcation and bifurcation zones were significantly low in protein content compared to the post-bifurcation zone ($P<0.01$) (Figure 3.1.11a). The cholesterol concentration was maximum in the first post-bifurcation section, significantly dropping ($P<0.001$) in section 4 before returning to the high concentration at the distal end of the plaque (Figure 3.1.11b). Like plaques A, B and C the neopterin levels had a significant high within the proximal section 1, the pre-bifurcation zone, with a concentration of 3.01 ± 0.01 nmole/g of plaque. Similarly to plaque A the neopterin also had a high concentration in the 2nd to last section within the post-bifurcation zone (Figure 3.1.11c). The α-tocopherol content was consistent along the plaque before decreasing significantly within the last two sections ($P<0.05$) (Figure 3.1.11d). TBARS had a maximum concentration within the first section with a concentration of 14.89 ± 0.52 nmole/g of plaque therefore the pre-bifurcation zone

was significantly high compared to the post-bifurcation region ($P<0.01$) (Figure 3.1.12a). Because the DOPA concentration increased along the length of the plaque from the proximal to the distal end (Figure 3.1.12c), the post-bifurcation zone had significantly more DOPA levels than the pre-bifurcation ($P<0.05$). The dityrosine concentration was similar in that it had a high level in the post-bifurcation section 6 (20.11 ± 0.03 nmole/g of plaque), and the majority of this protein oxidative product were in the latter three sections (Figure 3.1.12d). The protein carbonyls displayed no variation across the length of the plaque (Figure 3.1.12b).

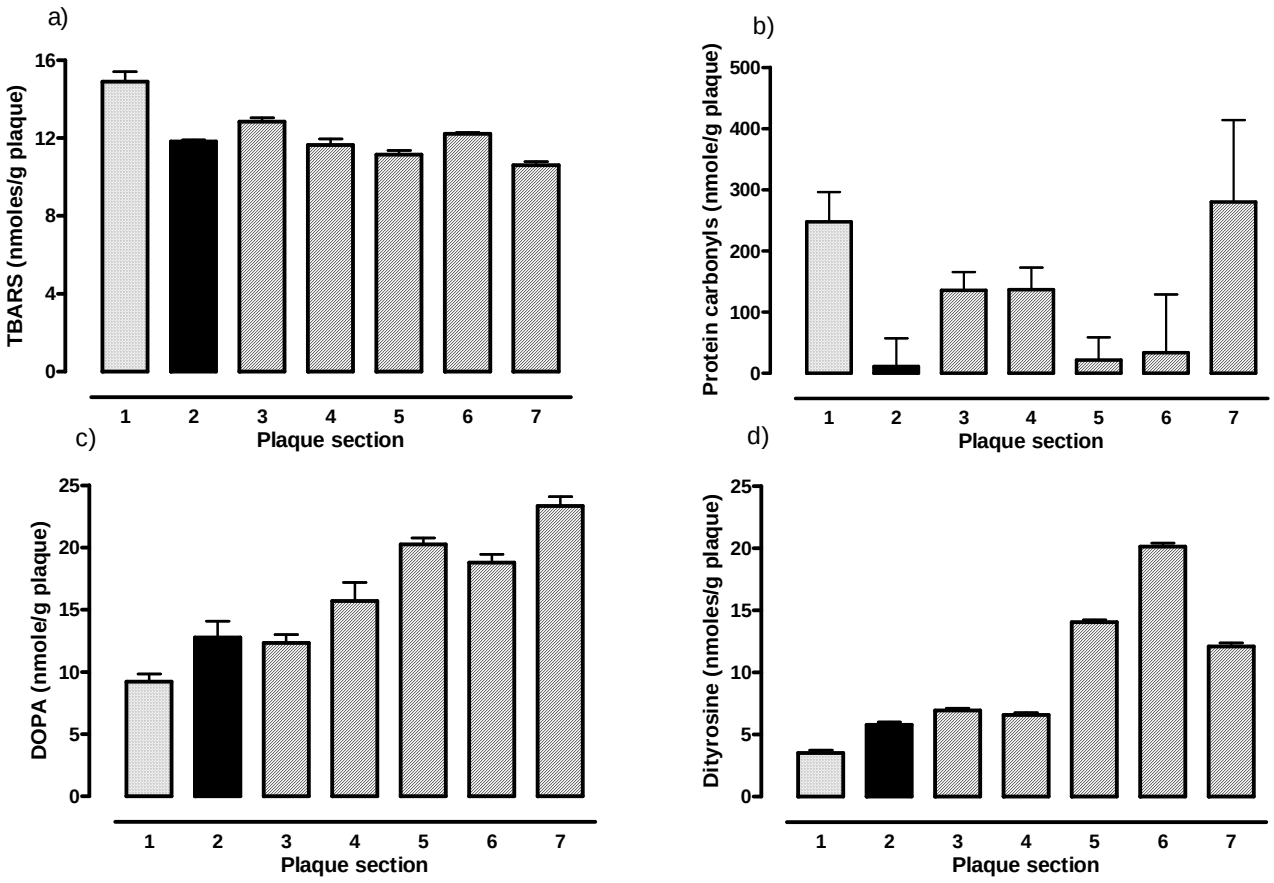

Figure 3.1.12 Lipid and protein oxidative product markers in plaque D
TBARS (a), protein carbonyls (b), DOPA (c) and dityrosine (d) were measured by either reverse phase HPLC or spectrophotometry. The dotted filled bar represent the pre-bifurcation section, solid bar the bifurcation section and the stripped bars the post-bifurcation sections. All bars were the mean ± SEM of triplicate samples.

Both DOPA and dityrosine concentrations were positively correlated with protein across the plaque ($P<0.01$) and ($P<0.05$) respectively, however not towards each other (Table 3.1.7). Within the oxidative markers, DOPA levels were negatively correlated towards TBARS concentrations ($P<0.05$), whereas the dityrosine levels had a negative correlation with α-tocopherol concentrations ($P<0.05$).

3.1.5 Plaque E (BB050507)

Plaque E had a stenosis of 80-95% and was taken from the right internal carotid artery. It was 30 mm in length with a total mass of 0.943 grams. Plaque E had a relatively small level of calcification compared to the previous plaques and was characterised with a thrombus observed within sections 3-5. For the majority of plaques there were associated symptoms induced within the patient. The presence of the disease within this patient was recently discovered and subsequently the patient was asymptomatic. Because of this the patient had only just begun taking the classic CAD medications; statins and aspirin. Therefore in the combined plaque analysis the patient was considered to be on neither of the medications.

Table 3.1.5 Clinical information of plaque E

Location	Right carotid artery	**Stenosis**	80-95%
Symptoms	Asymptomatic	**Gender**	M
Smoking status	Smoker	**Age**	60

Medication - Generic Name	**Purpose/Function**
Aspirin	Anti-inflammatory and anti-thrombotic
Simivastatin	Reduction in cholesterol and lipids
Metaprolol	Hypertension
Allopurinol	Gout
Alluretic	

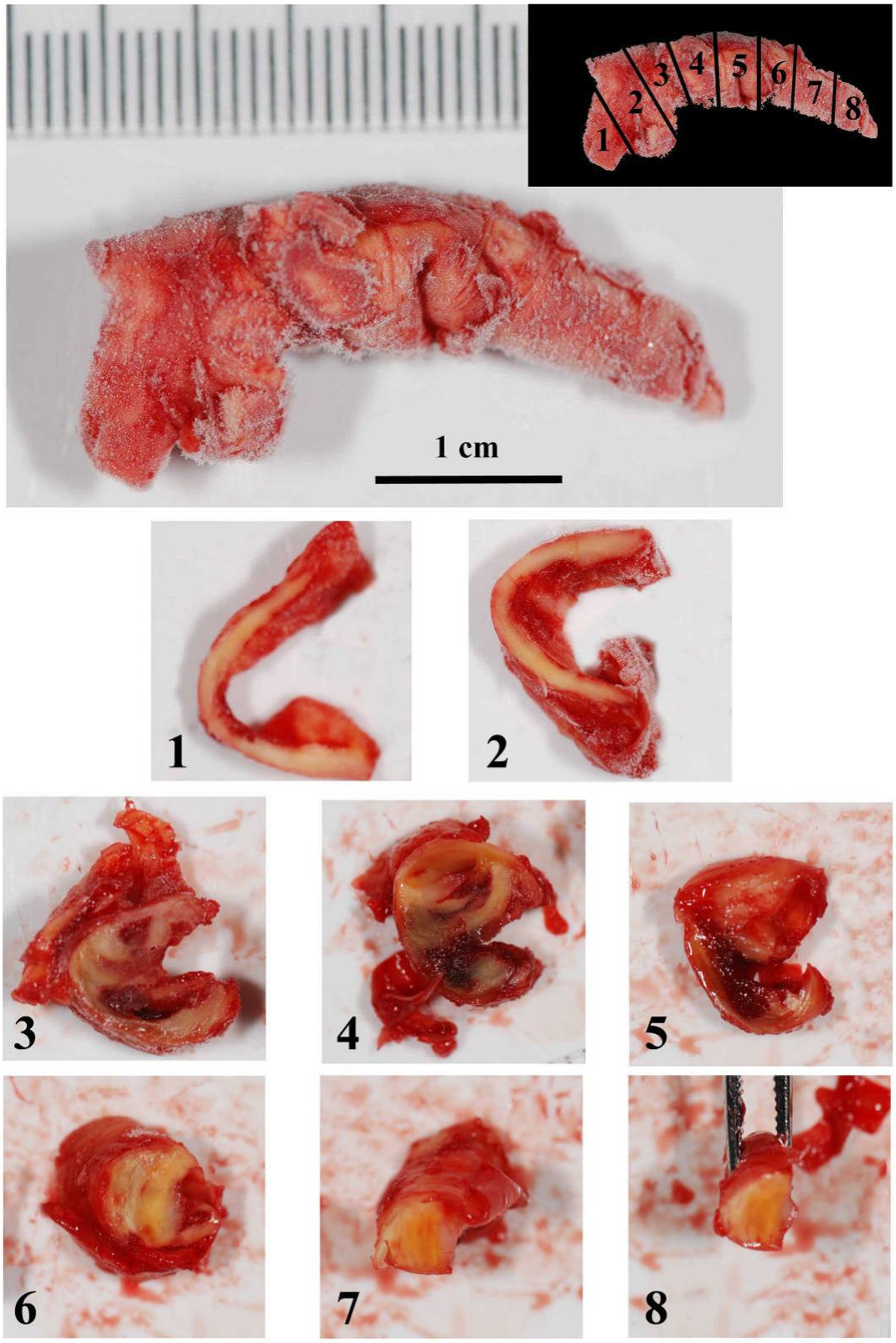

Figure 3.1.13 Sectioning and zones of plaque E
Plaque E was removed from the right carotid artery and homogenised into eight sections. Section 1 represents the pre-bifurcation zone, sections 2 and 3 the bifurcation zone, and sections 4-8 the post-bifurcation zone. Top right hand insert not to scale.

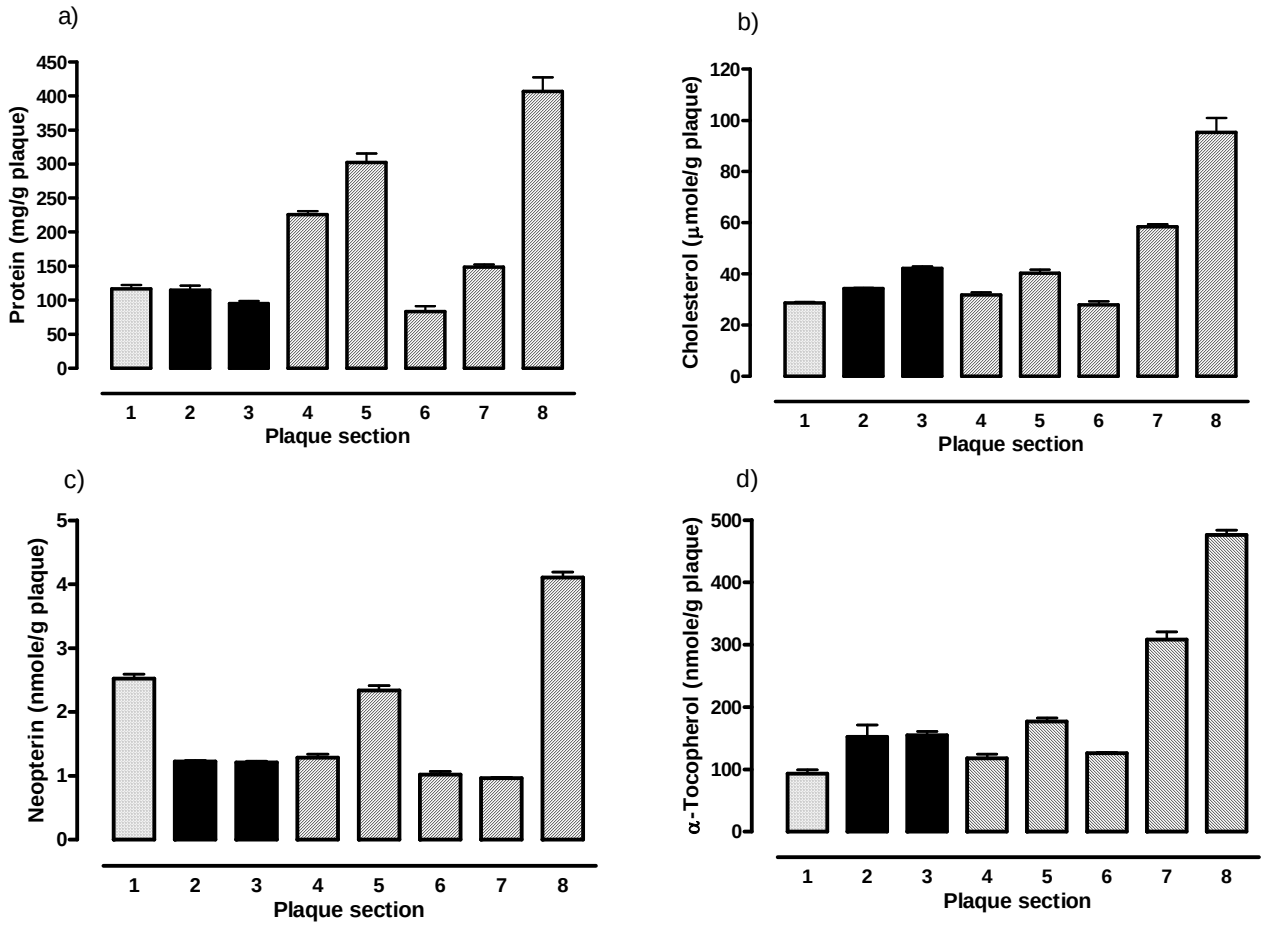

Figure 3.1.14 Protein, cholesterol, neopterin and α-tocopherol content within plaque E
Protein (a) and cholesterol (b) were measured by spectrophotometry and neopterin (c) and α-tocopherol (d) concentrations were determined by reverse phase HPLC. The dotted filled bar represents the pre-bifurcation zone, solid bars the bifurcation zone and the stripped bars the post-bifurcation zones. Each bar represents the mean ± SEM of triplicate samples.

The last section, section 8, contained the maximum concentrations of protein, cholesterol, neopterin and α-tocopherol detected within the plaque (Figure 3.1.14). The protein levels were also high within the first two post-bifurcation sections 4 and 5, whereas the neopterin also had high levels within the pre-bifurcation section. For α-tocopherol the majority of this antioxidant was found within the last two sections of the plaque. TBARS maximised in section 8, and along with dityrosine had high levels within the red 'gruel' sections 3, 4 and 5 (Figure 3.1.15a,d). Protein carbonyl and DOPA concentrations displayed no variation across this plaque. However when protein carbonyls was expressed as per gram of protein a zoning effect emerges with both the pre-bifurcation and bifurcation regions having higher levels than the post-bifurcation (data not shown).

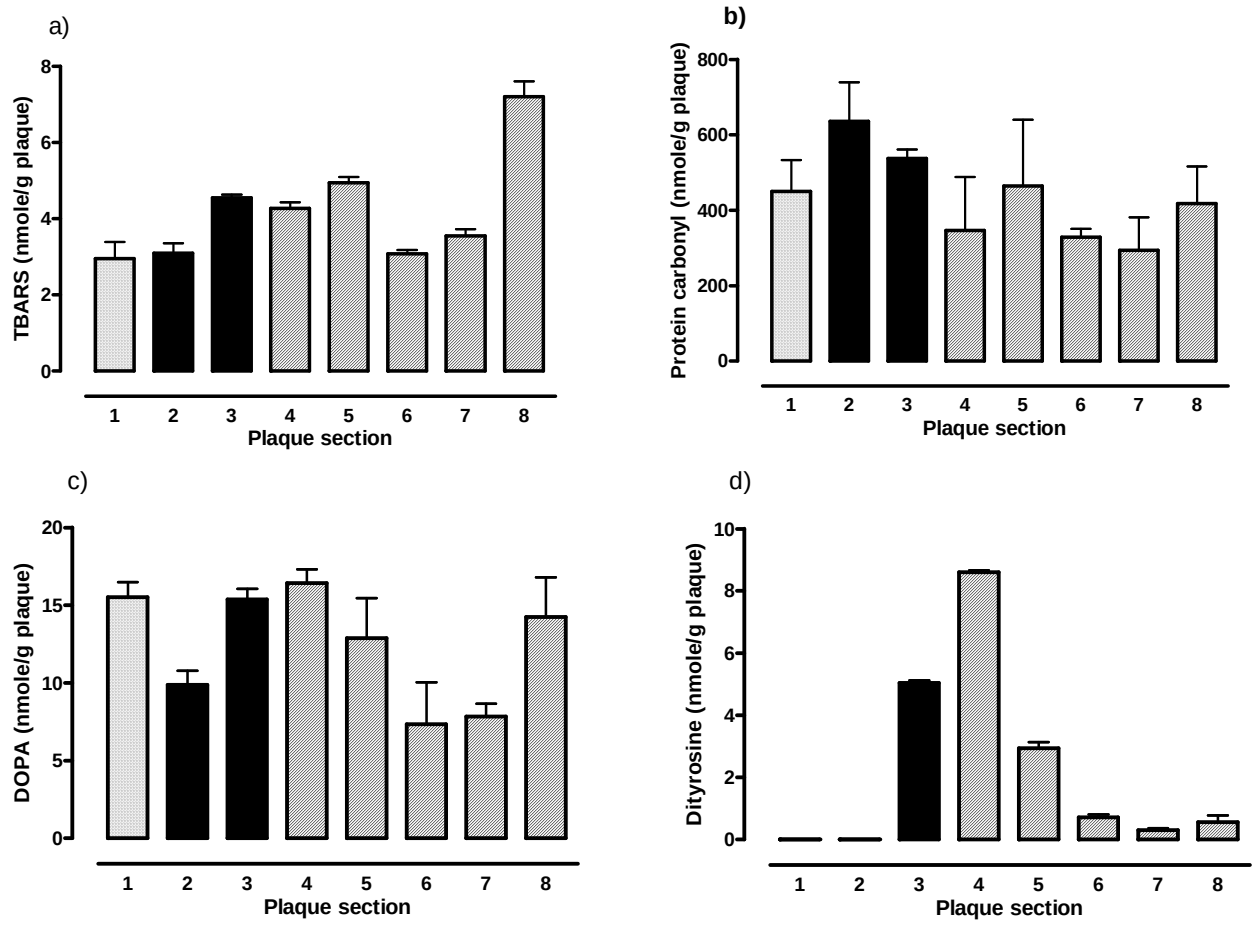

Figure 3.1.15 Lipid and protein oxidative product markers in plaque E
TBARS (a), DOPA (c) and dityrosine (d) were measured by reverse phase HPLC and protein carbonyls (b) via spectrophotometry. The dotted bar represents the pre-bifurcation section, solid bars the bifurcation sections and the stripped bars the post-bifurcation sections. Ear bar represents the mean ± SEM of triplicate samples.

The two lipid based analytes α-tocopherol and TBARS positively correlated ($P<0.05$) (Table 3.1.17) and both also correlated to cholesterol ($P<0.01$) and ($P<0.01$) respectively. This plaque was the only plaque to display correlations between all three lipid related components. Positive correlations between protein levels and two unrelated markers, cholesterol and TBARS were also observed.

3.1.6 Plaque F (TE120704)

Plaque F was characterised with 80-90% stenosis, 31 mm in length and a total mass of 0.692 grams. It was homogenised as a whole plaque because it was not suitable for sectioning. Therefore the marker concentrations are comparable to the average overall levels of previous plaques (Table I/II). Plaque F homogenate was also used for investigating the pterin, 7-ketocholesterol/α-tocopherol and AAS/GGS assays (section 3.2).

Table 3.1.6 Plaque F patient and clinical information

Location	Right common carotid artery	**Stenosis**	80-90%
Symptoms	Transient ischemic attack	**Gender**	M
Smoking status	Non smoker	**Age**	76

Medication - Generic Name	**Purpose/Function**
Aspirin	Anti-inflammatory and anti-thrombosis
Simvastatin	Reduction cholesterol and lipids
Atenolol	Hypertension
Bendrofluazide	Hypertension
Prazosin	Hypertension
Dipyridamole	Anti-thrombosis

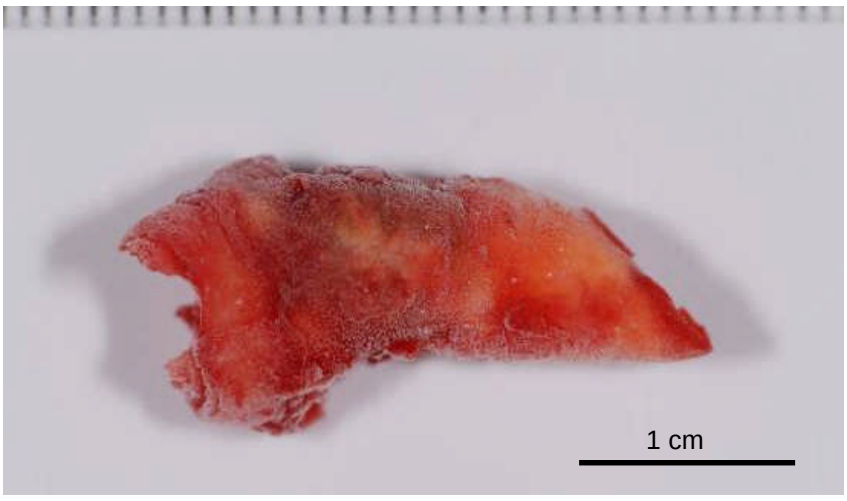

Figure 3.1.16 Plaque F morphology
Plaque F was homogenised whole under liquid nitrogen

Plaque F had a protein content of 91.76 ± 4.04 mg/g of plaque, very similar to the overall average of the plaques (Table I). The cholesterol and α-tocopherol concentrations were the highest recorded thus far in the study and the neopterin concentration was the lowest at 0.72 ± 0.01 nmole/g plaque. The TBARS, protein carbonyl, DOPA and dityrosine concentrations were all close to the overall average concentration of all the plaques with concentrations of 9.84 ± 0.68, 256.10 ± 56.94, 16.24 ± 1.63 and 3.94 ± 0.12 nmole/g of plaque respectively (Table II).

3.1.7 Individual plaque summary

In general the femoral plaques had overall lower concentrations of protein, cholesterol, α-tocopherol, DOPA and dityrosine but higher levels of lipid oxidation. Besides dityrosine, the overall α-tocopherol concentrations were the most variable between the plaques with a 37 fold difference between the plaque with the highest concentration in plaque F and lowest in plaque B. The overall neopterin concentration within each plaque ranged from 0.72-2.34 nmole/g of plaque between the six plaques. Within and between the first five plaques only one correlation occurred twice, a positive correlation between α-tocopherol and cholesterol (plaque C and E) (Table 3.1.17). However many of expected correlations did occur at least once within the five plaques, highlighting the differences between and within the plaque.

The lipid soluble antioxidant, α-tocopherol had a significant correlation with every marker within plaques A-E. The relationship was positive towards neopterin, cholesterol, TBARS, protein and protein carbonyl concentrations, but negative to both DOPA and dityrosine concentrations within different plaques (Table 3.1.17). Neopterin concentrations displayed a correlation towards TBARS and dityrosine, but not protein carbonyl or DOPA levels. Within plaques C and D the ‘gruelly’ sections generally had higher concentrations of the oxidative markers. Of the oxidative markers TBARS, DOPA and protein carbonyl levels all had a correlation with each other within one of the five plaques. All correlations where positive except between DOPA and TBARS. When relating to the appropriate compound of origin, TBARS and cholesterol concentrations positively correlated (Plaque E) and DOPA and dityrosine positively correlated with protein levels however this occurred within the same plaque (Plaque D).

Table 3.1.7 Correlations of inflammatory and oxidative markers within plaques A-E and between plaques A-N

Significant correlations were determined based on the average of each section (n=3) within plaques A-E. N is the number of sections within each plaque. Combined plaque analysis was preformed on plaques A, C-E, G-N, where N is the collated number of sections of the plaques. For neopterin correlations plaques G-J were excluded. Protein was expressed in mg/g plaque, cholesterol μmole/g plaque and neopterin, α-tocopherol, TBARS, protein carbonyl, DOPA and dityrosine as nmole/g plaque. Where stated, per cholesterol, the α-tocopherol and TBARS were expressed μmole/mole of cholesterol, and per protein, the DOPA, dityrosine and protein carbonyls were expressed per nmole/gram of protein. Statistical significance represented by P<0.05 * P<0.01 ** P<0.001 ***

Markers	r(Pearson)	P value		N
Plaque A				
protein vs. α-tocopherol	0.8027	0.016	*	8
neopterin vs. protein	0.9827	0.000	***	8
neopterin vs. α-tocopherol	0.7741	0.024	*	8
neopterin vs. TBARS	0.7200	0.044	*	8
α-tocopherol vs. protein carbonyls	0.8693	0.005	**	8
TBARS vs. protein carbonyls	0.8465	0.008	**	8
α-tocopherol (per cholesterol) vs. protein carbonyls (per protein)	0.7807	0.022	*	8
Plaque B				
DOPA vs. protein carbonyls	1.0000	0.040	*	3
α-tocopherol vs. TBARS (per cholesterol)	-0.9974	0.046	*	3
α-tocopherol vs. DOPA (per protein)	-0.9984	0.036	*	3
Plaque C				
α-tocopherol vs. cholesterol	0.7982	0.031	*	7
α-tocopherol vs. DOPA	-0.8694	0.011	*	7
DOPA vs. cholesterol	-0.9267	0.003	**	7
dityrosine vs. cholesterol	0.7546	0.050	*	7
dityrosine vs. neopterin	-0.8092	0.027	*	7
α-tocopherol vs. dityrosine (per protein)	-0.7909	0.034	*	7

DOPA (per protein) vs. protein carbonyls (per protein)	0.8157	0.025	*	7
Plaque D				
protein vs. DOPA	0.9122	0.004	**	7
protein vs. dityrosine	0.8540	0.014	*	7
α-tocopherol vs. dityrosine	-0.8328	0.020	*	7
TBARS vs. DOPA	-0.8432	0.017	*	7
tocopherol (per cholesterol) vs. TBARS (per cholesterol)	0.8969	0.006	**	7
Plaque E				
protein vs. cholesterol	0.7316	0.039	*	8
protein vs. TBARS	0.8898	0.003	**	8
cholesterol vs. α-tocopherol	0.9875	0.000	***	8
cholesterol vs. TBARS	0.8348	0.010	**	8
α-tocopherol vs. TBARS	0.7702	0.025	*	8
α-tocopherol (per cholesterol) vs. DOPA (per protein)	0.7742	0.024	*	8
Combined data analysis				
TBARS vs. cholesterol	-0.2983	0.005	**	87
α-tocopherol vs. cholesterol	0.2604	0.015	*	87
α-tocopherol vs. protein	0.5132	0.000	***	87
α-tocopherol vs. protein carbonyls	0.2804	0.009	**	87
neopterin vs. protein carbonyls	0.3807	0.003	**	59
protein carbonyls vs. protein	0.3025	0.004	**	87
neopterin vs. protein	0.3615	0.005	**	59
dityrosine vs. cholesterol	0.4313	0.000	***	87
dityrosine vs. DOPA	0.3294	0.002	**	87
α-tocopherol vs. DOPA (per protein)	-0.2800	0.009	**	87

3.1.8 Combined plaque analysis

Due to the small sample set (n=5) and the apparent complexity of the plaques, correlations within the individual plaques (plaques A-E) did not occur more than once with one exception (section 3.1.7). With a higher number of plaque samples the more likely common factors and correlations will emerge. This research was a continuation from a PhD (Firth, 2006) and Masters (Flavall, 2008) research which had collectively analysed the same markers within eight plaques. Thus to better understand the processes occurring within these plaques, the entire database of 13 plaques (excludes plaque F) was statistically analysed to identify any underlying trends within the inflammatory and oxidative markers along with other influential factors (Table 3.1.8).

All 13 plaques were in an advanced state of the disease displaying from 60-90% stenosis. The patients presented with a range and combination of symptoms including stroke, transient ischemic attacks (temporary blockage of blood flow), amaurosis fugax (temporary loss of vision) and dysphemia (temporary loss of speech). The morphology of the 13 plaques was classified by the overall shape of the plaque. The difference between morphological shapes were very distinctive as each plaque was either in the form of a Y shape where both branches were similar in size, had a smaller secondary branch, or was linear with no side protrusions. Another qualitative characteristic noted was overall composition assessed during homogenisation and classified as being either heavily calcified, contained an obvious thrombus or did not strongly have either of these features.

The location of the plaque either in the carotid or femoral artery may play a role in the concentration and/or localisation of the markers within the plaques. However, only plaques A and B were removed from the femoral arteries and were also from the same patient (Table 3.1.8). Therefore any differences observed between the locations may be due to patient variations, thus location was not considered in the analysis. Like plaques A-E the effects of zoning were assessed to see if variation existed between these regions in relation to the inflammatory and oxidative markers. Long term medication is another possible influential factor affecting plaque growth. Except for the femoral plaque patient all patients were on aspirin, however not all patients where on statins therefore this effect on plaque morphology and patients symptoms where also analysed (Table 3.1.8).

To assess the correlations between these plaques one way- and factorial-analysis of variance (ANOVA) were preformed. Where required data was logarithmically transformed. For the combined plaque analysis plaques G-J were excluded from the neopterin correlations because their concentrations were determined by the trichloricacetic acid method (section 3.2.1). This method has since been replaced with the more accurate acetonitrile method (section 2.2.4A).

Table 3.1.8 Summary of clinical and patient information of plaques A-N

Plaque	Total mass (g)	Morp.	Composition	Section N	Location				Symptoms	Meds
					LC	RC	LF	RF		
A	1.156	linear	calcified	8			√		Unknown	S
B	0.474	linear	calcified	3				√	Unknown	S
C	0.814	Y	neither	7	√				TIA	A
D	1.238	small	thrombosis	7		√			stroke	SA
E	0.943	linear	thrombosis	8		√			asymptomatic	N
F	0.692	linear	unknown	whole		√			TIA	SA
G	0.909	linear	neither	6		√			TIA	A
H	2.857	small	calcified	7		√			Stroke	SA
I	1.500	small	neither	8		√			TIA	SA
J	0.763	small	thrombosis	7	√				Stroke	SA
K	1.306	Y	calcified	7	√				TIA	SA
L	0.822	Y	thrombosis	6		√			AF	SA
M	0.507	small	calcified	6	√				Stroke	A
N	0.377	Y	thrombosis	6	√				AF	A

Overall morphology (Morp.) Y - Y shaped, small - small secondary branch and linear
Overall composition (Composition) thrombosed, calcified and neither
Section – number of sections each plaque was homogenised in to
Arterial location of plaque: LC– left carotid, RC – right carotid, LF – left femoral and RF – right femoral
Patient Symptoms (Symptoms) TIA – transient ischemic attack, AF – amaurosis fugax
Patient Medication (Meds) S – statins alone, A – aspirin alone, SA – statins and aspirin, N – neither

3.1.8.1 Combined plaque correlations

Between the 13 plaques cholesterol positively correlated to α-tocopherol ($P<0.05$) supported by the fact that LDL is the main source of α-tocopherol and possibly cholesterol (Table 3.1.17). The negative relationship between cholesterol and TBARS concentrations ($P<0.001$) indicates that at higher cholesterol content there is less lipid peroxides present. The positive correlation between neopterin and protein levels ($P<0.01$) (Table 3.1.17) was also observed in plaque A.

Even though protein carbonyl levels show little if any variation across individual plaques overall it displayed a positive correlation towards α-tocopherol ($P<0.01$), neopterin ($P<0.01$) and protein levels ($P<0.01$) (Table 3.1.17). This is the only oxidation marker that positively correlated to both α-tocopherol and neopterin.

Significant correlations observed in the combined plaque analysis, but not within any individual plaques, included the above mentioned correlations between protein carbonyl concentration with protein ($P<0.01$) and neopterin levels ($P<0.01$). This indicates that protein carbonyls do have relevant relationships with some markers but this was only observed when all plaques were included in the analysis. Within the protein oxidative markers, dityrosine and DOPA concentrations positively correlated ($P<0.01$) but protein carbonyls did not to either. This was another correlation observed in the combined plaque analysis that was not seen within individual plaques along with the positive correlation between dityrosine and cholesterol ($P<0.001$). This further supports the diversity among atherosclerotic plaques.

3.1.8.2 Variation in marker concentration associated with zones

Across the 13 plaques the post-bifurcation section had significantly high protein and cholesterol levels compared to the bifurcation ($P<0.05$) and pre-bifurcation ($P<0.01$) zones respectively (Figure 3.1.17 a,b). As was observed with plaques A-E in the individual plaque analysis the neopterin had significantly high levels within the pre- and post-bifurcation sections ($P<0.01$) (Figure 3.1.17 c). This is opposite of the lipid peroxidation marker TBARS which has a lower concentration in the pre- and post-bifurcation sections ($P<0.01$) (Figure 3.1.17 c,e). The free radical specific protein

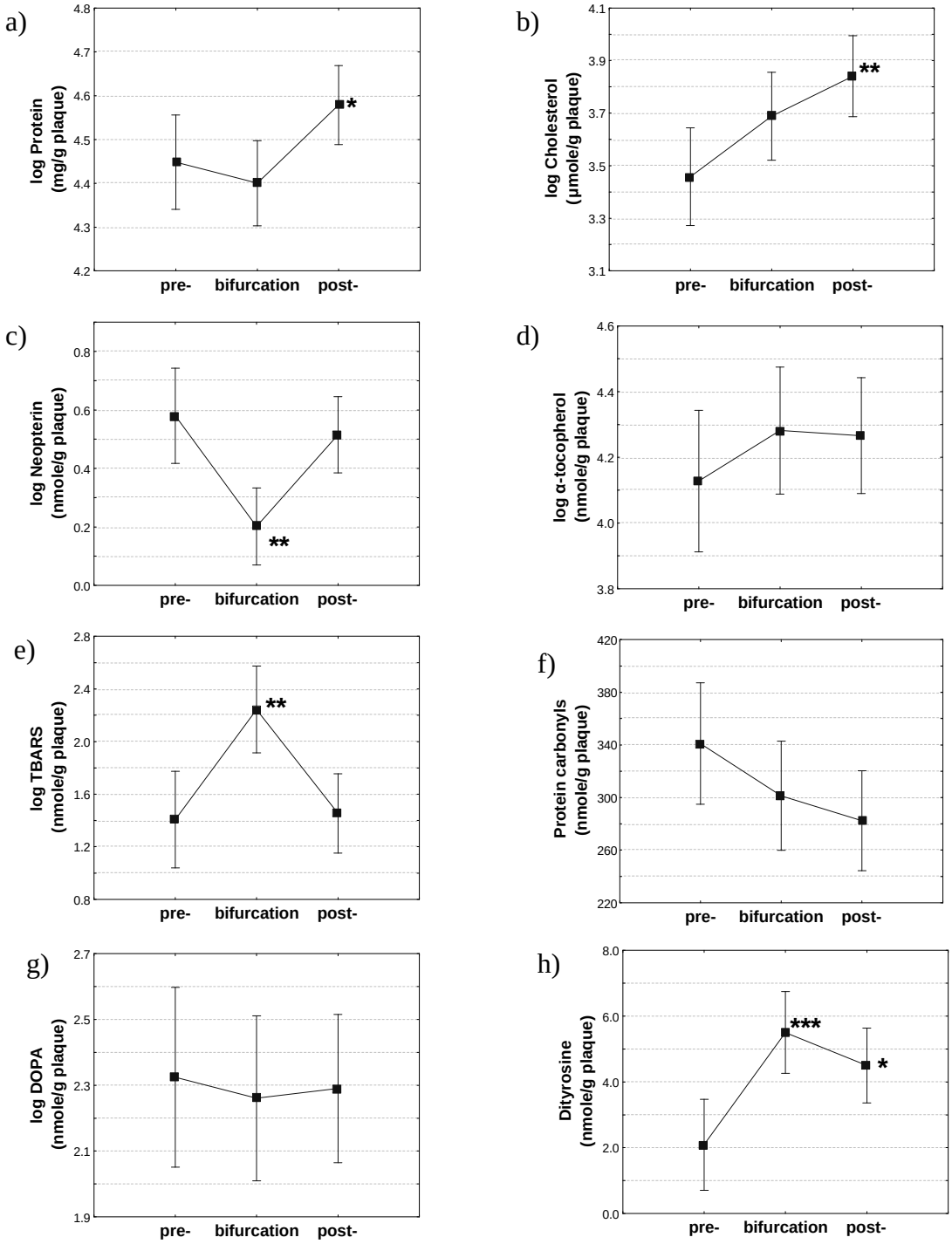

Figure 3.1.17 Effects of zoning on the concentration of the inflammatory and oxidative markers within plaques A-N

Data from each section from plaques A-N (N=13) were classified into either pre-bifurcation (pre-), bifurcation or post-bifurcation (post-) zones (as described in section 2.3). The variation between the concentrations of protein (a), cholesterol (b), neopterin (c), α-tocopherol (d), TBARS (e), protein carbonyl (f), DOPA (g) and dityrosine (h) within each zone was assessed by one way-ANOVA and Tukey's test. Displayed are the LS means and vertical bars represent 95 % confidence intervals. For the neopterin data only plaques A-E and K-N were included (N=9). Significant differences represent P<0.05*, P<0.01** and P<0.001*** to the other zones.

oxidation product dityrosine had higher levels in the bifurcation and post-bifurcation zones (Figure 3.1.17 h), suggesting that more free radical damage is occurring at these locations. Low shear stress occurs within these zones therefore increased oxidative stress (Chatzizisis et al., 2007) providing a site for the production of dityrosine inducible free radicals. Concentrations of the lipid soluble antioxidant α-tocopherol and protein oxidation products DOPA and protein carbonyls display no variation between the zones (Figure 3.1.17 d,f,g).

3.1.8.3 Variation in marker concentration associated with overall plaque composition

The plaques with a thrombus have higher protein content (Figure 3.1.18 a) presumably due to the increased presence of blood proteins. These plaques also had high levels of α-tocopherol and dityrosine (Figure 3.1.18 d,h). For the calcified plaques there were significantly low levels of protein, cholesterol, α-tocopherol, DOPA and dityrosine (Figure 3.1.18 a,b,d,h). However there is no variation between the categories for neopterin, TBARS and protein carbonyls (Figure 3.1.18 c,e,f). For the plaques that are not in either category (neither) the concentration of protein, α-tocopherol and dityrosine was between that of the thrombosed and calcified plaques.

When the thrombosed, calcified and neither plaques were analysed for variation between the zones, the trend was similar to that of analysing the whole plaque in each overall compositional state. This suggests that the zoning had little effect on the concentration of the markers when the compositional state was taken into consideration (Figure 3.1.18). Notable differences in the trends identified were higher levels of cholesterol, α-tocopherol and dityrosine in the bifurcation of neither plaques and higher protein carbonyls in the pre-bifurcation zone compared to the bifurcation zone of calcified plaques (data not shown).

3.1.8.4 Interaction between overall composition and overall morphology

As seen before, the thrombosed plaques had high protein content compared to both calcified and neither plaques which was true regardless of plaque shape (Figure 3.1.19 a). The calcified plaques generally had lower concentrations of protein, neopterin, DOPA and dityrosine however plaque morphology was influential with the concentration of cholesterol, α-tocopherol and TBARS (Figure 3.1.19).

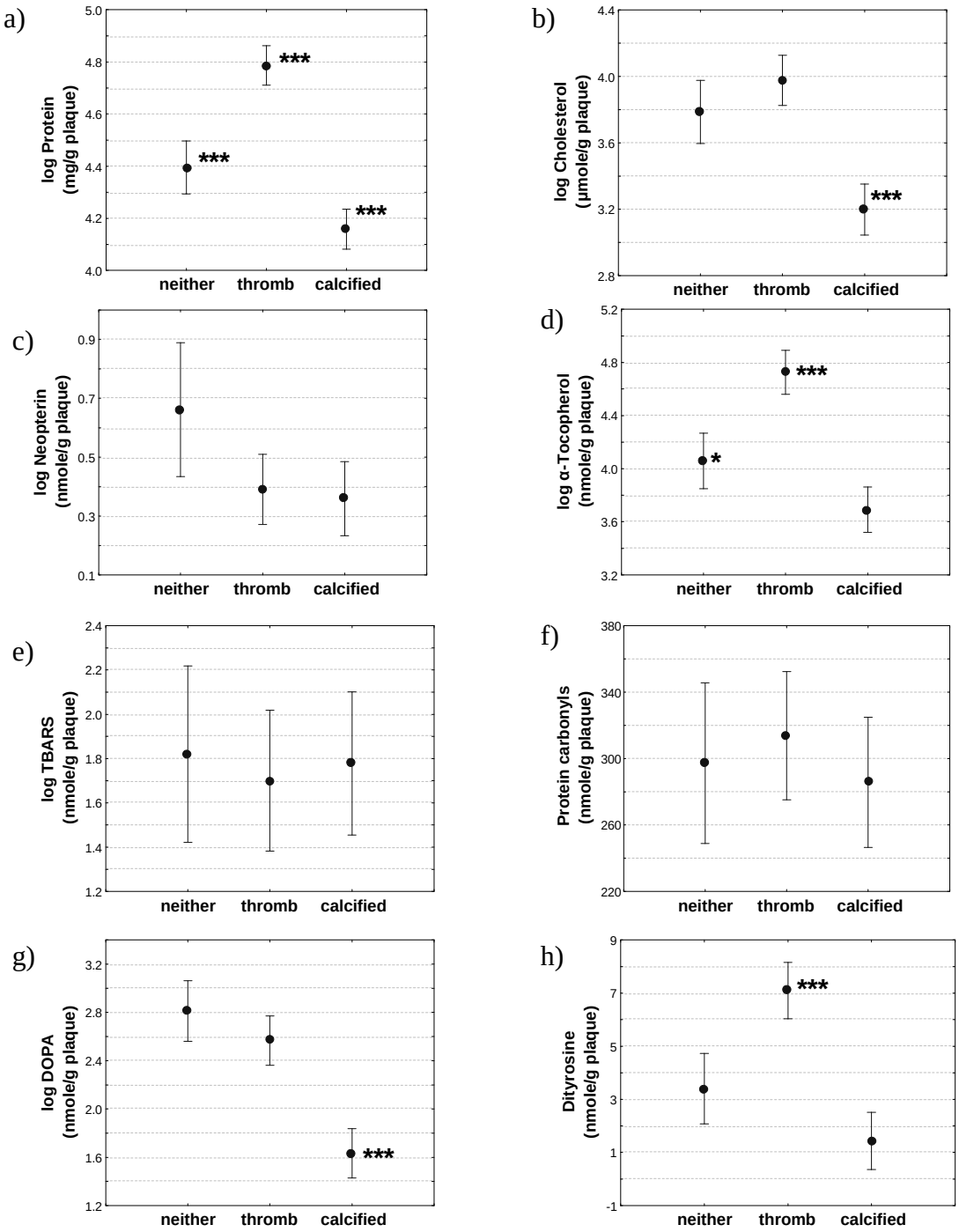

Figure 3.1.18 Influence of the overall plaque composition on the variation of inflammatory and oxidative markers between plaques A-N

Plaques A-N were qualitatively classified as being either thrombosed (thromb) (n=5), calcified (n=5) or neither (n=3). The data from the plaques were analysed as described in section 2.3. The variation in the concentrations of protein (a), cholesterol (b), neopterin (c), α-tocopherol (d), TBARS (e), protein carbonyls (f), DOPA (g) and dityrosine (h) were assessed by performing one way-ANOVA and Tukey's test. Displayed are the LS means and vertical bars represent 95 % confidence intervals. For the neopterin data only plaques A-E and K-N were included (thrombosed (n=4), calcified (n=4) and neither (n=1)). Significant differences represent $P<0.05$*, $P<0.01$** and $P<0.001$ to the other compositional states.

Within the linear plaques the protein, cholesterol and DOPA concentrations were lower in the calcified linear plaques but had higher TBARS concentrations (Figure 3.1.19). The thrombosed linear plaques were high in protein carbonyls compared to a lower level in the linear neither which may be due the presence of blood proteins and the thrombotic cascade event introducing an increase in oxidative stress. The Y shaped plaques had higher α-tocopherol levels regardless of compositional state compared to the other morphological shaped plaques (Figure 3.1.19d). Similarly, the cholesterol was statistically the same between the different compositional states and the concentration was also the same across the different morphologies (Figure 3.1.19b). Along with dityrosine, the DOPA and TBARS levels were lower in the Y shaped calcified plaques. This compares to the higher DOPA and TBARS content in the neither calcified plaques. Regardless of compositional state the α-tocopherol was low and cholesterol high in the small branched plaques (Figure 3.1.19b,d), indicating a lower proportion of α-tocopherol per cholesterol in the small branched plaques. Like the linear and Y shaped plaques the thrombosed small branched plaques had higher protein than the calcified or neither plaques. Along with this the dityrosine was higher in the thrombosed compared to the calcified and neither plaques. Neopterin showed no difference between either of the morphologies or compositional state.

Overall the DOPA concentration was generally higher in the neither plaques, the morphology of the plaque may play a role in the concentration of protein carbonyls in the neither and thrombosed plaques, TBARS concentration only differed across the Y shaped plaques, dityrosine was higher in the Y shaped plaques and the morphological shape may be influential on α-tocopherol concentration.

3.1.8.5 Interaction between symptom presented and overall morphology

Of the 11 patients (femoral plaque patient was excluded), four had strokes, four had transient ischemic attacks (TIA), two had amaurosis fugax (AF), and one patient was asymptomatic. The morphology of the plaque may have an influence on the symptoms suffered because the AF inducing plaques were both Y shaped and the stroke inducing plaques all had a small secondary branch. TIA inducing plaques were represented by all three different morphological shapes. In terms of the markers it was found that the Y shaped plaques generally had higher concentrations. Protein, α-tocopherol and protein carbonyl levels were statistically the same within the plaques

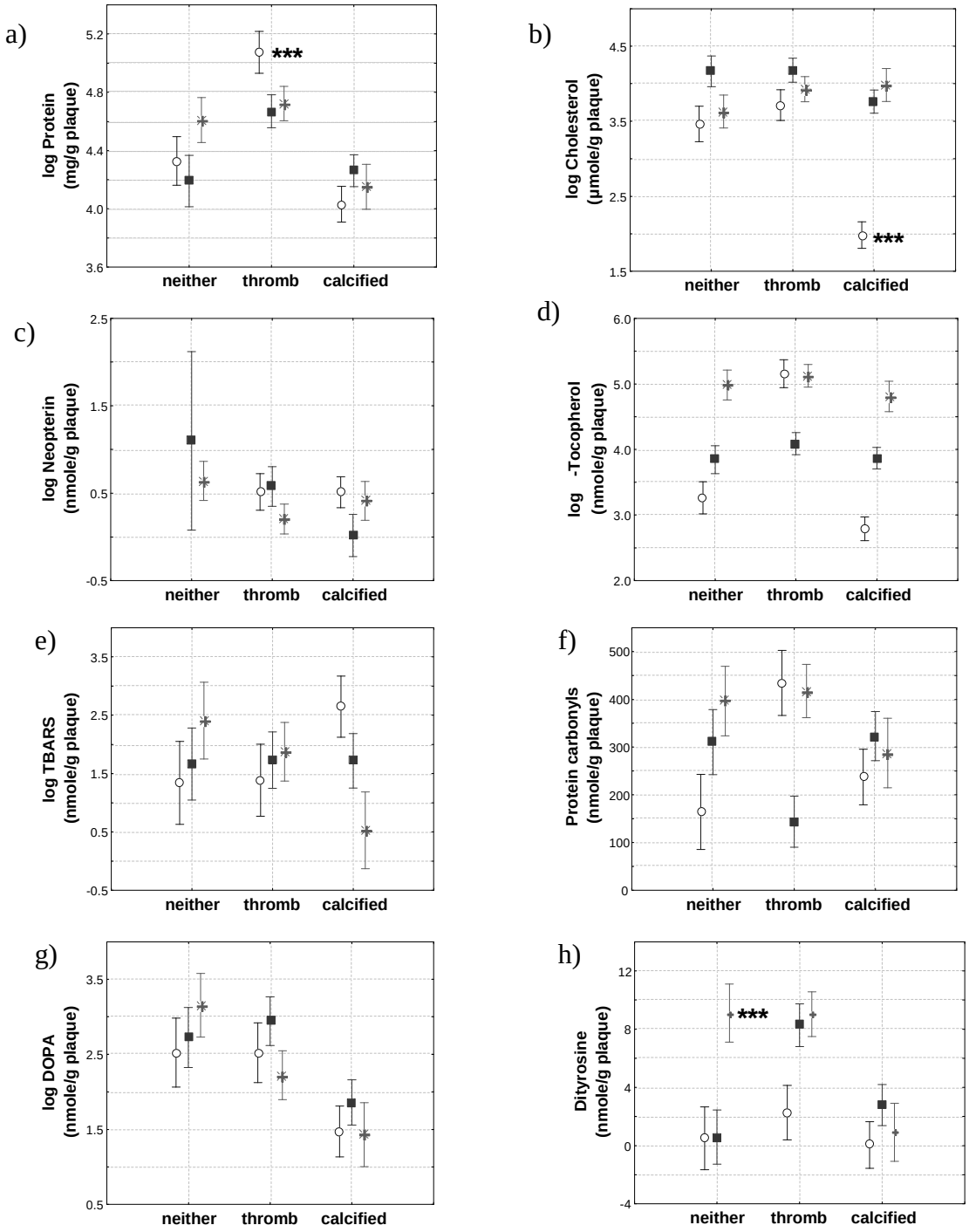

Figure 3.1.19 Interactions of overall composition and overall morphology of plaques in the concentration of the inflammatory and oxidative markers between plaques A-N

Plaques A-N were classified by composition as either calcified (n=5), thrombosed (thromb) (n=5) or neither (n=3) as well overall morphology as either Y shaped (✳) (n=4), small secondary branch (■) (n=5) or linear (○) (n=4). Factorial-ANOVA was performed on the data (as described in section 2.3) to identify any interactions towards protein (a), cholesterol (b), neopterin (c), α-tocopherol (d), TBARS (e), protein carbonyls (f), DOPA (g) and dityrosine (g) concentrations. Displayed are the LS means and vertical bars represent 95% confidence intervals. For neopterin only plaques A-E and K-N were analysed. Significant differences represented P<0.05*, P<0.01**, P<0.001*** to all other points, except dityrosine top three points significant to all but each other.

associated with stroke and TIA events and again within the AF and asymptomatic plaques where the AF and asymptomatic groups had significantly higher levels than the stroke and AF groups. This was not the case for the other markers.

Following the above mentioned trend the protein concentration was higher in the plaques that induced AF and asymptomatic events (Figure 3.1.20a). The cholesterol appeared to be influenced by the morphology of the plaque where the small branched plaques had the highest level of cholesterol, the linear plaques the lowest and the Y shaped plaques in between (Figure 3.1.20b). Due to the smaller sample size for neopterin analysis (N=9) the neopterin only differed between the plaques that induced TIA and AF events which are both Y shaped plaques. Otherwise the neopterin was consistent between the symptoms (Figure 3.1.20c). The antioxidant α-tocopherol followed the same trend as protein with high levels in the TIA and asymptomatic plaques (Figure 3.1.20d). To some extent the protein carbonyl concentrations also followed this trend where the highest levels of protein carbonyls occurred in the AF and asymptomatic plaques (Figure 3.1.20f). The dityrosine had the highest levels in the AF plaques compared to the linear and small branched inducing TIA plaques (Figure 3.1.20h). TBARS and DOPA showed no variation within the markers when the morphology and symptoms suffered were taken into consideration (Figure 3.1.20e,g).

The small branched plaques showed no difference when categorised as either stroke or TIA inducing plauques, except with dityrosine (Figure 3.1.20h). The Y shaped plaques again showed no difference in the concentration of markers between the TIA and AF inducing plaques. This was true except for neopterin and dityrosine, where the TIA inducing plaques had higher neopterin and the AF inducing had higher dityrosine. The linear plaques differed only in the protein, α-tocopherol and protein carbonyls concentrations which were higher in the asymptomatic plaque compared to the plaques that induced TIA events.

Overall, the trends observed indicate that the concentration of the protein, α-tocopherol and protein carbonyls had a correlation with the symptoms suffered. When the plaques were further categorised to the morphology of the plaque the symptoms suffered did not have a role in the concentration of the markers. The major exception to that was dityrosine and protein (Figure 3.1.20a,h).

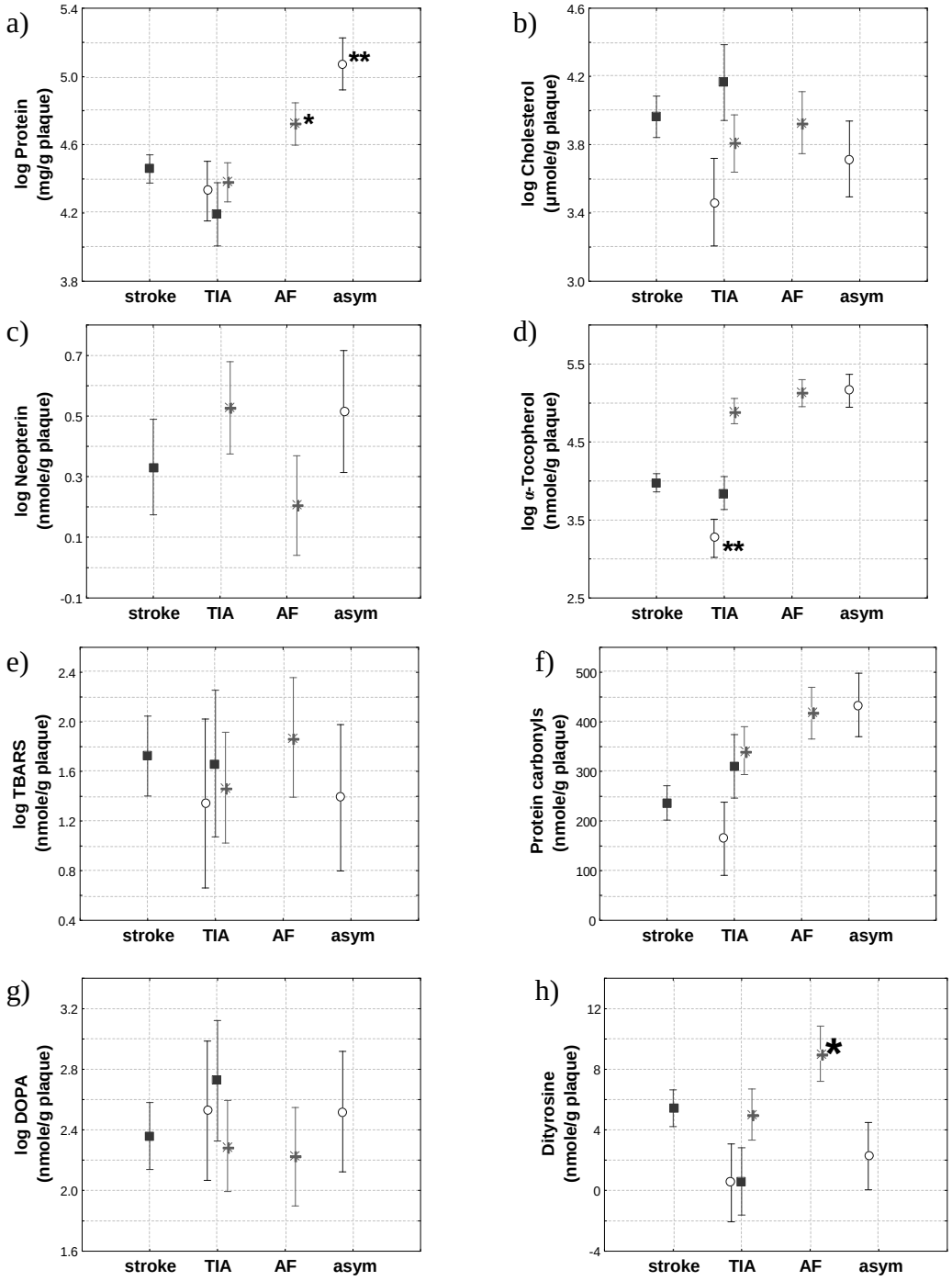

Figure 3.1.20 Interactions between symptoms presented and plaque morphology to the variation of inflammatory and oxidative marker concentrations between plaques C-N

Plaques A-N induced either stroke (n=4), transient ischemic attack (TIA) (n=4), amaurosis fugax (AF) (n=2) events or were asymptomatic (asym) (n=1). Plaques were either Y shaped (✳) (n=4), small secondary branch (■) (n=5) or linear (○) (n=2) in morphology. Factorial-ANOVA was performed on data (as described in section 2.3) to identify any interactions in terms of protein (a), cholesterol (b), neopterin (c) α-tocopherol (d), TBARS (e), protein carbonyls (f), DOPA (g), and dityrosine (h) concentrations. Displayed are the LS means and vertical bars represent 95% confidence intervals. For neopterin only plaques A-E and K-N were analysed. Significant differences represented by P<0.05*, P<0.01** and P<0.001***

3.1.8.6 Interaction between patient medication and symptom presented

All patients have been on medication for a relatively long period (excluding the asymptomatic patient). Aspirin is taken as an anti-inflammatory and statin as a lipid lowering drug (Chapman et al. 2007). Therefore the combination of these drugs may influence the processes occurring within the plaque feeding on the plaque morphology and possibly the symptoms the patient may later present. Therefore a factorial-ANOVA was performed to see if the drug combination and symptoms presented by the patient could explain some of the variations between these plaques.

In the four patients on aspirin alone, the AF plaques had higher protein, α-tocopherol and TBARS content (Figure 3.1.21). The TIA plaques had lower cholesterol and higher neopterin, and the stroke suffers had lower cholesterol, neopterin and dityrosine. This was similar for the six patients on both aspirin and statins, the AF suffers have higher α-tocopherol and protein carbonyls. The TIA suffers had lower TBARS and dityrosine and the stroke suffers had no significant variation between the markers.

In other words, the stroke inducing plaques exposed to both aspirin and statins have higher cholesterol, dityrosine and DOPA, than the aspirin alone exposed plaques. The TIA plaques had no significant difference between medication treatments. The AF plaques differ in that the statin and aspirin exposed plaques had higher neopterin and lower TBARS compared to the aspirin alone exposed plaque which had the opposite relationship.

3.1.8.7 Combined plaque analysis summary

In this analysis the zoning and overall composition of the plaques were the strongest predictors of the variation in marker concentration across and between the plaques respectively. When two factors were considered in combination the trends, if any, were weak possibly due to the small sample size. In the overall composition and morphology analysis both factors only appeared to affect the concentration of cholesterol in the linear calcified plaques, dityrosine within the neither Y shaped and linear thrombosed plaques, the protein carbonyls in the small branched thrombosed plaques and the α-tocopherol in the linear thrombosed plaques. In the symptoms and morphology analysis there were no distinct variations between the plaques. In the symptoms and medication

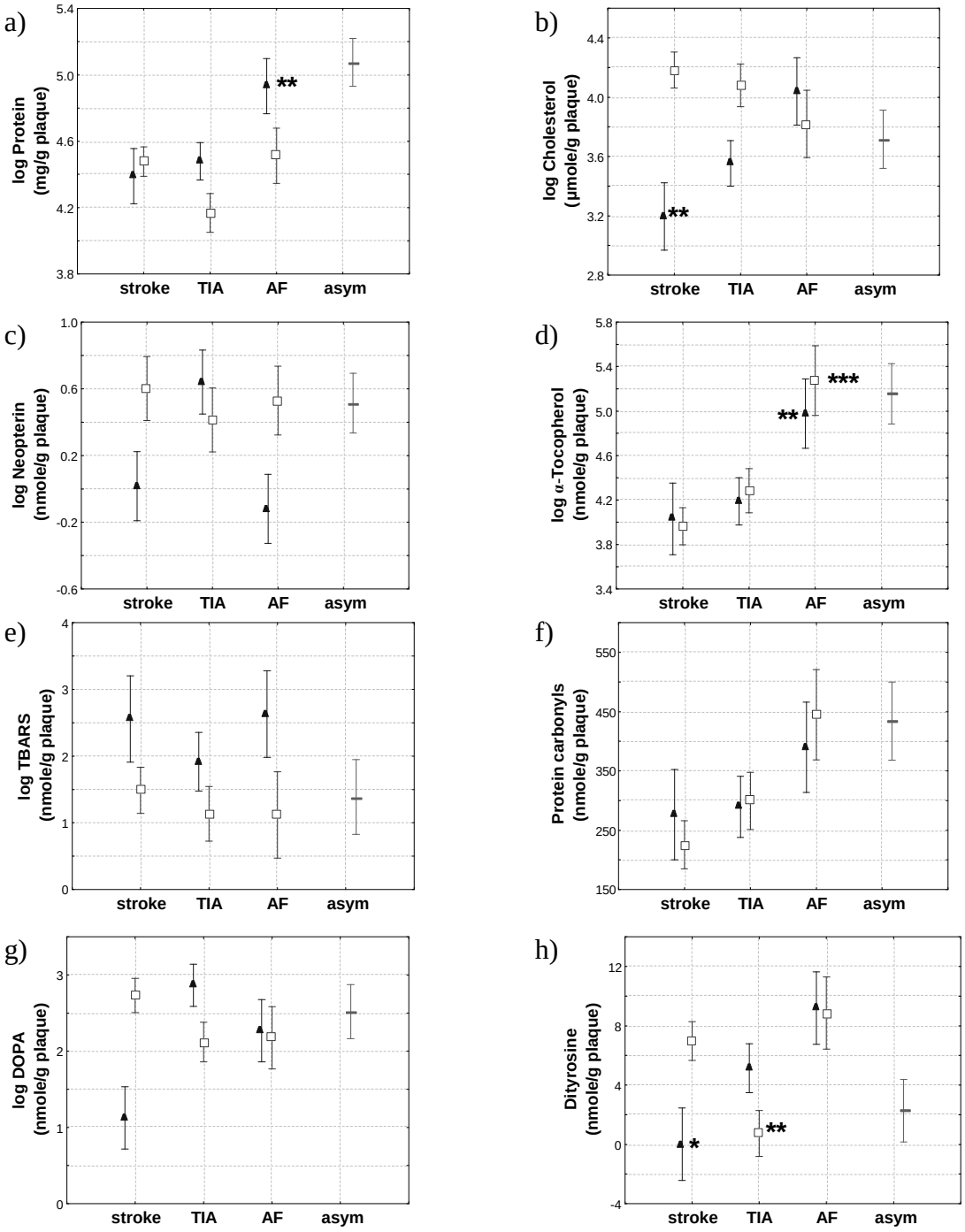

Figure 3.1.21 Interactions of symptoms presented and medication in the variation of the inflammatory and oxidative marker concentrations between plaques C-N

Symptoms induced by plaques A-N were either stroke (n=4), transient ischemic attack (TIA) (n=4), amaurosis fugax (AF) (n=2) or asymptomatic (n=1). Medication included aspirins only (▲) (n=4) statins and aspirin (○) (n=6) or neither (—) (n=1). Factorial-ANOVA was performed data (as described in section 2.3) to identify any interactions based on the concentration of protein (a), cholesterol (b), neopterin (c) α-tocopherol (d), TBARS (e), protein carbonyls (f), DOPA (g), and dityrosine (h). Display are the LS means and vertical bars represent 95 % confidence intervals. For neopterin analysis only plaques A-E and K-N were included. Significant differences represented by P<0.05*, P<0.01** and P<0.001***

analysis these factors combined only affected the concentration of protein within the aspirin alone AF plaque, the neopterin aspirin alone TIA plaques and the DOPA and dityrosine in the aspirin alone stroke plaque. Many of these categories represent one to two plaques therefore other factors that influence each particular plaque may influence the variation observed and not observed within these analyses.

3.2 Investigating assays and additional markers for detection within atherosclerotic plaques

3.2.1 Neopterin and 7,8-dihydroneopterin assay

The pterin assay was recently improved by using acetonitrile for the induction of protein precipitate within samples compared to trichloroacetic acid (Flavall et al., 2008). The change in solvent allows a greater detection of neopterin within both plasma and plaque. The pterin assay is able to quantify both neopterin and 7,8-dihydroneopterin (7,8-NP). 7,8-NP itself has little to no fluorescence therefore it is quantified by it's oxidation to neopterin (section 2.2.4 A), creating a total neopterin concentration. The 7,8-NP is calculated by subtracting the neopterin concentration from the total neopterin level. Within plaque samples there was no significant difference between the concentration of neopterin compared to total neopterin, indicating there is no 7,8-NP present in the plaques. 7,8-NP is quite labile therefore to ensure this was an accurate result and not due to loss of 7,8-NP during preparation, the acidic iodide, pH levels and presence of endogenous free iron were investigated. It was already established within our laboratory that the ascorbate was not interfering with the detection of the total neopterin.

The oxidation of 7,8-NP to neopterin is induced by the IO_3^- in the acidic iodide solution (5.4% I_2, 10.8% KI in 1 M HCl). To determine if the molarity of the HCl in the acidic iodide solution was affecting the ability to detect 7,8-NP, the concentration of HCl in the acidic iodide was altered to non-acidic (no HCl) and 0.5 M. The concentration of neopterin in healthy plasma was 25.4 ± 2.1 nM and using the non-acidic iodide the total neopterin was significantly high ($P<0.05$) detecting 7,8-NP at a concentration of 10.1 ± 2.3 nM (Figure 3.2.1 a). The concentrations and ratio of neopterin to 7,8-NP agrees with previously reported levels in healthy plasma (Flavall et al. 2008)

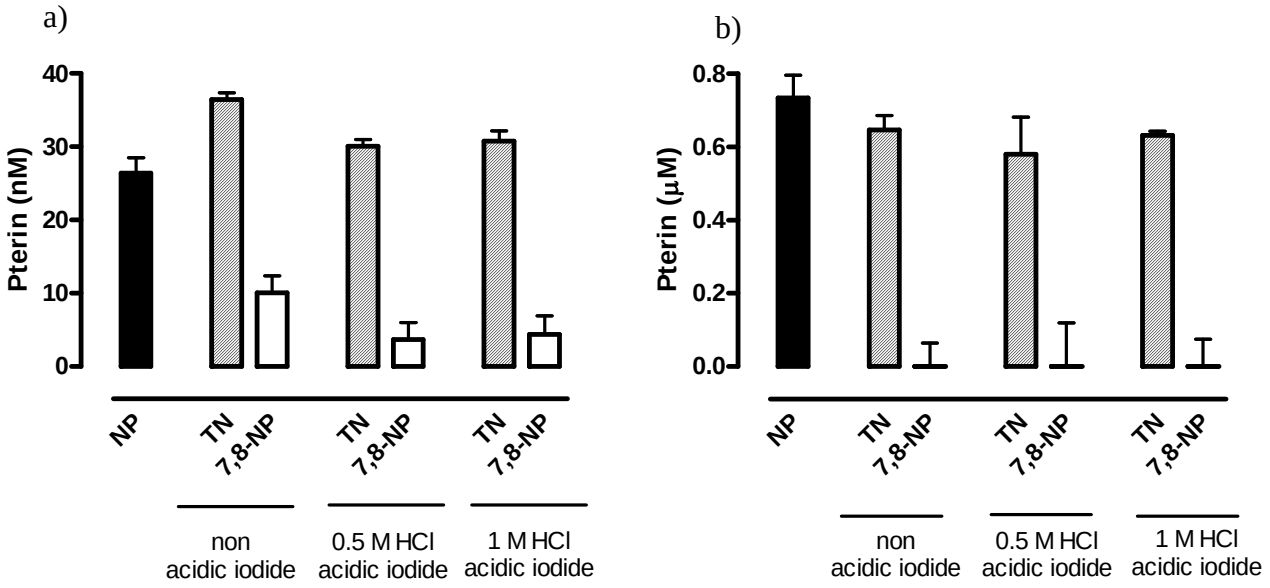

Figure 3.2.1 Effect of HCl molarity in acidic iodide solutions on the detection of 7,8-dihydroneopterin within plasma and plaque
The concentration of neopterin (NP) and total neopterin (TN) in plasma (a) and plaque (b) treated with different acidic iodide solution. Each bar represents the mean ± SEM of duplicate samples.

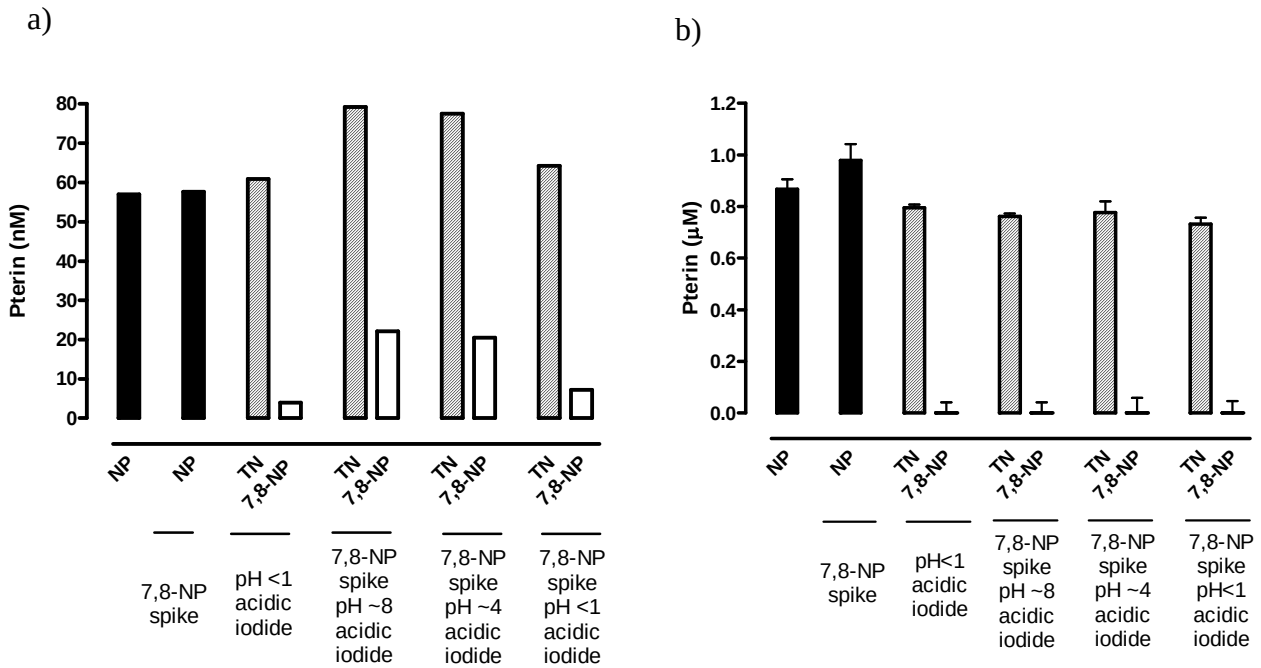

Figure 3.2.2 Effect acidic iodide pH on the ability to detect 7,8-dihydroneopterin spikes in plasma and plaque
Neopterin (NP), total neopterin (TN) and 7,8-dihydroneopterin (7,8-NP) concentrations were measured in plasma and plaque E. Spiked samples contained an additional 20 nM 7,8-NP. Each bar represents mean ± SEM of duplicate samples.

The total neopterin values from the 0.5 M and 1 M HCl acidic iodide solutions were statistically the same as neopterin, detecting 7,8-NP concentrations at 3.4 ± 2.3 nM and 4.4 ± 2.6 nM respectively. Plaque F neopterin levels were the same as previously determined (Figure 3.2.1 b) (section 3.1.6), and the neopterin versus total neopterin concentrations for all acidic iodide treatments were statistically the same. This suggests that the molarity of HCl in the acidic iodide solutions tested were not responsible for the lack of 7,8-NP detected within the plaques.

The molarity of HCl had an effect on the plasma measurements, but not on the plaque, therefore the pH of the acidic iodide was investigated. The pH values were adjusted to an alkaline pH range ~8, slightly acidic pH range ~4 and acidic iodide pH<1. To ensure there was 7,8-NP present within the plasma and plaque to detect the samples were spiked with 20 nM 7,8-NP. Within plasma 91.1% and 82.7% of the 20 nM 7,8-NP spike was returned after treatment with the pH~8 and pH~4 iodide solutions respectively (Figure 3.2.2a). The pH<1 acidic iodide solution only returned 16.5% of the 20 nM 7,8-NP spike from plasma. Within the plaque all three acidic iodides failed to detect the 7,8-NP spike.

Plaques are considered a highly oxidative environment (Smith et al., 1992), and a component within the plaque that maybe facilitate this is the presence of free iron at high concentrations. The iron maybe able to convert the 7,8-NP to 7,8-dihydroxanthopterin via Fenton reactions (section 1.2). This would underestimate the true concentration of 7,8-NP within the sample. To remove the iron an iron chelator, deferoxamine was added to 7,8-NP spiked plaque samples above a concentration reported to almost completely inhibit deoxyribose degradation in the presence of plaque gruel (Smith et al., 1992).

The concentration of neopterin and total neopterin in plaque F was the same in the absence and presence of 200 μM DFO, indicating that the DFO was not interfering with the neopterin detection or concentration (Figure 3.2.3). To ensure there was sufficient 7,8-NP present within the plaque to detect, the samples were spiked with 11 μM 7,8-NP. Because 1-2 μM was detected with plaques this was considered a more physiologically relevant concentration compared to the 20 nM 7,8-NP spike in the previous experiment. The neopterin concentration within the 7,8-NP spike samples was double that of neopterin in the control samples because 7,8-NP has a low level of fluorescence (Figure 3.2.3). Within the 7,8-NP spiked samples the acidic iodide (1 M HCl), returned 51% of the

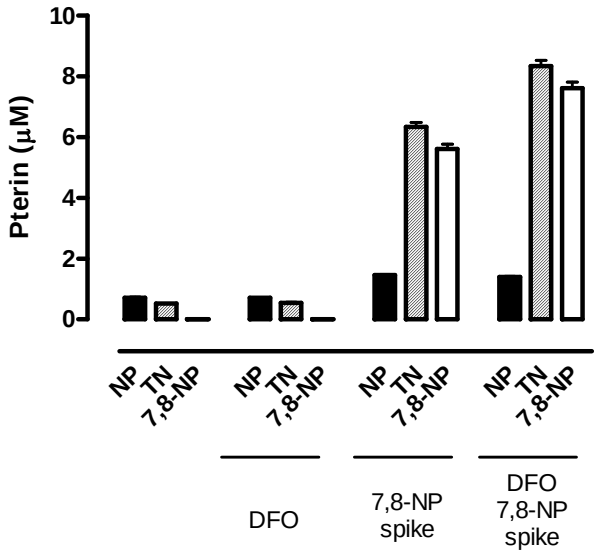

Figure 3.2.3 Effect of deferoxamine on the ability to detect neopterin and 7,8-dihyroneopterin in plaque samples
Neopterin (NP) and total neopterin (TN) concentrations were measured in plaque F samples in the presence or absence of 200 μM deferoxamine and/or 11 μM 7,8-NP. Each bar represents mean ± SEM of triplicate samples.

added 7,8-NP. Within the DFO and spiked treated samples 69.2% of the 7,8-NP was detected. This was a significant increase however it is still underestimating the concentration of 7,8-NP spiked within the plaque homogenate.

3.2.2 Simultaneous quantification of 7-ketocholesterol and α-tocopherol

The oxysterol 7-ketocholesterol (7-KC) is one of the three oxysterols detected in oxLDL and plaque that is known to exert cytotoxic properties, along with 25- and 27-hydroxyl cholesterols (Stocker and Keaney, 2004). OxLDL is cytotoxic to cells and our laboratory has found that different batches of oxLDL induce variable LD_{50} towards U-937 cells and human monocyte derived macrophages. The concentration of 7-KC in oxLDL may have an influential role in determining the potency and therefore the toxicity towards these cells. Because 7-KC is cytotoxic to vascular cells (Larsson et al., 2006) it may play a role in the death of macrophages, SMC and endothelial cells within the plaque. Future work on plaques will include the measurement of 7-KC within the sections. This will provide information on its quantity and spatial localisation across the plaques therefore possible interactions with lipid hydroperoxides, protein oxidation, α-tocopherol and neopterin.

The original method (Kritharides et al., 1993) was modified within our laboratory for the determination of conjugated ester dienes in combination with α-tocopherol in human plasma exposed to peroxyl radicals (Osborn, 2006). Here the same method was applied for the detection of 7-KC and α-tocopherol. An advantage to this assay is it simultaneously determines the concentration of 7-KC and α-tocopherol (section 2.2.5B) therefore may replace the original α-tocopherol assay for plaque analysis (section 2.2.4B), and at the same time provide additional information on the occurrence of lipid oxidation therefore reducing the amount of sample required for analysis.

The 7-ketocholesterol (7-KC) content measured within LDL (Figure 3.2.4) is in agreement with concentrations reported by Steffen et al. (2006) and Chang et al. (1997) (Table 3.2.1). The 7-KC

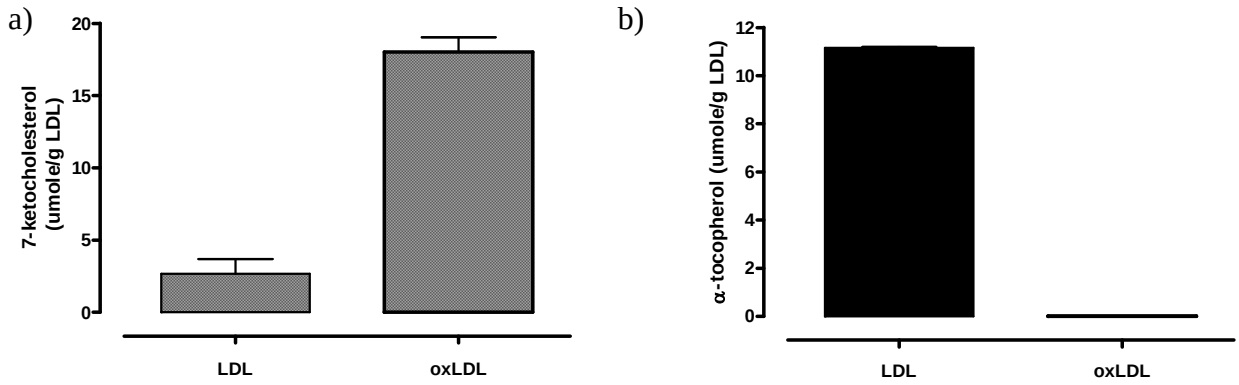

Figure 3.2.4 7-Ketocholesterol and α-tocopherol content in LDL and oxLDL
The 7-ketocholesterol (a) and α-tocopherol (b) were measured by the 7-KC method in 1 mg/mL of LDL and oxLDL prepared from the same batch. Each bar represents the mean ± SEM of triplicate samples.

Table 3.2.1 7-Ketocholesterol content in LDL and copper mediated oxidised LDL

LDL (µmole/g LDL)	Cu^{2+} incubation time (hours)	oxLDL (µmole/g LDL)	Reference
2.68 ± 1.01	24	18.00 ± 1.02	This study
2.37 ± 1.26*	3.33	35.14 ± 5.29*	Steffen et al. (2006)
2.93 ± 0.59§	3.33	15.4 ± 2.20§	Chang et al. (1997)

* Values calculated based on 31.64% of LDL is cholesterol (Esterbauer et al., 1992)
§ Values calculated based on 22% of LDL is protein (Esterbauer et al., 1992) and oxLDL measurement read off graph

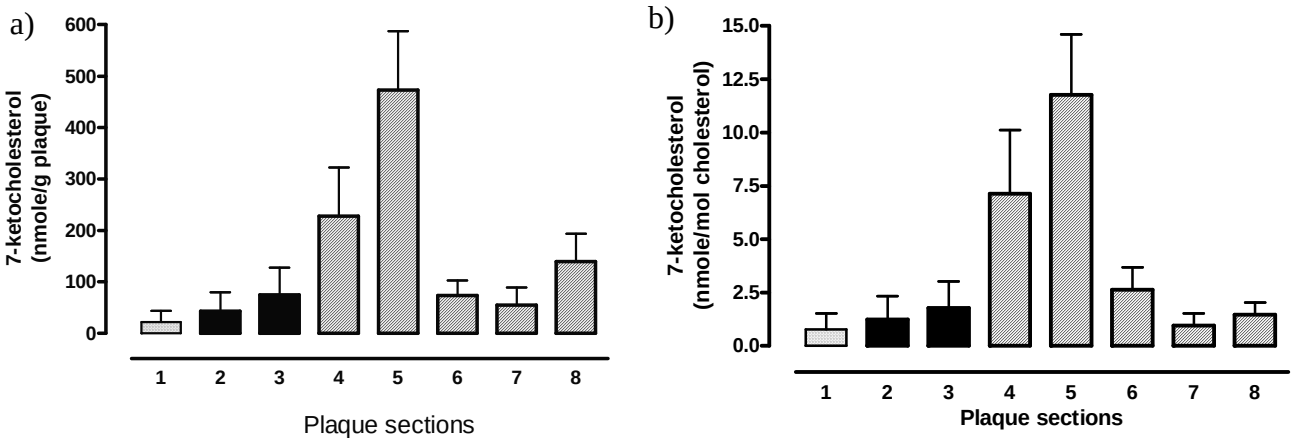

Figure 3.2.5 7-Ketocholesterol content within plaque E determined by the 7-ketocholesterol/α-tocopherol assay
The 7-ketocholesterol concentration per gram of plaque (a) and per mole of cholesterol (b) were measured by reverse phase-HPLC with a mobile phase of 54 isopropanol: 44 acetonitrile: 2 water. The dotted bar represents the pre-bifurcation zone, the solid bars represent the bifurcation zone and the stripped bars represents the pos-bifurcation zone. Each bar represents the mean ± SEM of triplicate samples.

concentration increased 7-fold after 24 hours incubation with copper ions (Figure 3.2.4a). The 7-KC concentration was in the same magnitude as reported by Steffen et al. (2006) and Chang et al. (1997). As was expected and previously reported (Esterbauer et al. 1992) the α-tocopherol content declined from 11.2 ± 0.047 μmole/g of LDL to almost zero within the oxLDL after incubation with copper (Figure 3.2.4b). The 7-KC concentration within plaque F was 136.7 ± 11.5 nmole/g of plaque. Within plaque E the average 7-KC concentration was 138.4 ± 54.8 nmole/g of plaque, with the maximum level detected within section 5, a post bifurcation section ($P<0.01$) (Figure 3.2.5).

Comparing the α-tocopherol concentration in plaque E detected by the original α-tocopherol and the 7-KC/α-tocopherol method (Figure 3.2.6), the concentrations in each corresponding section were on average 53% lower using the 7-KC/α-tocopherol method. Correlation between the two methods produced a linear regression value of $r^2=0.9183$ (Figure 3.2.6c) therefore the trend across the plaque for both methods is highly similar. This suggests a problem with the α-tocopherol solubility in the 7-KC/α-tocopherol mobile phase.

The 7-KC/α-tocopherol mobile phase consisted of 54 isopropanol: 44 acetonitrile: 2 water therefore had a polar solvent component compared to methanol, a non-polar mobile phase used for the

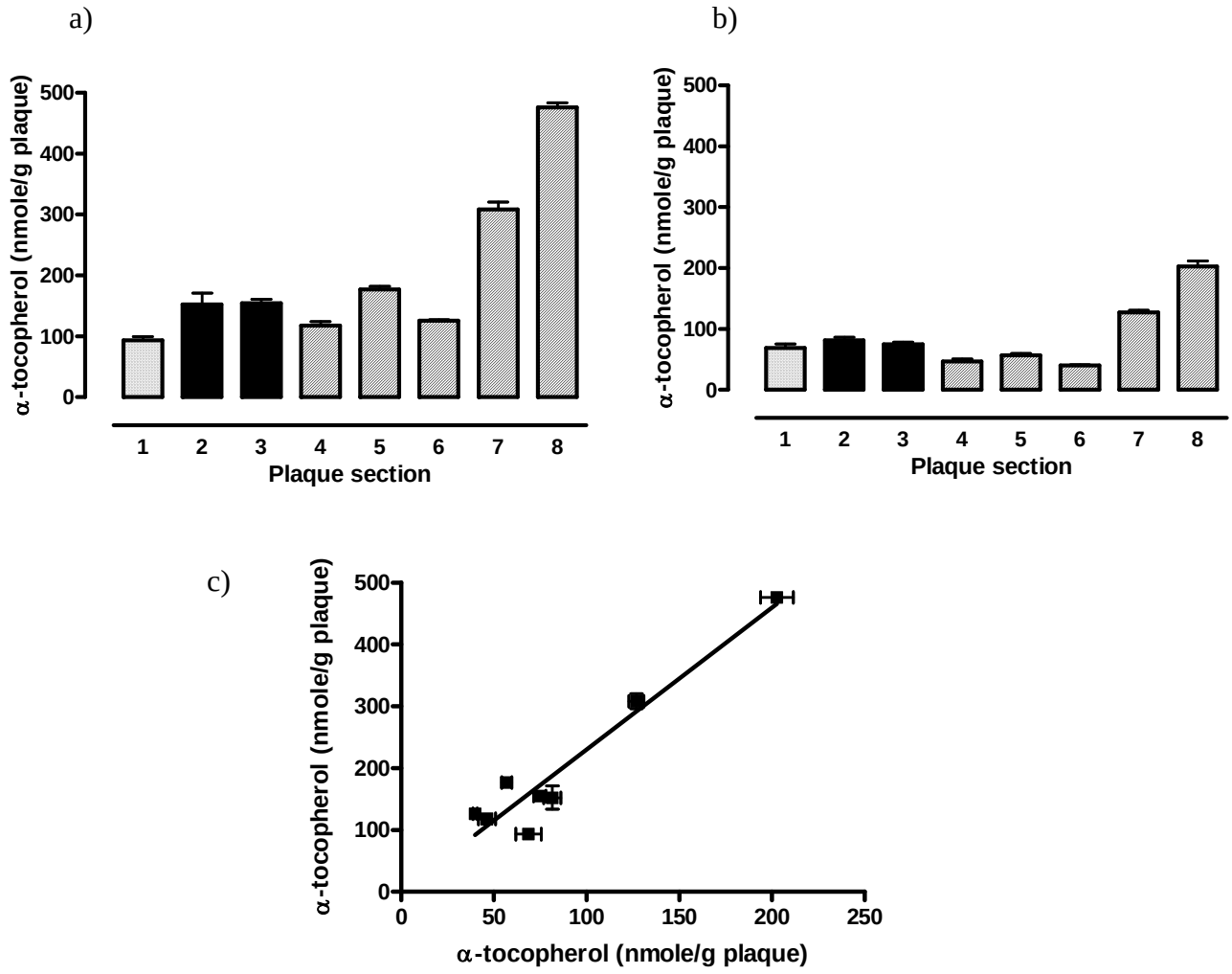

Figure 3.2.6 Comparison between the original α-tocopherol and the 7-ketocholesterol/α-tocopherol assay in the determination of α-tocopherol content within plaque E
The α-tocopherol content determined by the original α-tocopherol (a) and the 7-ketocholesterol/α-tocopherol (b) methods within plaque E, and the correlation between the two methods (c). The dotted filled bar represents the bifurcation, solid filled the bifurcation and the stripped bars the post-bifurcation zone. Each bar represents the mean ± SEM of triplicate samples.

original α-tocopherol assay. To investigate this further the mobile phase was modified to a ratio of 50 isopropanol: 50 acetonitrile. For the sample preparation the original α- tocopherol method was followed up to the point of re-solubilising the residue in the appropriate mobile phase. The α-tocopherol concentration across the plaque was significantly higher with the 7-KC/α-tocopherol method using the 50 isopropanol: 50 acetonitrile mobile phase compared to the original α-tocopherol method (Figure 3.2.7a). The correlation between the two methods gave a linear

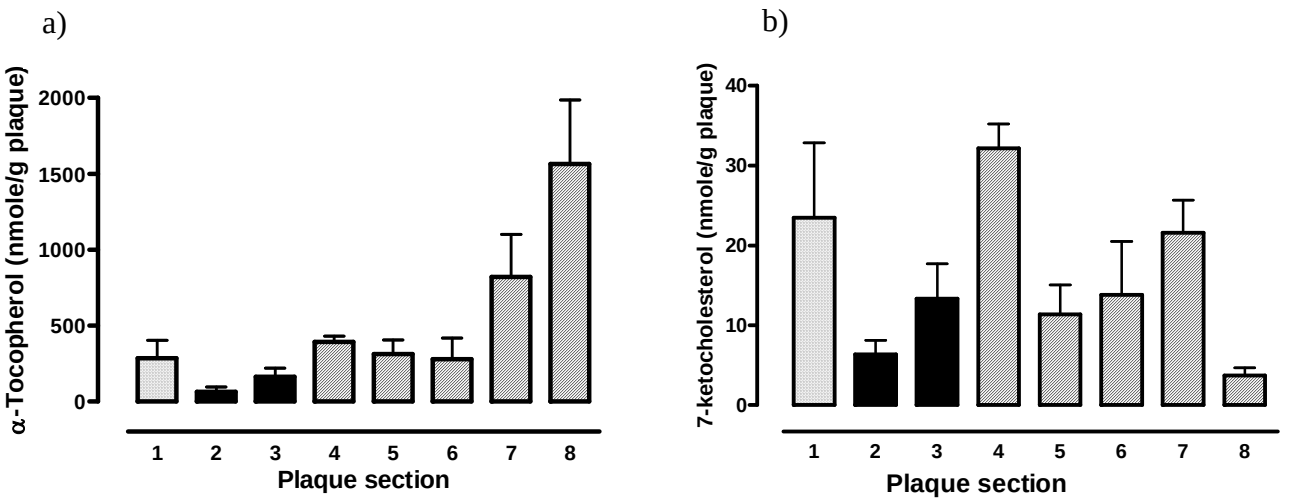

Figure 3.2.7 7-Ketocholesterol and α-tocopherol content within plaque E analysed using the 50 isopropanol: 50 acetonitrile mobile phase
7-Ketocholesterol (a) and α-tocopherol (b) content was determined using the modified 7-KC method. The mobile phase consisted of 50 isopropanol: 50 acetonitrile. The dotted bar represents the pre-bifurcation zone, the solid bars represent the bifurcation zone and the stripped bars represents the pos-bifurcation zone. Each bar represents the mean ± SEM of triplicate samples.

regression of r^2=0.8909 (graph not shown), again indicating the trend across the plaque was highly similar to the concentration detected with the original α-tocopherol method (Figure 3.2.6a). Opposite to α-tocopherol, the 7-KC levels detected using the 54 isopropanol: 44 acetonitrile: 2 water mobile phase compared to the 50 isopropanol: 50 acetonitrile mobile phase was significantly higher in the former mobile phase (Figure 3.2.7b). Furthermore, the error bars for the 7-ketocholesterol in both mobile phases were large (Figure 3.2.5a and 3.2.7b). This suggests a solubility issue for both α-tocopherol and 7-KC in the mobile phases.

3.2.3 Investigating the detection of AAS and GGS; a candidate for the replacement of the protein carbonyl assay

Currently our laboratory uses the well established 4-dinitrophenylhydrazine (DNPH) method for the detection of protein carbonyls (section 2.2.6 B). Using the DNPH method on plaque homogenate, a complex biological fluid, the standard errors within the triplicates are large, which may be masking any statistical differences in plaque sections within and between the plaques. For this reason a more accurate and reliable assay for protein carbonyls was investigated.

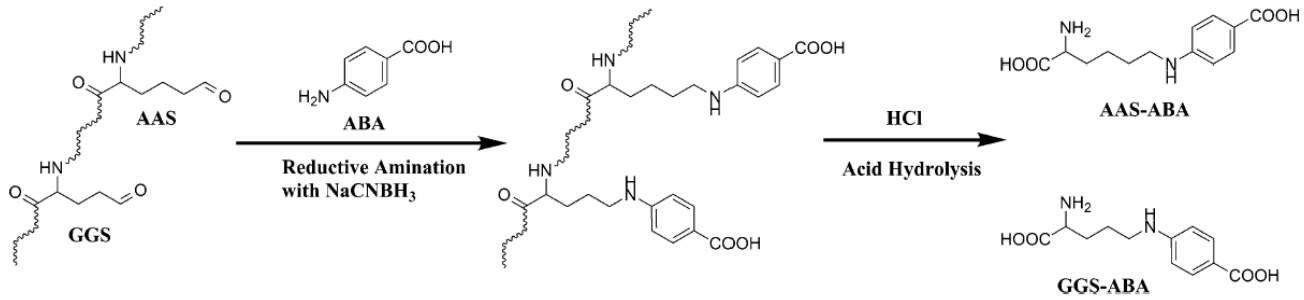

Figure 3.2.8 Derivatisation of the two main carbonyl oxidation products AAS and GGS
AAS and GGS putatively formed from free radical damage are reduced by sodium cyanoborohydride ($NaCNBH_3$) and conjugated to ABA. The derviatised protein undergoes acid hydrolysis to release the conjugates from the protein backbone and detected by reverse phase HPLC. Figure from Akagawa et al. (2006).

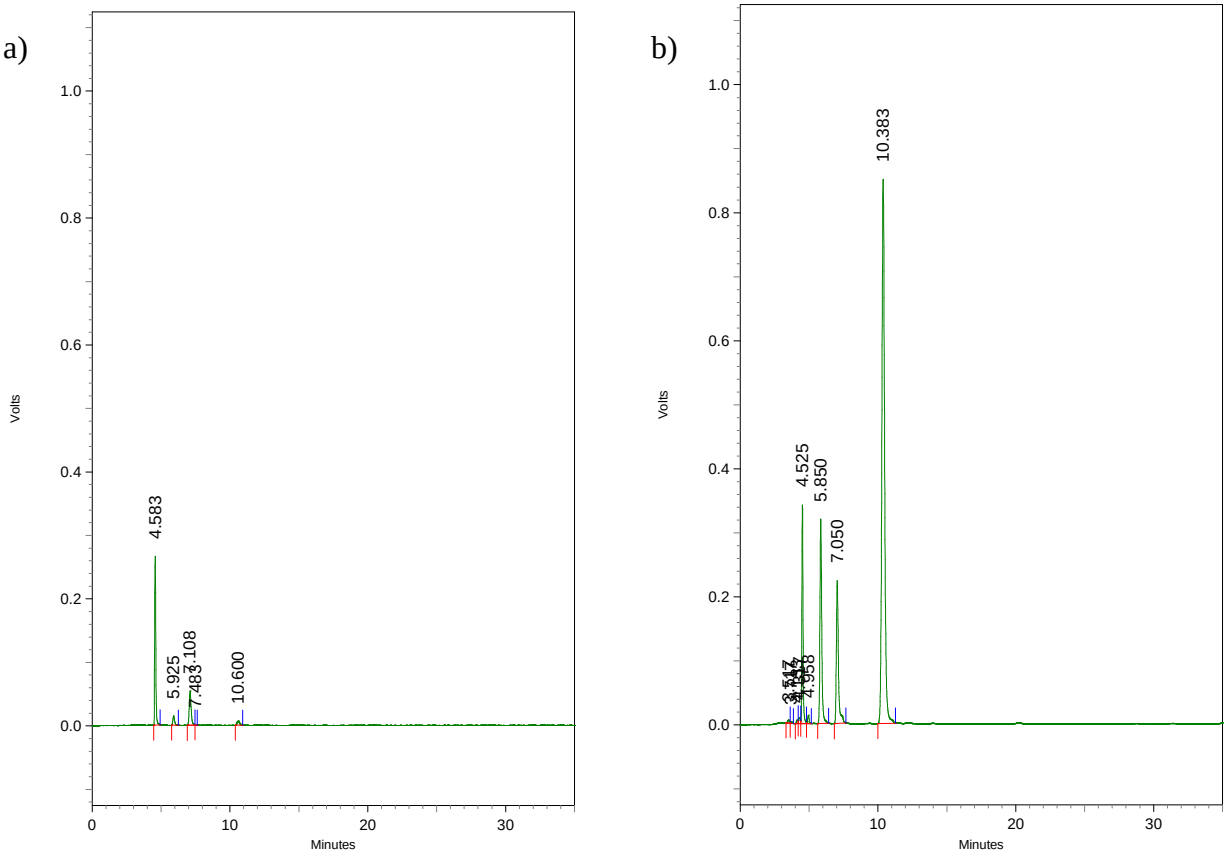

Figure 3.2.9 HPLC chromatagrams of AAS and GGS from BSA incubated with AAPH
2 mg/mL of BSA was incubated with 10 mM AAPH at 37º C and analysed using the modified HPLC method for the detection of AAS and GGS after zero hours (a) and 24 hours (b) incubation with AAPH. Peak one elutes within the 4th minute, peak two at the end of the 5th minute, peak three at the beginning of the 7th minute and peak four at the 10th minute.

Recently Akagawa et al. (2006) have developed a method which measures the two main oxidative products formed from protein carbonylation reactions via a highly sensitive HPLC method. This method detects the two main carbonyls derivatives α-aminoadipic semialdehyde (AAS) derived from lysine residues and γ-glutamic semialdehyde (GGS) derived from proline and arginine residues (Figure 3.2.8). To quantifiably detect AAS and GGS they are first converted to their corresponding hydroxyl amino acid using the mildly reducing agent sodium cyanoborohydride, before conjugating to the highly fluorescent aminobenzoic acid (ABA). Because ABA will react with any carbonyl moiety the oxidative products are retained within the protein backbone to avoid the derivatisation of the peptide skeletal carbonyls. The samples then undergo acid hydrolysis allowing the release of the AAS-ABA and GGS-ABA conjugates from the protein backbone. AAS-ABA and GGS-ABA are then separated via reverse phase HPLC and detected at an extinction and emission wavelengths of 283 and 350 nm respectively. Because these carbonyl moieties react with ABA in a one to one ratio the concentration of the AAS and GGS are quantified against a known concentration of ABA.

The assay was first investigated on a pure protein system, bovine serum albumin (BSA), and the AAS and GGS formation induced by the free radical initiator 2,2-azobis (2-aminopropane) dihydrochloride (AAPH). The chromatograms constantly produced four peaks with relatively consistent retention times of 4.5, 5.8-5.9, 7.0-7.1 and 10.1-10.6 minutes (Figure 3.2.9). Residual ABA elutes around the 7^{th} minute, confirmed by injecting a pure sample of ABA onto the HPLC system.

Taking into consideration the physical properties of AAS and GGS and as well as the properties of the HPLC column, the GGS-ABA is expected to elute first. It is highly unlikely that the first peak is either AAS-ABA or GGS-ABA, because even though the peak areas do vary across treatments they do not increase in relation to increased exposure time to AAPH nor with increased BSA concentration (data not shown). This leaves the second peak to be the GGS-ABA compound and the fourth peak to be AAS-ABA.

In BSA exposed to peroxyl radicals, the concentration of AAS and GGS increased 208 fold and 38 fold respectively over the 24 hour incubation period (Figure 3.2.10). The AAS concentration had

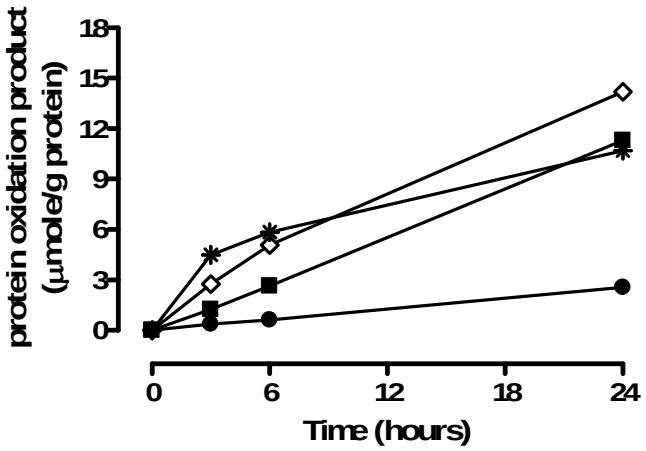

Figure 3.2.10 Concentration of AAS, GGS, protein carbonyls and protein hydroperoxides in BSA incubated with AAPH
2 mg/mL BSA was incubated with 10 mM AAPH at 37C and aliquots taken at the specified times and analysed for protein carbonyls (◇) by the DNPH method, the protein hydroperoxides (*) via the FOX assay and AAS (■) and GGS (●) by the modified HPLC method. Data was corrected against its corresponding zero time point and each time point represents mean ± SEM of triplicate samples.

significantly increased from the basal level by three hours ($P<0.001$) and the GGS had significantly increased after six hours ($P<0.01$) (Figure 3.2.10).

The modified HPLC carbonyl assay was compared to other protein oxidation methods including the FOX and the DNPH protein carbonyls assay on BSA (Figure 3.2.10). The FOX assay determines the concentration of PrOOH a protein modification similar to protein carbonyls (see section 3.3). In agreement with a previous study the basal levels of GGS were higher than AAS in BSA (Requena et al., 2001) with a concentration of 71.0 ± 6.8 and 54.7 ± 5.7 nmole/g protein respectively. The concentration of AAS, GGS and protein carbonyls had increased linearly after 24 hours incubation with AAPH (Figure 3.2.10). Initially the PrOOH had a faster rate of formation before slowing down after six hours. At time zero the AAS and GGS accounted for 6% of the protein carbonyls. This basal level was lower than Akagawa et al. (2006) reported at 23% and even lower than the 88% detected by Requena et al. (2001). With iron catalysed oxidation of BSA the AAS and GGS concentration increased, however the proportion of AAS and GGS to total protein carbonyls decreased from 88% to 51% (Requena et al. 2001). In this study after 24 hours exposure to peroxyl radicals 86% of the protein carbonyls was attributed to AAS and GGS. Between the protein carbonyls and AAS and GGS the linear regression was $r^2=0.9822$ and 0.9841 respectively. This

indicates that the rate of formation of AAS and GGS has a high agreement to the formation of the total protein carbonyls formed on BSA supporting that AAS and GGS are the two main protein carbonyl products. The linear regression between AAS and GGS was r^2=0.9990 also supporting that these two carbonyl derivatives form via similar kinetics.

The assay was also investigated on a biological system, human plasma. Small endogenous antioxidants were removed from the plasma by dialysis to increase the AAPH induced oxidation of the proteins (see section 3.3). After 12 hours both AAS and GGS increased by 126 nmole/g of protein a 9 and 4 fold increase of AAS and GGS respectively relative to the basal levels (Figure 3.2.11a,b).

Within plasma the rates of formation of AAS, GGS and PrOOH (Figure 3.2.11) were similar to that of BSA. The PrOOH concentration increased over the time period but displayed different rates of formation compared to AAS and GGS. The PrOOH concentration increased at a faster rate than AAS and GGS before starting to plateau after eight hours (Figure 3.2.11c). Opposite to this the AAS and GGS initially formed at a slower rate until the eight hour time point before increasing the rate of formation between eight and ten hours (Figure 3.2.11a,b).

Further comparisons were made between the DNPH method and the modified HPLC method on the whole plaque homogenate of plaque F (section 3.1.6). The AAS and GGS attributed to 42% of the protein carbonyls detected by the DNPH method (Table 3.2.2). This indicates that a large proportion of protein carbonyls are not one of these two semialdehydes. The standard error of the mean for protein carbonyls was 25 % of the mean value and for AAS and GGS it was 4 and 3% respectively. This is a considerable improvement to the error rate for the measurement of protein oxidation within this plaque.

Table 3.2.2 Protein carbonyl, AAS and GGS content in plaque F

	nmole/g protein*
Protein carbonyls	2791 ± 713
AAS	950 ± 41
GGS	225 ± 6

* mean ± SEM of triplicate samples

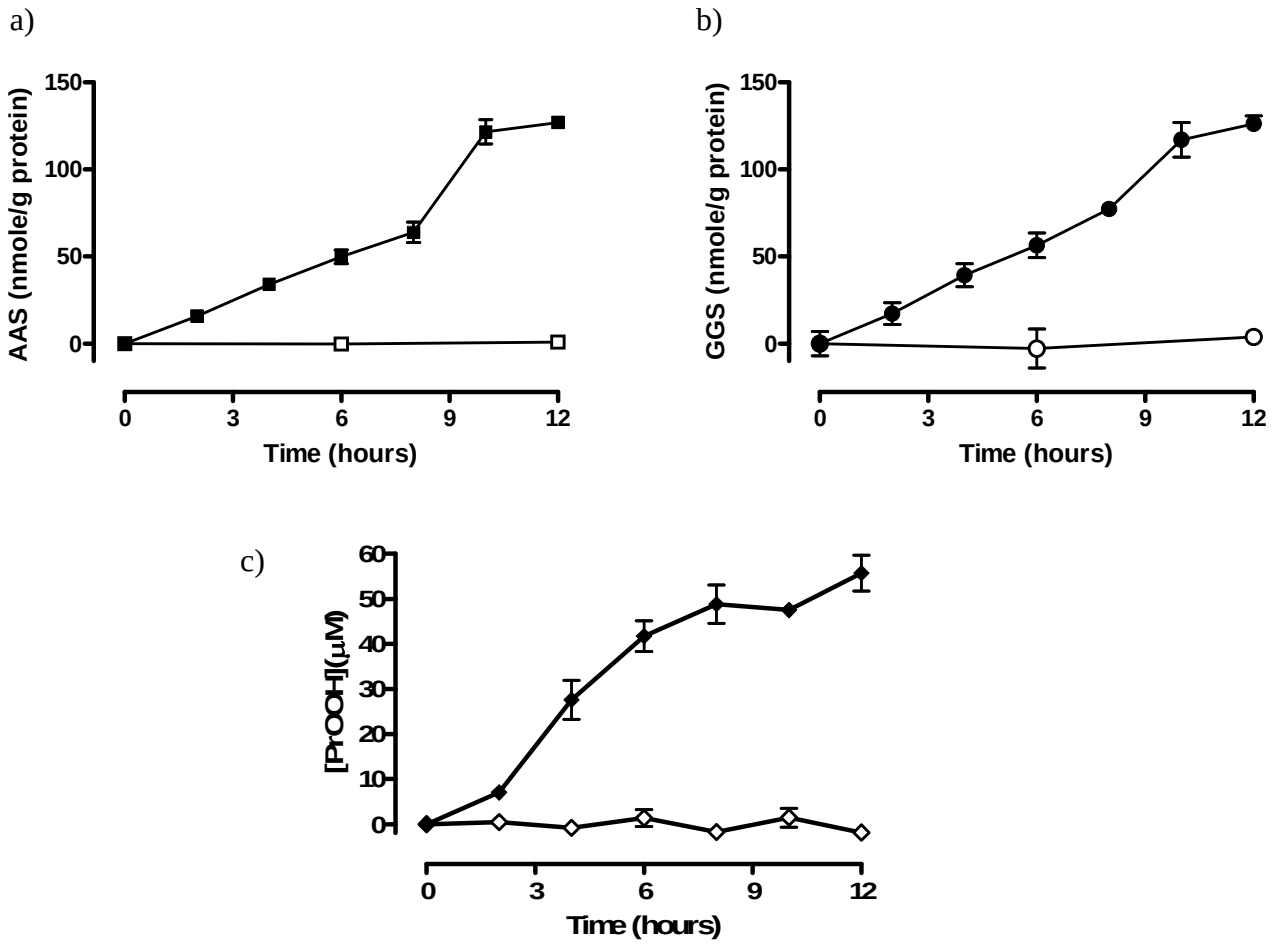

Figure 3.2.11 AAS, GGS and protein hydroperoxide formation in dialysed plasma incubated with AAPH

Dialysed plasma was incubated with AAPH at 37ºC (filled symbols) and without AAPH (open symbols) and aliquots were removed at specified time points and analysed for AAS (a) and GGS (b) by the modified HPLC method and protein hydroperoxide (PrOOH) (c) by the acetic acid FOX assay. Each data point was corrected against its corresponding zero time point. For AAS and GGS each point represents the mean ± SEM of duplicate samples and PrOOH triplicate samples.

3.2.4 Investigation of protein oxidation in human plasma

Protein oxidation is a key oxidative process within plaques and is linked to the oxidation of lipids and cell mediated death. To better understand the process and components involved in protein oxidation within the plaque, oxidation of plasma was investigated. Many of the antioxidants within plasma have been reported within plaque (Frei et al., 1988; Stocker and Keaney, 2004). Therefore, by investigating the mechanism and kinetics of protein hydroperoxidation formation within plasma

and the relationship of antioxidants to protein oxidation may provide a platform to elucidating the mechanisms involved in protein oxidation occurring within plaques.

Human plasma contains many antioxidants providing a defence against oxidative stress. These antioxidants include ascorbic acid, α-tocopherol, uric acid, bilirubin, albumin and protein thiols which are capable of scavenging the oxidants or breaking the chain to oxidative damage formation (Frei et al., 1988).

Under thermal decomposition AAPH forms peroxyl radicals and in the presence of BSA, a pure protein system, induces the formation of protein hydroperoxides (PrOOH) at an immediate and rapid rate (Figure 3.2.12). Human plasma exposed to peroxyl radicals produced a lag phase period before any significant protein hydroxide formation began (Figure 3.2.13a). A previous study (Yang, 2005) hypothesised that was due to protein thiol protective mechanism as the concentration of protein thiols reduced to almost zero before any significant PrOOH formation began. When plasma was dialysed it removed small molecular weight antioxidants and consequently when dialysed plasma was incubated with peroxyl radicals the lag phase was abolished (Figure 3.2.13b). In the

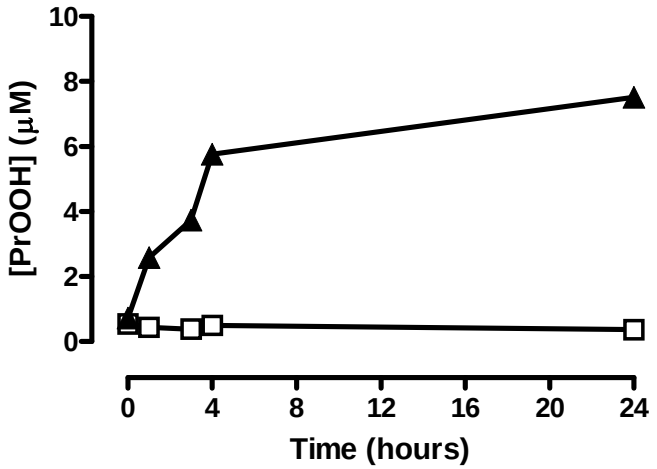

Figure 3.2.12 Protein hydroperoxide formation in BSA incubated with AAPH
2 mg/mL BSA was incubated with (▲) and without (□) 10 mM AAPH at 37ºC. Aliquots were taken at specified time points and PrOOH measured via the acetic acid FOX assay. Data was corrected against its corresponding zero time points and represents the mean ± SEM of triplicate samples.

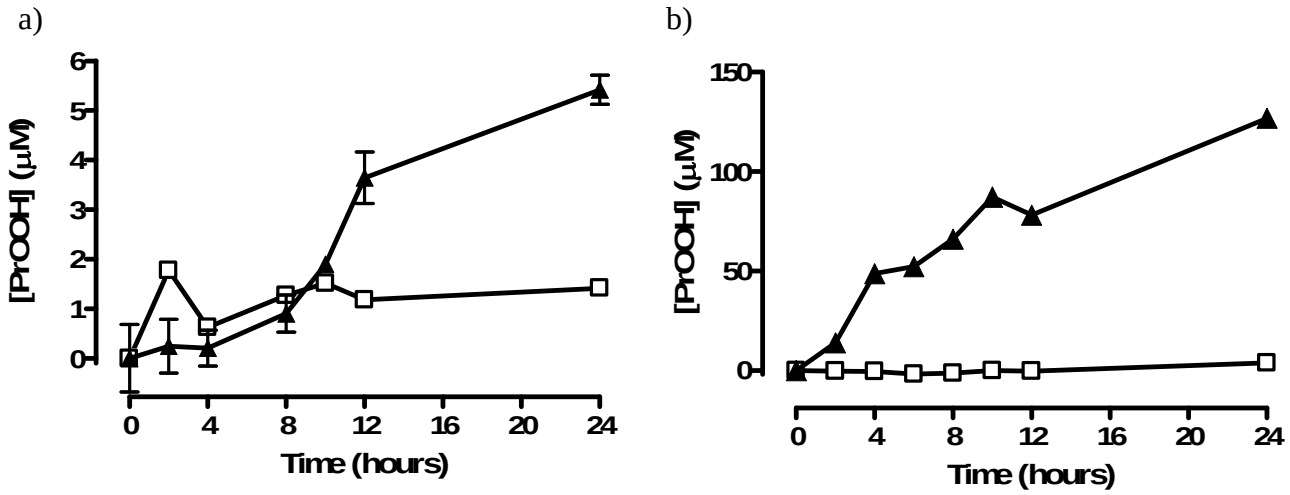

Figure 3.2.13 Protein hydroperoxide formation in plasma incubated with AAPH
Whole plasma (a) and dialysed plasma (b) where incubated with (▲) and without (□) 10 mM AAPH at 37ºC. Aliquots were taken at specified time points and analysed for PrOOH concentration using the acetic acid FOX assay. Data was corrected against its corresponding zero time point and represents the mean ± SEM of triplicate samples.

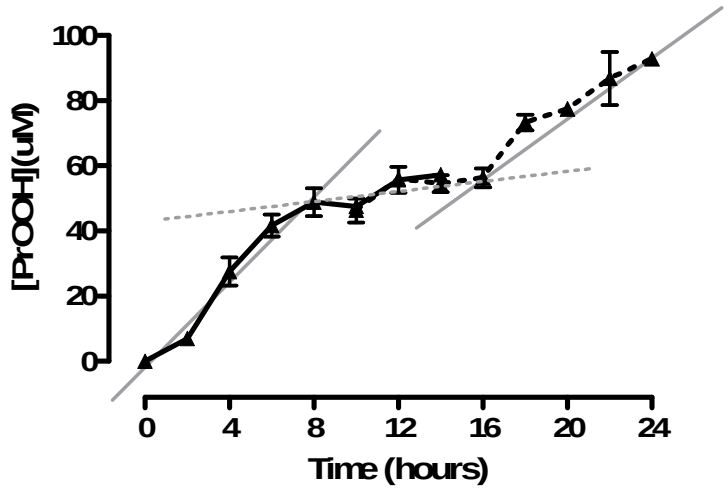

Figure 3.2.14 Protein hydroperoxide formation within dialysed plasma incubated with AAPH
Dialysed plasma was incubated with 10 mM AAPH at 37º C for 24 hours. Aliquots were taken at specified time points and PrOOH concentration determined by acetic acid FOX assay. Data was collated from two experiments, experiment a (solid black line) and experiment b (dashed black line). The grey solids line were times of rapid PrOOH formation and dashed grey stationary PrOOH concentration. Data was corrected against its corresponding zero time point and represents the mean ± SEM of triplicate samples.

dialysed plasma the protein thiol concentration and rate of loss was similar to the whole plasma indicating that the protein thiols are not responsible for this lag phase. The previous studies (Ling, 2003; Osborn, 2006; Yang, 2005) have found that a combination of uric acid, ascorbic acid and α-tocopherol are responsible for the initial lag phase (as seen in Figure 3.2.13a), as dialysed plasma supplement with physiological concentrations of uric and ascorbic acid re-establishes the lag phase observed within whole plasma.

Yang (2005) also identified a second lag phase occurring within dialysed plasma after 10-12 hours incubation with AAPH. Measuring the accumulation of PrOOH in dialysed plasma in two hour increments over 24 hours the initial lag phase was abolished as before and a second lag phase occurred beginning at eight hours and continuing until 16 hours (Figure 3.2.14), confirming the presence of the latter lag phase. The PrOOH formation began at a rate of 6.1 μmole/hour between zero and eight hours, plateauing between eight and 16 hours with a rate of 0.9 μmole/hour before increasing to a rate of 4.8 μmole/hour. Because the plasma was dialysed it suggested the latter lag phase was due to the scavenging of high molecular weight protein/s, hypothesised to be either albumin or apolipoprotein. If these proteins were providing a protective effect then on a gel electrophoresis the intensity and/or position of the corresponding band would change with increasing exposure to AAPH. In plasma incubated without AAPH and at the zero time points of the plasma with AAPH, two bands are evident between the 45 and 36 kDa markers (Figure 3.2.15)

After four hours incubation the low sharper band of the two had disappeared or merged with the other higher molecular weight band (Figure 3.2.15). This indicates that the alteration to this protein was occurred early before the second lag phase and therefore most likely not associated with the second lag phase. Apolipoprotein B has a molecular weight of ~515 kDa larger than the gel can separate. There was no change to the level of human serum albumin (~71 kDa).

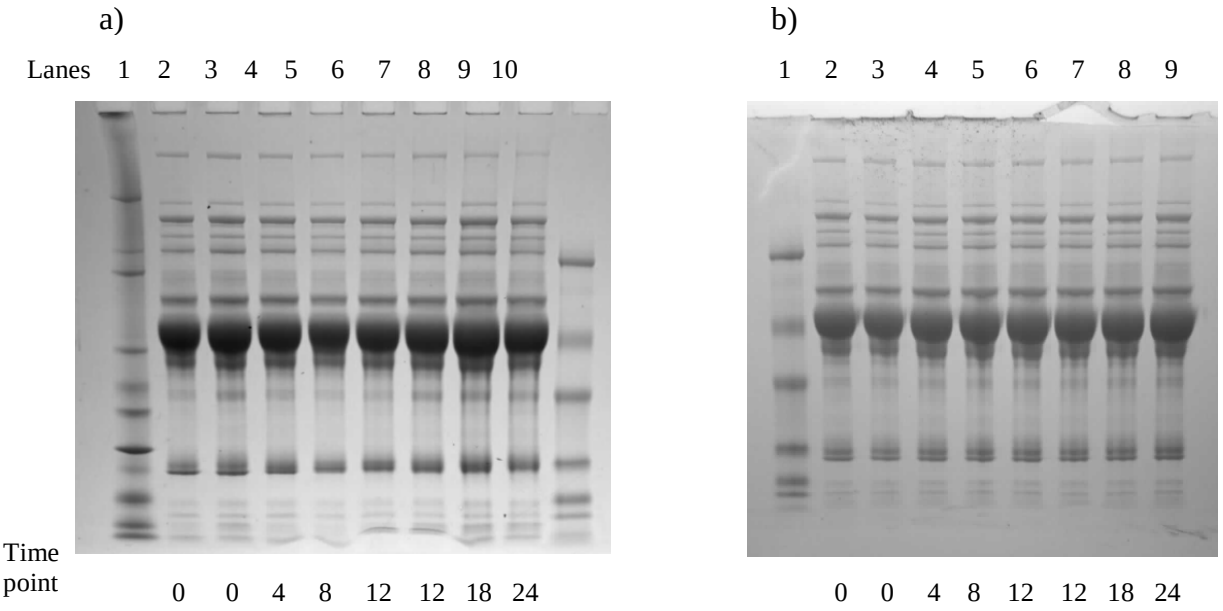

Figure 3.2.15 Gel electrophoresis of dialysed plasma incubated with and without AAPH
Dialysed plasma was incubated with (a) and without (b) 10 mM AAPH at 37ºC and aliquots were taken at specified time points and applied to gel electrophoresis. For both gels, lane 1 was loaded with a high range marker, lane 2 after zero hours incubation with AAPH (experiment a), lane 3 zero hours (experiment b), lane 4 four hours (experiment a), lane 5 eight hours (experiment a), lane 6 12 hours (experiment a), lane 7 12 hours (experiment b), lane 8 18 hours (experiment b), lane 9 24 hours (experiment b) and in the gel (a) lane 10 was a low range ladder. High range band sizes from top to bottom 205, 116, 97, 84, 66, 55, 45, 36, 29, 24 and 20 kDa bands. Low range band sizes from top to bottom 117, 85, 49, 34, 25 and 19 kDa.

Discussion

Cardiovascular disease, including atherosclerosis, is the major cause of morbidity and mortality within the developed world (Danilevicius et al., 2007; Helderman et al., 2007). There is no doubt that atherosclerotic plaque formation is a complex process involving multiple mechanisms. In the beginning of the plaque project it was hypothesised these plaques would have similar overall concentration of the markers as well as a similar spatial variation across the plaques. However, this is not the case. Evident through this study advanced atherosclerotic plaques are diverse in their biochemical composition. The plaques analysed have conclusively shown a lack of consistent correlations across the plaques (Table 3.1.7). For example only a significant correlation between α-tocopherol and cholesterol occurred twice within individual plaques (Plaques C and E). A variation in oxidative and inflammatory marker concentration was also observed in the overall concentrations between the plaques (Table I,II). For example the average overall cholesterol content within plaque F was 14 fold higher than within plaque B and the average overall dityrosine content within plaque J was 232 fold higher than in plaque A. Therefore the factors responsible for the concentration and spatial localisation of the markers measured within these plaques may be influenced by different mechanisms and/or combination of these mechanisms. If this holds true then these different factors which maybe influencing the initiation and progression of these plaques may also be driving different degrees and type of this disease as seen within the advanced state atherosclerotic plaques in this study.

Yet several significant correlations emerged between the markers within the combined plaque analysis that was not observed within individual plaques (Table 3.1.7). Furthermore the analysis between plaques zones (Figure 3.1.17) and between different overall plaque compositions (Figure 3.1.18) shows the concentration of the oxidative and inflammatory markers across and between the plaques have significant trends. These significant trends and correlations may exist because of the occurrence of common mechanism and/or influences on the concentration of the oxidative and inflammatory markers within the plaques. This suggests that even though the plaques individually are all different in their biochemical composition, there are potentially common features like that of zoning associated with shear stress and the overall plaque composition that have an influential role in the concentration of these markers within and across the plaques.

4.1 Comparison of the marker concentrations within atherosclerotic plaques to published literature

Except for neopterin, all of the markers quantified within this study have previously been quantified within atherosclerotic plaques (Adachi et al., 2007; Carpenter et al., 1995; Fu et al., 1998; Li et al., 2006; Nishi et al., 2002; Suarna et al., 1995). Despite the plaques having varied average concentrations of oxidative and inflammatory markers between the plaques, the majority of the overall average concentration of these markers within the plaques (Table I,II) agree with concentrations that have previously been measured.

This laboratory was the first to quantify the level of neopterin within both carotid and femoral plaques via HPLC (Firth et al., 2008; Gieseg et al., 2008a). At the same time neopterin was detected in coronary plaques via immunohistochemical staining in conjunction with SMC, macrophages, T cells and neutrophils, but its concentration was not quantified (Adachi et al., 2007). Our study showed the highest average concentration of neopterin detected within a plaque was 2.34 μM (Table I). Within this study the overall average concentration of α-tocopherol within 14 plaques was 112.41 ± 10.09 nmole/g plaque. In agreement with this, Carpenter et al. (1995) determined an average (± SD) α-tocopherol concentration of 156 ± 118 nmole/g tissue within 19 plaques. The α-tocopherol level in this study, expressed as α-tocopherol per cholesterol, had an average concentration of 2.49 ± 0.19 mmole/mole of total cholesterol. Suarna et al. (1995) detected an average (± SD) concentration of 6.4 ± 4.8 mmole/mole of free cholesterol within 11 femoral and carotid plaques. The α-tocopherol within this study was adjusted against the total cholesterol of the plaques whereas Suarna et al., (1995) adjusted against the free cholesterol content of the intima. Thus the α-tocopherol measurements within plaques determined by both Suarna et al. (1995) and Carpenter et al. (1995) agree with this study.

In our study the overall average concentration of DOPA and dityrosine was 13.75 ± 1.43 and 4.41 ± 0.81 nmole/g plaque respectively. These measurements agree with previous DOPA and dityrosine average values (± SD) measured in carotid plaques of 14.26 ± 3.80 and 4.75 ± 5.17 nmole/g of plaque respectively (Fu et al., 1998). In conjunction with the highly oxidative environment of plaques, the overall average protein carbonyl content (3.77 ± 0.47 μmole/g protein) was considerably high compared to normal tissue (approximately 1 nmole/g protein) (Davies et al., 1999). Via an ELISA method a protein carbonyl concentration of 21.1 μmole/g protein within the

gruel of aortic and carotid plaques was detected (Li et al., 2006). Furthermore, within carotid plaques a noticeably higher TBARS average (± SD) of 36.4 ± 4.2 nmole/g tissue has been reported (Nishi et al., 2002), compared to the overall average TBARS concentration within this study at 14.32 ± 2.26 nmole/g plaque. Like that of the protein carbonyl measurements (Li et al., 2006), Nishi et al. (2002) quantified the oxidative marker via a different method to this laboratory possibly accounting for the discrepancies between the studies. The solvents within the butanol/absorption method employed to quantify the lipid peroxides include highly volatile solvents which can cause the overestimation of lipid peroxide content within the sample. However the femoral plaques A and B had TBARS values within and above the range (Table II) published by Nishi et al. (2002).

4.2 Correlations between the marker concentrations across the atherosclerotic plaques

Correlations between neopterin, α-tocopherol and the lipid and protein oxidative markers across the plaques may provide insight into the interactions and influences the oxidative marker have on one another, whether α-tocopherol exerts a anti- or pro- oxidant effect towards protein and lipid oxidation and if the macrophage associated neopterin relates to the oxidative damage observed in the plaques.

Protein and Cholesterol

It may be hypothesised that the variation of the spatial concentration of protein and cholesterol may have a major influence of the concentration of the resulting oxidative product. Across the individual and combined analysis this is not conclusively seen. The strongest trend occurs between α-tocopherol and cholesterol concentration within individual plaques and combined data, as LDL is the major source of α-tocopherol (Esterbauer et al., 1992). LDL may also be a major contributor to the cholesterol content within plaques as LDL cholesterol is thought to be the main source of cholesterol within macrophage foam cells (Kruth et al., 2002). In terms of TBARS formed from PUFAs located predominantly within the LDL, the cholesterol level only significantly correlated to TBARS content within one plaque where it also correlated with α-tocopherol concentration. Protein is the substrate for protein carbonyls, DOPA and dityrosine yet the concentration of DOPA and dityrosine only significantly correlated with protein content within one plaque. In the combined plaque analysis, protein positively correlated to protein carbonyl content, the formation of which is

non-specific. The specificity of DOPA and dityrosine may explain why correlations with protein levels were only observed once within an individual plaque. This indicates that even though the concentration of protein and cholesterol will play some role in the degree of oxidative damage, other major influences are occurring. This includes the degree and nature of oxidative stress as well as the availability of protein and cholesterol particles. Remodelling may also alter the location of the protein, cholesterol and/or markers through the formation and degradation of the extracellular matrix, the migration and proliferation of SMC, as well as cycles of thrombi formation and subsequent healing. Another factor to consider is DOPA is not an end product as it can be involved in further oxidation reactions (Dean et al., 1997; Fu et al., 1998) Therefore its formation and detoxification will be dependent on these factors in combination with the protein concentration. This is why caution is required when interrupting DOPA results.

Neopterin

Within the combined data, neopterin and protein concentrations have a strong positive relationship. This correlation was seen within one of the two individual heavily calcified plaques (Plaque A), but not the other possibly due to its size (Plaque B). Flavall (2008) also reported this significant correlation within heavily calcified plaques. A possible reason why this relationship was not seen within the thrombosed plaques is because the higher concentrations of protein introduced by the presence of a thrombus may alter the spatial variation of protein across the plaques. The presence of the calcified deposits predominantly within the middle sections of plaques will have a pronounced effect on the mass of the section. This will decrease the concentration of the neopterin and protein per gram of tissue within these sections. Within a type II-like alveolar epithelial cell line neopterin at physiologically relevant plaque concentrations inhibited ATP mediated increase in intracellular calcium (Hoffmann et al., 2002). Alternatively neopterin and 7,8-NP both increased the intracellular calcium in human monocyte line cells putatively for the activation of the monocytes (Woll et al., 1993). Therefore along with oxLDL and lipid accumulation (Tang et al., 2006) neopterin may have a role in the process of cellular mineralisation.

7,8-NP could not be detected within these plaques, yet as 7,8-NP is the only known precursor to neopterin, 7,8-NP must have been present within the plaques at some point. Subsequent loss of 7,8-NP appears to occur by its conversion to either neopterin or its other byproduct 7,8-dihydroxanthopterin (Figure 1.6). The micromolar concentration of neopterin suggests that 7,8-NP

present within particular microlocations across the plaque could reach low to mid micromolar concentrations of 7,8-NP, especially within the peripheral regions of the plaque. This is plausible because within coronary plaques the majority of neopterin was associated with macrophages and these cells were significantly correlated towards MPO associated neutrophils (Adachi et al., 2007). Therefore the hypochlorous acid produced from the MPO could convert 7,8-NP to neopterin within the macrophage rich regions increasing the proportion of neopterin to 7,8-dihydroxanthopterin. Thus neopterin may represent the greater proportion of 7,8-NP in these regions. Besides the possibility that 7,8-NP may act as an antioxidant by reaching sufficient concentrations *in vivo*, the formation of oxLDL, TBARS and protein oxidation still occurs. Taking into consideration the properties of neopterin and 7,8-NP described within literature, the ratio and therefore the antioxidant and pro-oxidant balance between the 7,8-NP and neopterin may play an influential role in modulating oxidative stress within the plaque and therefore plaque processes and development (Gieseg et al., 2008a).

The co-localisation of high levels of neopterin with TBARS (plaque A) and neopterin with protein carbonyls (combined data) suggests that the 7,8-NP may have failed to protect the lipids and protein from oxidation. Alternatively, the majority of 7,8-NP was already oxidised to neopterin/7,8-dihyroxanthopterin therefore the lipids and protein lacked this protective mechanism allowing the formation of the protein carbonyls and lipid peroxidation. Within plaque A the neopterin and protein concentrations had a significant positive correlation (Table 3.1.7). At sites of high protein and neopterin, lower DOPA and dityrosine concentrations were found, suggesting that the 7,8-NP may be protecting the tyrosine residue from oxidation. This is supported by the DOPA and dityrosine content occurring within the middle sections of plaque A whereas the majority of neopterin and protein levels occurred within the peripheral sections (Figures 3.1.2, 3.1.3). Within plaque C, which had a relatively high degree of protein oxidation levels (Table II), the neopterin had a similar relationship to dityrosine that is high neopterin to low dityrosine levels. Also observed within this plaque was a significant negative correlation between α-tocopherol and DOPA concentrations. The protective effect of α-tocopherol indicates a high radical flux was occurring within this plaque which may also explain how 7,8-NP may be protecting against dityrosine formation. Because neopterin is not the only byproduct of 7,8-NP the interactions between 7,8-NP and protein and lipids speculated above can only be confirmed by directly measuring the 7,8-NP and possibly the 7,8-dihydroxanthopterin concentrations within and across the plaques.

α-Tocopherol

With the exception of plaque B, the individual plaques all displayed a relationship between α-tocopherol and at least one marker. α-Tocopherol had a negative correlation towards DOPA and dityrosine observed within different plaques. This indicates α-tocopherol is acting as an antioxidant. The formation of DOPA and dityrosine on the tyrosine residue can be mediated by the hydroxyl or peroxyl radical (Davies et al., 1999). α-Tocopherol is able to scavenge hydroxyl radicals but because of its rapid rate of reaction the opportunity to scavenge it will depend on the location of the hydroxyl radical formation. It is more likely the α-tocopherol is scavenging the peroxyl radicals that can mediate DOPA and dityrosine formation. Because α-tocopherol appears to protect one plaque from DOPA and another from dityrosine formation indicates that again other factors and mechanisms maybe involved in tyrosine oxidation. Within the combined plaque data the TBARS and cholesterol concentrations negatively correlated as well as a positive correlation between α-tocopherol and cholesterol levels. Therefore at sites of high cholesterol there were high levels of α-tocopherol and low levels of TBARS indicating that overall the α-tocopherol maybe protecting the lipids from lipid peroxidation. Along with the antioxidant properties of α-tocopherol, the positive correlations towards TBARS (Plaque E) and protein carbonyl concentrations (combined data) reveal α-tocopherol undergoing pro-oxidant activity involving tocopherol mediated peroxidation (TMP). Under a low radical flux the α-tocopherol via a much slower rate of reaction can initiate the lipid hydroperoxide chain reaction leading to malondialdehyde formation suggested by the positive relationship between α-tocopherol and TBARS within plaque E. However, this may be a minority relationship as the opposite relationship is inferred in the combined plaque data as discussed above. The TMP action may occur within the majority of plaques at some point because within the combined analysis α-tocopherol positively correlated to the protein carbonyls which both in turn positively correlated to protein the substrate for protein carbonyls (Table 3.1.7). In the presence of native and mildly oxLDL a human serum ultrafiltrate containing compounds with a molecular weight below 500 inhibited and accelerated oxidation respectively. The pro-oxidative properties were associated with uric acid, α-tocopherol and copper towards the preformed lipid hydroperoxides on the mildly oxLDL (Patterson et al., 2003). This demonstrates that the environment in which these antioxidants are in dictates the properties it will exert on the biomolecular components. Studies have shown that plaque supports an oxidative environment which can mediate cellular death and oxidation of molecules (Li et al., 2006; Smith et al., 1992). This study has shown that the spatial organisation of the oxidative products and therefore this

oxidative environment varies. Therefore it can not be surprising that α-tocopherol can undertake both antioxidant and TMP action within atherosclerotic plaques.

Oxidative markers

Within plaque A TBARS and proteins carbonyl levels correlated. It is known that lipid breakdown products like malondialdehyde can mediated the formation of protein carbonyls (Berlett and Stadtman, 1997). In plaque D the opposite relationship was observed with a negative correlation between DOPA and TBARS concentrations. Within the combined data the only oxidative markers to relate to one another was the positive correlation between DOPA and dityrosine levels. This was also observed by Flavall et al. (2008) indicating that overall these two markers appear to be formed by the same process within the artery wall. DOPA and dityrosine can be induced by similar oxidants (Davies et al., 1999), notably through hypochlorous acid and hydroxyl radical mediated damage (Gieseg et al., 1993; Sutherland et al., 2003), whereas many different mechanisms and oxidants can induce the formation of protein carbonyls (section 1.2.1.1). In all plaques the concentration of DOPA was higher than dityrosine, but not every plaque or section contained detectable levels of dityrosine. Considering dityrosine is only formed through free radical mediated mechanisms and within these dityrosine free plaques the concentration of DOPA was within the lower range, suggests that the hydroxyl radical/HOCl/peroxyl radicals involved in DOPA and dityrosine formation was reduced. In combination, the tyrosine residues may be protected via antioxidants like α-tocopherol, ascorbic acid, uric acid and 7,8-NP among others. Protein carbonyl concentration positively correlated to TBARS and DOPA levels within two different individual plaques. Because TBARS and DOPA can further mediate oxidative reactions they may contribute to the formation of the protein carbonyls. Therefore, along with the radicals and oxidants, the oxidation markers themselves may play a role in inducing further oxidative damage.

Femoral plaques

Plaques A and B formed within the left and right common femoral branches respectively. These femoral plaques had higher TBARS, lower cholesterol and α-tocopherol, a DOPA and dityrosine concentration within the lower range and neopterin content within the higher range of the 12 carotid plaques (Tables I/II). As both the femoral plaques have this relationship towards the carotids this could indicate that external factors could influence the plaque biochemical composition. However both the femoral samples were taken from the same patient so it is difficult to gauge from this data

alone whether these differences between the femoral and carotid plaques are a patient or location effect.

4.3 External factors influencing the concentration and/or spatial localisation of the markers in atherosclerotic plaques

Although the biochemical components within the plaques play a substantial role in the localisation and occurrence of oxidative, antioxidants and inflammatory markers across and within the plaques external factors cannot be ruled out. The importance of shear stress in the locality of plaque formation is well established (Chatzizisis et al., 2007; Helderman et al., 2007), along with the risk factors including hyperlipidemia, diabetes and obesity (Abedin et al., 2004; Libby et al., 2002). The effects of aspirin and statins on human plaque biochemical composition have not been investigated either. Therefore it is essential to examine these factors since they may participate in either the initiation or progression of the plaque or the clinical outcome of the patient.

4.3.1 The influence of zoning on the variation of the marker concentrations across the plaques

The level of shear stress differs across the length of the plaque and is known to disrupt the function of the endothelial cells. Since the endothelial cells are the barrier between the circulating blood and tissue, the shear stress may also influence processes like the ability of the LDL to accumulate and therefore affect the concentration of cholesterol and α-tocopherol across the plaque (Chapman, 2007). The cholesterol content was higher within the post-bifurcation zone which may be explained by the occurrence of low and/or oscillatory endothelial shear stress (ESS) (Figure 3.1.17b). Low ESS is reported to increase the ability of lipids to accumulate (Chatzizisis et al. 2007). This is not reflected within the α-tocopherol content as it does not significantly vary across the pre-, post- and bifurcation regions (Figure 3.1.17d). However, α-tocopherol can have a temporal variation due to its antioxidant and pro-oxidant effects. Ascorbic acid, a co-antioxidant towards α-tocopherol has been identified within plaques (Suarna et al., 1995), therefore the temporal and spatial concentration of ascorbic acid could have a considerable effect of the temporal and spatial concentration of α-tocopherol.

Neopterin was significantly higher in the pre- and post-bifurcation regions (Figure 3.1.17a). The bifurcation was predominantly the location where the plaque begins to significantly narrow the arterial passage potentially altering the level of ESS. The level of neopterin was lower within the bifurcation region possibly due to this change in shear stress. Low ESS which can occur before the point of stenosis activates NF-κβ which in turn induces the expression of γ-interferon (Chatzizisis et al., 2007). In the presence of macrophages the γ-interferon stimulates the synthesis and secretion of 7,8-NP. Thus a higher synthesis of 7,8-NP could explain the higher neopterin located within the pre-bifurcation. Plaque gruel was generally located predominantly within the bifurcation and the proximal end of the post-bifucation region. Gruel from carotid plaques has been shown to be highly cytotoxic to human monocyte derived macrophages inducing apoptosis due to the phagocytosis of aldehydes and hydroperoxide products (Li et al., 2006). Therefore the macrophages present within these sites are most likely dead hence the lack of neopterin present. In combination with this the significantly high neopterin levels in the pre- and post-bifurcations may also be due to macrophages concentrated within the shoulder regions of the plaques (Stary et al., 1995) making these sites metabolically active. As previously mentioned the majority of neopterin associated macrophages significantly correlated towards MPO associated neutrophils (Adachi et al., 2007). Therefore the MPO produced hypochlorous acid could convert 7,8-NP to neopterin producing the high neopterin levels observed in the pre- and post-bifurcation regions. The association between the macrophages and neutrophils also supports the role of neopterin acting to enhance oxidative species and 7,8-NP protecting its cell of origin. Another possible cause to the low level of neopterin within the bifurcation might be the low conversion ratio of 7,8-NP to neopterin. Peroxyl radicals can convert 7,8-NP to 7,8-dihydroxanthopterin rather than neopterin (Figure 1.6). Within the bifurcation zone a significantly high level of TBARS was observed (Figure 3.1.17). Thus the more peroxyl radicals present for the 7,8-NP to react with the less neopterin formed. Also 7,8-NP is a known peroxyl radical scavenger (Gieseg et al., 2003; Ottel et al., 1997) therefore a low concentration of 7,8-NP may allow a high occurrence of lipid oxidation mediated by the peroxyl radicals.

The peroxyl radicals from the lipid peroxide decay may also contribute to the significant dityrosine content within the bifurcation region of the plaques (Figure 3.1.17h). Alternatively the tyrosyl radicals may induce lipid peroxidation. The occurrence of MPO induced tyrosyl radicals during lipid peroxidation in LDL has been reported supporting an influential relationship between the two oxidative product pathways (Savenkova et al., 1994). However, this does not explain the high

concentrations of dityrosine within the post-bifurcation region where the TBARS levels are significantly low. Because macrophage associated neopterin within plaques had a strong correlation to MPO associated neutrophils (Alachi et al., 2007) and MPO activity can generate the tyrosyl radical (Leeuwenburgh et al., 1997), the high neopterin levels within the post-bifurcation region associated with high MPO maybe responsible for the high dityrosine observed within the post-bifurcation region. Why this is not seen within the pre-bifurcation where there are also high levels of neopterin may be because there is a significantly low concentration of protein present therefore less substrate for the HOCl to act upon. This trend is not observed with DOPA and protein carbonyl concentrations possibility because DOPA and protein carbonyls are formed from various mechanisms that include non free radical and oxidant pathways (sections 1.2.1.1 and 1.2.1.3). The contributions from these paths may obscure the contributions of the free radical/oxidant mechanisms masking possible trends DOPA or protein carbonyls may have towards neopterin and TBARS.

4.3.2 The influence of the overall plaque composition on the variation of the marker concentrations between the plaques

The protein concentration in the thrombosed plaques was significantly high compared to the neither plaques and the calcified plaques. Thrombosed plaques have a considerable amount of blood components associated internally within the plaque. The increased blood components may explain the higher protein content of these plaques. The high dityrosine levels observed within the thrombosed plaques may also be the result of the high protein levels present. The concentrations of α-tocopherol, dityrosine and protein associated with the calcified plaques were significantly low and associated with the thrombosed plaques the concentration of these markers were significantly high. Within the neither plaques the concentration of α-tocopherol, dityrosine and protein were between the levels detected within the thrombosed and calcified plaques (Figure 3.1.18a,d,h), therefore the neither plaques may represent an intermediate state between heavily calcified plaques and plaques that have formed significant thrombi.

As discussed (section 4.1) the highly calcified plaques had significantly low protein levels. This was associated with a high level of calcium deposits increasing the mass of the sections and decreasing the concentration of protein per gram of tissue. This high proportion of the plaque mass attributed to the calcium deposits within the sections of highly calcified plaque might also extend in

relation to the low concentrations of cholesterol, α-tocopherol, DOPA and dityrosine observed in the calcified plaques. However, this effect is not observed with neopterin, TBARS and protein carbonyl levels therefore will not be the only factors involved in the spatial localisation of these markers within the calcified plaques. In fact these three markers show a lack of effect across all three difference plaque composition types. Despite this the overall composition of the plaque had a significant influential role in the overall concentration of the LDL associated components and the tyrosine oxidation markers.

4.3.3 The influence of patient medication and symptoms presented on the variation of the marker concentrations between the plaques

Medications

A study on the effect of statins on the cellular and lipid composition of carotid plaques concluded that the statin treated groups contained lower cholesterol than the controls (Crisby et al., 2001). Furthermore, coronary lesions exposed to statins had a significant decrease in the total and LDL cholesterol content (Burgstahler et al., 2007). Within the statin alone treated patients the concentration of cholesterol, α-tocopherol, protein, DOPA and dityrosine was low in the plaques when examined. These plaques were the two femoral plaques therefore any differences associated with taking statins alone will also be influenced by the highly calcified state of these plaques and an individual patient effect. Between the seven plaques from statins and aspirin treated patients and the four plaques from aspirin alone treated patients there was low cholesterol within the aspirin alone group where the α-tocopherol content in the plaques remained unaltered. This indicates that within this small sample size the statins were not reducing the total cholesterol content within the advanced plaques studied. In patients undergoing elective coronary angiography the serum neopterin levels were lower in the patients that were on a statin (Walter et al., 2003). This was opposite to what was found in this study. In the plaques of statins and aspirin treated patients, the neopterin concentration was higher than the plaques from aspirin alone treated patients. With the low cholesterol and neopterin levels in the plaques of aspirin alone treated patients the TBARS and protein were significantly high compared to the plaques of statin and aspirin treated patients. The other three oxidative markers DOPA, dityrosine and protein carbonyls were statistically the same between the two medication groups. This supports the proposal that both aspirin and statin may have overlapping effects by directly or indirectly acting on the same or similar mechanisms involved in protein oxidation. Assessed by a meta-analysis of many studies the clinical benefits of taking statins

clearly indicated a reduction in clinical events. The aspirin analysis was not so conclusive (Hennekens and Schneider, 2008). When both aspirin and statin are consumed in conjugation the clinical benefits were even higher (Chapman, 2007; Hennekens and Schneider, 2008), with the suggestion that a combination of statin and aspirin may have synergetic effects (Chapman, 2007). Within this study the combination of taking both aspirin and statins do not confer any significant difference in the biochemical composition of the plaques compared to aspirin alone treated patients.

Medication versus the symptoms presented

The marker concentrations displayed a general trend in the overall concentration of the plaque when the symptom induced by the plaque was taken into consideration. The protein, α-tocopherol and protein carbonyls were statistically high within the plaque that induced amaurosis fugax (AF) and asymptomatic events compared to the plaques that induced stroke and transient ischemic attack (TIA) events. This maybe because within the AF group all three plaques were thrombosed plaques. As discussed these plaques had higher levels of protein and α-tocopherol, however the marker trends between the symptom groups do not completely follow the thrombosed/calcified/neither categories. This is because two thrombosed plaques along with two calcified plaques occur within the stroke group therefore the presence of thrombi can not totally explain the significant difference observed between the high levels of protein, α-tocopherol and protein carbonyls in the plaque induced AF group to the low levels in the stroke group.

The variation of the marker concentration within the plaques had no significant defining trends when the medication consumed by the patient was taken into consideration along with the symptom presented. This maybe because within the medication combinations exposed to the plaques (aspirin alone and statins and aspirin combined), all of the symptoms suffered (stroke, AF and TIA) and plaque overall composition states (thrombosed, calcified and neither) are represented within both medication groups. Thus it is a combination of the plaque state and patient medication that may play a role within the overall and spatial variation of these markers across the plaques. And it is these variations which may affect the stability of the plaque contributing to the symptom presented by the patient.

4.4 Investigating current and new markers for quantification within the atherosclerotic plaques

Theses additional studies identify further markers that could be included in future plaque analysis which may provide further elucidation of mechanisms and interactions occurring within theses plaques.

4.4.1 Detection of 7,8-dihydroneopterin

The inability to detect 7,8-NP within plaques samples was either because 7,8-NP is not present within plaques or the solutions involved in the preparation of the samples was interfering with 7,8-NP/neopterin detection. Healthy plasma was reported to have a ratio of 78-NP to neopterin at 2:1 (Flavall et al., 2008). 7,8-NP was not being detected within this biological fluid either, indicating error was occurring by the preparation of the samples. Within the acidic iodide solutions the molarity and pH of the hydrochloric acid was altered and made no impact on 7,8-NP detection within plaque. This also occurred with the pH experiment where the plaque homogenate was spiked with 20 nM of 7,8-NP. A 7,8-NP concentration of 20 nM was physiological relevant for plasma (Flavall et al., 2008) but is unlikely to be for plaque, since 1-2 μM of neopterin was detected within these samples (Table I). Plaques have been shown to support a high oxidative environment (Smith et al. 1992), therefore the addition of the 20 nM 7,8-NP may have been rapidly converted to neopterin or 7,8-dihydroxanthopterin within the plaque homogenate.

The plasma treated with the non-acidic iodides at a pH of approximately 8 and 4 returned nearly the full 7,8-NP spike. This suggests that the low pH level of the acidic iodide was interfering with 7,8-NP. Lorente et al. (2004) reported the fluorescence of neopterin was dependent on the pH values tested at pH 5-5.5 and 10-10.5, giving a higher fluorescence emission at the lower pH value. The pH of the acidic iodide treated samples would be lower than the neopterin samples. The samples were injected into a pH buffered mobile phase onto the HPLC. Therefore the pH difference of the sample injects may not be a problem. The total neopterin values of the plaque treated with different acidic iodides was significantly the same (Figure 3.2.2b). This further supports that the different pH levels of the acidic iodide treated samples are not significantly quenching the fluorescence of neopterin within plaque. The quenching of neopterin within plasma may still be an issue because of

the lower basal concentration of neopterin relative to plaque. To overcome this problem within plasma more investigations into the properties of the acidic iodide solution is required.

Within plaque gruel, redox active iron and copper had been detected at a concentration of 0.03-7.2 μM and 0.2-28.6 μM respectively (Smith et al. 1992). The presence of these reduced ions may mediate the underestimation of 7,8-NP by its conversion to 7,8-dihydroxanthopterin (Figure 1.6). The inability of deferoxamine (DFO) a strong iron chelator, to fully return the 7,8-NP spike indicates that there may not be sufficient chelator present to bind up all the iron within the sample. Though this is unlikely as 100 μM DFO nearly completely inhibited DNA modification induced from plaque gruel (Smith et al., 1992). Another possibility is that a substantial concentration of reduced copper is present mediating the oxidation of 7,8-NP to 7,8-dihydroxanthopterin. Further investigation is required to determine the consequence of redox active iron and copper and possibly other oxidants in the presence of 7,8-NP. The detection of 7,8-dihydroxanthopterin and direct detection of 7,8-NP would also shred light onto this problem.

4.4.2 The oxysterol 7-ketocholesterol

Numerous studies have identified that 7-KC is cytotoxic towards various cells including epithelial cells (Rodriguez et al., 2004), aortic SMC (Hughes et al. 1994), human vascular endothelial cells, fibroblasts derived from HUVECs cells, human artery SMC and MRC5 human fibroblasts (Lizard et al., 1994). Therefore it would be reasonable to hypothesis that the concentration of 7-KC within oxLDL may play a role in determining the different toxicity levels of oxLDL observed towards human macrophages. This would require a database of the 7-KC and α-tocopherol content of each batch of LDL and oxLDL prepared within the laboratory along with the LD_{50} of the oxLDL towards human monocyte derived macrophages.

Using the method defined by Kritharides et al. (1993) the 7-KC concentration increased in oxLDL 7 fold after 24 hours incubation with copper. In other studies the 7-KC content in oxLDL increased 5 fold (Chang et al., 1997) and 15 fold (Steffen et al.) after 200 minutes incubation with copper. Because the 7-KC concentration within the native LDL agrees between the studies (Table 3.2.1) and the 7-KC content in the oxLDL are within the same magnitude (Table 3.2.1) the differences may be associated with only one batch of oxLDL being measured in this study. Therefore the

inherent donor variation like the presence and quantity of a combination of antioxidants within the LDL including α-tocopherol, β-carotene, ubiqinol-10 and lycopene (Esterbauer et al., 1992; Jessup et al., 1990) may account for the difference observed between the studies in the increase of 7-KC content in LDL after incubation with copper.

Studies have identified 7-KC as a cytotoxic component with plaques (Larsson et al., 2006; Lizard et al., 1999). The 7-KC concentration and spatial localisation could potentially be added to the list of oxidative markers measured within the plaque, as a specific marker to cholesterol oxidation. The average concentration of 7-KC detected within plaque E using the original Kritharides et al. (1993) method was 138.38 ± 54.82 nmole/g plaque considerably higher than a previously published value of 0.25 ± 0.16 nmole/g tissue in aortic plaques (Garcia-Cruset et al., 2001). The average 7-KC concentration as expressed per mole of cholesterol within plaque E was 3.46 ± 1.39 mmole/mole of cholesterol. This is within the same magnitude as the average concentration (± SD) of 0.6 ± 0.4 mmole/mole of free cholesterol reported in femoral and carotid plaques (Suarna et al., 1995). As is evident from the plaque analysis the variation of oxidative products between plaques is large. For example the overall average of TBARS expressed as nmole per mole of cholesterol varies between plaques from 13.8 to 0.1 (Table I), therefore the differences observed between the 7-KC measurement in this study to others may be associated with the inherent differences of the biological sample and method used.

To replace the original α-tocopherol method with the 7-KC/α-tocopherol method it is essential the α-tocopherol concentrations detected agree between the two. The 7-KC/α-tocopherol method was detecting lower levels of α-tocopherol using Kritharides et al. (1993) original mobile phase and higher α-tocopherol levels when the water component of the mobile phase was removed. The opposite trend was observed for 7-KC in the different mobile phases. This suggests that the α-tocopherol and 7-KC from the plaques has a different solubility between the two mobile phases. Therefore, it is difficult to determine which conditions provide a more accurate reading of α-tocopherol within the plaque. In the original α-tocopherol method for plaque E the average α-tocopherol concentration was 4.4 ± 0.3 and with the 7-KC/α-tocopherol method it was 1.9 ± 0.1 mmole/mol of total cholesterol. Both α-tocopherol measurements within plaque E were within the range of the average α-tocopherol concentration (± SD) within femoral and carotid plaques with 6.3 ± 4.8 mmole/mol free cholesterol (Suarna et al., 1995). Therefore, more investigation is required to

determine under which conditions the 7-KC/α-tocopherol method will provide accurate measurements of α-tocopherol within plaque.

4.4.3 Determining the concentration of the two main protein carbonyl products via HPLC analysis; a candidate for the replacement of the protein carbonyl assay

α-Aminoapidic semialdehyde (AAS) and γ-glutamic semialdehyde (GGS) have recently been acknowledged for their potential as markers of protein oxidation (Akagawa et al., 2006; Akagawa et al., 2005; Daneshvar et al., 1997; Requena et al., 2001). Akagawa et al. (2006) developed a HPLC based assay for the detection of AAS and GGS. Using this assay on BSA and human plasma incubated with AAPH derived peroxyl radicals and in plaque, there were consistently four distinct peaks on the HPLC chromatograms (Figure 3.2.9). In the original publication, GGS-ABA elutes around the 7^{th} minute and AAS-ABA at the 20^{th} minute. Within this study the method had been modified using a different mobile phase and column, changing the solubility and elution times of the conjugates. To confirm exactly which peaks are which known solutions of ASA-ABA and GGS-ABA are required to be injected onto the modified HPLC system and retention times noted, however the complete synthesis of AAS-ABA and GGS-ABA is complex (Akagawa et al., 2006) and beyond the scope of this project.

In agreement with Akagawa et al. (2006) the AAS concentration was higher than GGS in oxidised BSA. A previous study have found that 10% of the lysine residues and only 1% of the arginine residues within BSA were modified after 24 hours incubation with 10 mM AAPH (Cassidy, 2003), supporting the higher increase in AAS compared to GGS. The opposite was reported in BSA incubated with free iron inducing a higher concentration of GGS compared to AAS (Requena et al., 2001). The proportion of protein carbonyls that was accounted for by AAS and GGS were also different between the three studies. In this study AAS and GGS accounted for 6% of the protein carbonyls at the basal level and 86% of the protein carbonyls after 24 hours incubation with peroxyl radicals. Compared to a basal level of 23% (Akagawa et al., 2006) and 88% (Requena et al., 2001) before oxidation and 51% after iron mediated oxidation (Requena et al., 2001). The differences may be attributed to the different oxidation systems and the purity of the BSA (different suppliers).

Within dialysed plasma the AAS and GGS rate of formation was opposite to that of protein hydroperoxide (PrOOH) formation (Figure 3.2.11). Initially the PrOOH formation was rapid before slowing down after eight hours incubation with peroxyl radicals. The AAS and GGS formation was slow before increasing after eight hours exposure to AAPH. This supports the idea that the breakdown products of PrOOH can mediate the formation of protein carbonyls, which has been shown to occur on lysine and proline residues (Davies, 1996). Therefore the PrOOH decay may be responsible for the increased rate of AAS and GGS formation occurring after eight hours in dialysed plasma.

Within plaques, the apoB protein within LDL may contribute to the presence of AAS and GGS observed within plaque F (Table 3.2.2). Proline and arginine residues within the apoB protein of LDL are highly susceptible towards γ-glutamic semialdehyde formation. During LDL oxidation and in the presence of iron a 117 fold increase in γ-glutamic semialdehydes was reported (Pietzsch, 2000). To investigate if the apoB protein makes a significant contribution to the AAS and GGS formation within the plaque, the concentration of AAS and GGS to the spatial concentrations of the LDL based components 7-KC, cholesterol and α-tocopherol across plaques may confirm this hypothesis.

The ratio of AAS and GGS to protein carbonyl concentration within plaques may not be constant and this assay is more time consuming than the protein carbonyl spectrophotometric assay. But a major advantage to the HPLC based assay is it measures specific protein carbonyl products, not just the generic protein carbonyl structures as the DNPH method does. This allows speculation of the possible reaction pathways that lead to the formation of AAS and GGS, as well as the relative concentrations of these compounds *in vivo*. Furthermore in plaque F the HPLC assay had a lower statistical error in the measurements of AAS and GGS compared to protein carbonyls detected by the DNPH method (Table 3.2.2). Moreover the high linear regression values of the protein carbonyls towards both AAS and GGS in BSA (section 3.2.3) indicate that AAS and GGS have a similar kinetic relationship to the overall formation of protein carbonyls. This kinetic relationship between protein carbonyl formation and AAS and GGS formation may also apply within the environment of plaques. Therefore the AAS and GGS HPLC assay is a good candidate to replace the protein carbonyl DNPH assay in plaque analysis.

4.4.4 Antioxidants and proteins involved in plasma protein hydroperoxide formation

When plasma was exposed to AAPH derived peroxyl radicals a lag phase occurs for 6-8 hours before any significant protein hydroperoxide (PrOOH) formation occurs. When the plasma was dialysed removing all the small molecular weight antioxidants like uric acid, ascorbic acid, bilirubin and protein thiols the lag phase was abolished, and a second lag phase emerges between the 8-16 hour time points. Studies confirmed it was the combined effect of uric acid and ascorbic acid that was responsible for the initial lag phase (Osborn, 2006; Yang, 2005). The second lag phase that occurs in the dialysed plasma was attributed to protein thiols. When the accumulation of PrOOH reached a particular level the thiols could act as a radical sink by transferring the position of the damage from a carbon centred location to a thiol group (Davis et al. 1993) effectively stabilizing the concentration of PrOOH present. Yang (2005) showed that the protein thiols were completely oxidised somewhere between the 12-24 hour time period. This study confirmed that the rate of increase of PrOOH formation before the lag phase was similar to the rate of increase post lag phase (Figure 3.2.13). Because these rates are similar this indicates that the protein thiols presumably have no major effect on the PrOOH formation until the PrOOH reaches a certain threshold concentration represented at the 8 hour time point by the lag phase.

The exact identity of the proteins modified during the oxidation process was difficult to determine. A gel electrophoresis of the plasma proteins showed a 34 kDa protein with two distinct bands in the control treatment (Figure 3.2.15b). After two hours incubation with AAPH the 34 kDa protein remained unaltered. After fours exposure with peroxyl radicals the two bands began to merge losing their sharp appearance (Figure 3.2.15a). Ascorbic acid is fully consumed within plasma after two hours incubation with peroxyl radicals (Osborn, 2006) and the 34 kDa protein was altered after two hours suggesting this protein maybe protected by the ascorbic acid. Uric acid may not protect the 34 kDa protein from oxidation as it is still present after two hours (Osborn, 2006). The 34kDa protein may also contain thiol groups. The oxidation of protein thiols by the peroxyl radicals could potential alter the migration pattern of the protein on the gel accounting for the difference observed in the 34 kDa protein after fours hours exposure to peroxyl radicals. This is difficult to interpret because the identity of the protein/s involved remains unknown.

The human serum albumin (HSA) protein with a molecular weight of ~71 kDa was clearly identified on the gel. Its intensity and size of the band remained unchanged throughout the incubation with AAPH. HSA is the main source of protein thiols within plasma (Yang, 2005) and as discussed above the protein thiols were the chief component responsible for the second lag phase observed between eight-16 hours. The lack of a change may be because the oxidation of the thiols is not altering enough of the HSA to change its migration pattern on the gel. Bilirubin is another antioxidant present within plasma and the majority of it is bound to HSA (Neuzil and Stocker, 1993). Bilirubin is able to scavenge AAPH derived peroxyl radicals (Frei et al., 1988), therefore the HSA may be protected via the bilirubin. Yang (2005) showed that bilirubin is completely oxidised after 4 hours exposure to peroxyl radicals. Therefore it cannot fully explain why the HSA migration pattern remains unaltered after 24 hours incubation with AAPH.

Patterson et al. (2003) demonstrated a plasma ultrafiltrate was able to inhibit copper mediated LDL oxidation. Associated with this antioxidant effect was uric acid (Patterson et al., 2003), an antioxidant which has been identified within plaques. The uric acid and ascorbic acid were predominantly in the extracellular space of the plaques (Suarna et al., 1995) providing opportunity for the protection of proteins and lipids. Due to the role of uric acid, ascorbate acid, α-tocopherol and protein thiols have in the prevention of protein hydroperoxide formation within plasma it may be hypothesised that these antioxidants may have a role in the antioxidant protection towards proteins against free radicals and oxidants produced with plaques. To investigate this further the spatial organisation of uric acid and ascorbic acid in relation to the oxidative markers and α-tocopherol could be included within the study of atherosclerotic plaques.

4.5 Summary

The major finding of this project is that atherosclerotic plaques are different in their biochemical composition spatially across and between plaques. Plaque progression and growth are dynamic processes which may give explanation to why protein and cholesterol generally do not correlate to their corresponding oxidative product, and why in turn these oxidative products do not correlate with one another. This illustrates that the environment of micro locations as well as the whole plaque will dictate the relationship and ability of oxidative markers to influence each other. The

strongest external factor to account for the spatial variation of marker concentration appeared to be zoning, possibly associated with shear stress. The high level of protein and cholesterol within the post-bifurcation regions supports the low ESS occurring at this location. The inverse relationship between neopterin and TBARS supports what is known between peroxyl radicals and 7,8-NP. As outlined by Helderman et al. (2007) the type of shear stress will play a role in the localisation of macrophages, SMC and lipids across the plaque. The plaques vary morphologically therefore the type, degree and combination of shear stress exerted on different locations may be different providing the variation in marker concentrations observed within and between the plaques.

The neopterin concentration detected within the plaques reached low micromolar concentrations. Therefore it is possible that the 7,8-NP levels within particular locations within the plaque may also reach these levels *in vivo*. To conclusively determine this requires the direct measurement of 7,8-NP. An additional measurement of 7,8-dihydroxanthopterin would also provide information to the reaction of 7,8-NP and infer the environment 7,8-NP was secreted by the macrophages since neopterin and 7,8-dihydroxanthopterin are formed by different oxidants reacting with 7,8-NP.

As was demonstrated within plasma more than one antioxidant was attributed to the full antioxidant protection against peroxyl radicals towards protein. This most likely extends to that of plaques in which antioxidants may act alone or in synergy for the protection of cells, extracellular matrix and the LDL present. This does depend however on the spatial organisation of the antioxidants a factor not applicable to plasma. α-Tocopherol may have exerted both antioxidant and pro-oxidant properties observed within the plaques. There were significant negative correlations with DOPA (Plaque C) and dityrosine (Plaque D) concentrations suggesting a protective effect and significant positive correlations with TBARS (Plaque E) and protein carbonyl (combined plaque data) concentrations suggesting a pro-oxidative effect. This dual role of α-tocopherol has also been reported for uric acid (Patterson et al., 2003).

As suggested by this study, the inclusion of other markers measured within in each plaque, 7-KC, uric acid and ascorbic acid, may provide additional information on the relationships and mechanisms of oxidants, free radicals and antioxidants which may drive this complex and diverse disease.

References

Abedin, M., Tintut, Y., and Demer, L. L. (2004). Vascular calcification: Mechanisms and clinical ramifications. *Arteriosclerosis, Thrombosis, and Vascular Biology* **24:** 1161-1170.

Adachi, T., Naruko, T., Itoh, A., Komatsu, R., Abe, Y., Shirai, N., Yamashita, H., Ehara, S., Nakagawa, M., Kitabayashi, C., Ikura, Y., Ohsawa, M., Yoshiyama, M., Haze, K., and Ueda, M. (2007). Neopterin is associated with plaque inflammation and destabilisation in human coronary atherosclerotic lesions. *Heart* **93**(12)**:** 1537-1541.

Akagawa, M., Sasaki, D., Kurota, Y., and Suyama, K. (2005). Formation of α-aminoadipic and γ-glutamic semialdehydes in proteins by the Mallard reaction. *Annals of the New York Academy of Sciences* **1043:** 129-134.

Akagawa, M., Sasaki, D., Ishii, Y., Kurota, Y., Yotsu-Yamashita, M., Uchida, K., and Suyama, K. (2006). New method for the quantitative determination of major protein carbonyls, α-aminoadipic and γ-glutamic semialdehydes: Investigation of the formation mechanism and chemical nature in vitro and in vivo. *Chemical Research in Toxicology* **19**(8)**:** 1059-1065.

Alcouffe, J., Caspar-Bauguil, S., Garcia, V., Salvayre, R., Thomsen, M., and Benoist, H. (1999). Oxidized low density lipoproteins induce apoptosis in PHA-activated peripheral blood mononuclear cells and in the Jurkat T-cell line. *Journal of Lipid Research* **40**(7)**:** 1200-1210.

Aldini, G., Dalle-Donne, I., Facino, R. M., Milzani, A., and Carini, M. (2007). Intervention strategies to inhibit protein carbonylation by lipoxidation-derived reactive carbonyls. *Medicinal Research Reviews* **27**(6)**:** 817-868.

Assoian, R. K., Fleurdelys, B., Stevenson, H. C., Miller, P. J., Madtes, D. K., Raines, E., W., , Ross, R., and Sporn, M. B. (1987). Expression and secretion of type 13 transforming growth factor by activated human macrophages. *Proceedings of the National Academy of Sciences of the United States of America* **84**(17)**:** 6020-6024.

Baier-Bitterlich, G., Fuchs, D., Murr, C., Reibnegger, G., Werner-Felmayer, G., Sgonc, R., Bock, G., Dierich, M. P., and Wachter, H. (1995). Effect of neopterin and 7,8-dihydroneopterin on tumor necrosis factor-κβ induced programmed cell death. *FEBS Letters* **364**(2)**:** 234-238.

Baier-Bitterlich, G., Baier, G., Fuchs, D., Bock, G., Hausen, A., Utermann, G., Pavelka, M., and Wachter, H. (1996). Role of 7,8-dihydroneopterin in T-cell apoptosis and HTLV-1 transcription in vitro. *Oncogene* **13**(10)**:** 2281-2285.

Baird, S. K., Reid, L., Hampton, M. B., and Gieseg, S. P. (2005). OxLDL induced cell death is inhibited by the macrophage synthesised pterin, 7,8-dihydroneopterin, in U937 cells but not THP-1 cells. *Biochimica et Biophysica Acta - Molecular Cell Research* **1745**(3)**:** 361-369.

Ball, R. Y., Stowers, E. C., Burton, J. H., Cary, N. R. B., Skepper, J. N., and Mitchinson, M. J. (1995). Evidence that the death of macrophage foam cells contributes to the lipid core of atheroma. *Atherosclerosis* **114**(1)**:** 45-54.

Beal, M. F. (2002). Oxidatively modified proteins in aging and disease. *Free Radical Biology and Medicine* **32**(9)**:** 797-803.

Berlett, B. S., and Stadtman, E. R. (1997). Protein oxidation in aging, disease, and oxidative stress. *Journal of Biological Chemistry* **272**(33)**:** 20313-20316.

Bevilacqua, M. P., Pober, J. S., Mendrick, D. L., Cotran, R. S., and Gimborne, J., M.A. (1987). Identification of an inducible endothelial-leukocyte adhesion molecule. *Proceedings of the National Academy of Sciences of the United States of America* **84:** 9238-9242.

Bostrom, K., Watson, K. E., Horn, S., Wortham, C., Herman, I. M., and Demer, L. L. (1993). Bone morphogenetic protein expression in human atherosclerotic lesions. *Journal of Clinical Investigation* **91:** 1800-1809.

Bowry, V. W., and Stocker, R. (1993). Tocopherol-mediated peroxidation. The prooxidant effect of vitamin E on the radical-initiated oxidation of human low-density lipoprotein. *Journal of the American Chemical Society* **115**(14)**:** 6029-6044.

Burgstahler, C., Reimann, A., Beck, T., Kuettner, A., Baumann, D., Heuschmid, M., Brodoefel, H., Claussen, C. D., Kopp, A. F., and Schroeder, S. (2007). Influence of a lipid-lowering therapy on calcified and noncalcified coronary plaques monitored by multislice detector computed tomography: Results of the New Age II Pilot Study. *Investigative Radiology* **42**(3)**:** 189-195.

Carpenter, K. L., Cheeseman, K. H., van der Veen, C., Taylor, S. E., Walker, M. K., and Mitchinson, M. J. (1995). Depletion of alpha-tocopherol in human atherosclerotic lesions. *Free radical research* **23**(6)**:** 549-558.

Cassidy, L. (2003). The localisation of oxidative damage to proteins. *Masters of Science*. University of Canterbury, Christchurch, New Zealand.

Chang, Y. H., Abdalla, D. S. P., and Sevanian, A. (1997). Characterization of cholesterol oxidation products formed by oxidative modification of low density lipoprotein. *Free Radical Biology and Medicine* **23**(2)**:** 202-214.

Chapman, M. J. (2007). From pathophysiology to targeted therapy for atherothrombosis: A role for the combination of statin and aspirin in secondary prevention. *Pharmacology and Therapeutics* **113**(1)**:** 184-196.

Chatzizisis, Y. S., Coskun, A. U., Jonas, M., Edelman, E. R., Feldman, C. L., and Stone, P. H. (2007). Role of Endothelial Shear Stress in the Natural History of Coronary Atherosclerosis and Vascular Remodeling. Molecular, Cellular, and Vascular Behavior. *Journal of the American College of Cardiology* **49**(25)**:** 2379-2393.

Cheeseman, K. H., and Slater, T. F. (1993). An introduction to free radical biochemistry. *British Medical Bulletin* **49**(3)**:** 481-493.

Chisolm, G. M., Hazen, S. L., Fox, P. L., and Cathcart, M. K. (1999). The oxidation of lipoproteins by monocytes-macrophages. Biochemical and biological mechanisms. *Journal of Biological Chemistry* **274**(37)**:** 25959-25962.

Chisolm, G. M., and Steinberg, D. (2000). The oxidative moification hypothesis of atherogenesis: An overview. *Free Radical Biology and Medicine* **28**(12)**:** 1815-1826.

Cox, B. E., Griffin, E. E., Ullery, J. C., and Jerome, W. G. (2007). Effects of cellular cholesterol loading on macrophage foam cell lysosome acidification. *Journal of Lipid Research* **48**(5)**:** 1012-1021.

Crisby, M., Nordin-Fredriksson, G., Shah, P. K., Yano, J., Zhu, J., and Nilsson, J. (2001). Pravastatin treatment increases collagen content and decreases lipid content, inflammation, metalloproteinases, and cell death in human carotid plaques: Implications for plaque stabilization. *Circulation* **103**(7)**:** 926-933.

Cyrus, T., Sung, S., Zhao, L., Funk, C. D., Tang, S., and Pratico, D. (2002). Effect of low-dose aspirin on vascular inflammation, plaque stability, and atherogenesis in low-density lipoprotein receptor-deficient mice. *Circulation* **106**(10)**:** 1282-1287.

Dalle-Donne, I., Giustarini, D., Colombo, R., Rossi, R., and Milzani, A. (2003). Protein carbonylation in human diseases. *Trends in Molecular Medicine* **9**(4)**:** 169-176.

Daneshvar, B., Frandsen, H., Autrup, H., and Dragsted, L. O. (1997). γ-Glutamyl semialdehyde and 2-amino-adipic semialdehyde: Biomarkers of oxidative damage to proteins. *Biomarkers* **2**(2)**:** 117-123.

Danilevicius, C. F., Lopes, J. B., and Pereira, R. M. R. (2007). Bone metabolism and vascular calcification. *Brazilian Journal of Medical and Biological Research* **40**(4)**:** 435-442.

Daugherty, A., Dunn, J. L., Rateri, D. L., and Heinecke, J. W. (1994). Myeloperoxidase, a catalyst for lipoprotein oxidation, is expressed in human atherosclerotic lesions. *Journal of Clinical Investigation* **94**(1)**:** 437-444.

Davies, M. J., Richardson, P. D., Woolf, N., Katz, D. R., and Mann, J. (1993). Risk of thrombosis in human atherosclerotic plaques: Role of extracellular lipid, macrophage, and smooth muscle cell content. *British Heart Journal* **69**(5)**:** 377-381.

Davies, M. J. (1996). Protein and peptide alkoxyl radicals can give rise to C-terminal decarboxylation and backbone cleavage. *Archives of Biochemistry and Biophysics* **336**(1)**:** 163-172.

Davies, M. J., Fu, S., Wang, H., and Dean, R. T. (1999). Stable markers of oxidant damage to proteins and their application in the study of human disease. *Free Radical Biology and Medicine* **27**(11/12)**:** 1151-1163.

Dayuan, L. I., Yang, B., and Mehta, J. L. (1998). Ox-LDL induces apoptosis in human coronary artery endothelial cells: Role of PKC, PTK, bcl-2, and Fas. *American Journal of Physiology* **275**(2 PART 2).

Dean, R. T., Fu, S., Stocker, R., and Davies, M. J. (1997). Biochemistry and pathology of radical-mediated protein oxidation. *Biochemical Journal* **324**(1)**:** 1-18.

Demer, L. L., Watson, K. E., and Bostrom, K. (1994). Mechanism of calcification in atherosclerosis. *Trends in Cardiovascular Medicine* **4**(1)**:** 45-49.

Demer, L. L., and Tintut, Y. (2003). Mineral exploration: Search for the mechanism of vascular calcification and beyond. The 2003 Jeffrey M. Hoeg Award lecture. *Arteriosclerosis, Thrombosis, and Vascular Biology* **23**(10)**:** 1739-1743.

Denz, H., Fuchs, D., Hausen, A., Huber, H., Nachbaur, D., Reibnegger, G., Thaler, J., Werner, E. R., and Wachter, H. (1990). Value of urinary neopterin in the differential diagnosis of bacterial and viral infections. *Klinische Wochenschrift* **68**(4)**:** 218-222.

Duggan, S., Rait, C., Platt, A., and Gieseg, S. P. (2002). Protein and thiol oxidation in cells exposed to peroxyl radicals is inhibited by the macrophage synthesised pterin 7,8-dihydroneopterin. *Biochimica et Biophysica Acta - Molecular Cell Research* **1591**(1-3)**:** 139-145.

Esterbauer, H., Gebicki, J., Puhl, H., and Jurgens, G. (1992). The role of lipid peroxidation and antioxidants in oxidative modification of LDL. *Free Radical Biology and Medicine* **13**(4)**:** 341-390.

Esterbauer, H., Wag, G., and Puhl, H. (1993). Lipid peroxidation and its role in atherosclerosis. *British Medical Bulletin* **49**(3)**:** 566-576.

Exner, M., Hermann, M., Hofbauer, R., Kapiotis, S., and Gmeiner, B. M. K. (2003). Free and peptide bound DOPA can inhibit initiation of low density lipoprotein oxidation. *Free Radical Research* **37**(11)**:** 1147-1156.

Firth, C. A. (2006). 7,8-Dihydroneopterin-mediated protection of low density lipoprotein, but not human macrophages, from oxidative stress. *Doctor of Philosophy*. University of Canterbury, Christchurch, New Zealand.

Firth, C. A., Yang, Y. T., and Gieseg, S. P. (2007). Lipid oxidation predominates over protein hydroperoxide formation in human monocyte-derived macrophages exposed to aqueous peroxyl radicals. *Free Radical Research* **41**(7)**:** 839-848.

Firth, C. A., Crone, E. M., Flavall, E. A., Roake, J. A., and Gieseg, S. P. (2008). Macrophage mediated protein hydroperoxide formation and lipid oxidation in low density lipoprotein are inhibited by the inflammation marker 7,8-dihydroneopterin. *Biochimica et Biophysica Acta* **1783**(6)**:** 1095-1101.

Flavall, E. (2008). Localisation of antioxidants and oxidative markers within the atherosclerotic plaque. *Masters of Science*. University of Canterbury, Christchurch, New Zealand.

Flavall, E. A., Crone, E. M., Moore, G. A., and Gieseg, S. P. (2008). Dissociation of neopterin and 7,8-dihydroneopterin from plasma components before HPLC analysis. *Journal of Chromatography B: Analytical Technologies in the Biomedical and Life Sciences* **863**(1)**:** 167-171.

Frei, B., Stocker, R., and Ames, B. N. (1988). Antioxidant defences and lipid peroxidation in human blood plasma. *Proceedings of the National Academy of Sciences of the United States of America* **85**(24)**:** 9748-9752.

Fu, S., Davies, M. J., Stocker, R., and Dean, R. T. (1998). Evidence for roles of radicals in protein oxidation in advanced human atherosclerotic plaque. *Biochemical Journal* **333:** 519-525.

Garcia-Cruset, S., Carpenter, K. L., Guardiola, F., Stein, B., and Mitchinson, M. J. (2001). Oxysterol profiles on normal arteries, fatty streaks and advanced lesions. *Free Radical Research* **35**(1)**:** 31-42.

Garner, B., and Jessup, W. (1996). Cell-mediated oxidation of low-density lipoprotein: The elusive mechanism(s). *Redox Report* **2**(2): 97-104

Gay, C., Collins, J., and Gebicki, J. M. (1999). Hydroperoxide assay with the ferric-xylenol orange complex. *Analytical Biochemistry* **273**(2)**:** 149-155.

Gebicki, J. M. (1997). Protein hydroperoxides as new reactive oxygen species. *Redox Report* **3**(2)**:** 99-110.

Gebicki, S., and Gebicki, J. M. (1999). Crosslinking of DNA and proteins induced by protein hydroperoxides. *Biochemical Journal* **338**(3)**:** 629-636.

Gieseg, S. P., Simpson, J. A., Charlton, T. S., Duncan, M. W., and Dean, R. T. (1993). Protein-bound 3,4-dihydroxyphenylalanine is a major reductant formed during hydroxyl radical damage to proteins. *Biochemistry* **32**(18)**:** 4780-4786.

Gieseg, S. P., and Esterbauer, H. (1994). Low density lipoprotein is saturable by pro-oxidant copper. *FEBS Letters* **343:** 188-194.

Gieseg, S. P., Reibnegger, G., Wachter, H., and Esterbauer, H. (1995). 7,8 Dihydroneopterin inhibits low density lipoprotein oxidation in vitro. Evidence that this macrophage secreted pteridine is an anti-oxidant. *Free Radical Research* **23**(2)**:** 123-136.

Gieseg, S. P., Maghzal, G., and Glubb, D. (2000). Inhibition of haemolysis by the macrophage synthesized antioxidant, 7,8- dihydroneopterin. *Redox Report* **5**(2-3)**:** 98-100.

Gieseg, S. P., Whybrow, J., Glubb, D., and Rait, C. (2001). Protection of U937 cells from free radical damage by the macrophage synthesized antioxidant 7,8-dihydroneopterin. *Free Radical Research* **35**(3)**:** 311-318.

Gieseg, S. P., Pearson, J., and Firth, C. A. (2003). Protein hydroperoxides are a major product of low density lipoprotein oxidation during copper, peroxyl radical and macrophage-mediated oxidation. *Free Radical Research* **37**(9)**:** 983-991.

Gieseg, S. P., Crone, E. M., Flavall, E. A., and Amit, Z. (2008a). Potential to inhibit growth of atherosclerotic plaque development through modulation of macrophage neopterin/7,8-dihydroneopterin synthesis. *British Journal of Pharmacology* **153**(4)**:** 627-635.

Gieseg, S., Leake, D. S., Flavall, E., Amit, Z., and Yang, Y. (2008b). Macrophage antioxidant protection within atherosclerotic plaques. *Frontiers in Bioscience* **Article in press**.

Gimbrone, M. A. (1999). Vascular endothelium, hemodynamic forces, and atherogenesis. *American Journal of Pathology* **155**(1)**:** 1-5.

Giulivi, C., and Davies, K. J. A. (1994). Dityrosine: A marker for oxidatively modified proteins and selective proteolysis. *Methods in Enzymology* **233:** 363-371.

Gniwotta, C., Morrow, J. D., Roberts II, L. J., and Kuhn, H. (1997). Prostaglandin F2-like compounds, F2-isoprostanes, are present in increased amounts in human atherosclerotic lesions. *Atherosclerosis, Thrombosis and Vascular Biology* **17**(11)**:** 3236-3241.

Goldstein, J. L., Ho, Y. K., Basu, S. K., and Brown, M. S. (1979). Binding site on macrophages that mediates uptake and degradation of acetylated low density lipoprotein, producing massive cholesterol deposition. *Proceedings of the National Academy of Sciences of the United States of America* **76**(1)**:** 333-337.

Grebe, S. O., Kuhlmann, U., and Muller, T. F. (2004). Elevated post-transplant levels of neopterin are associated with poorer long-term graft outcome. *Pteridines* **15**(3)**:** 113-119.

Guo, W., Morrisett, J. D., DeBakey, M. E., Lawrie, G. M., and Hamilton, J. A. (2000). Quantification in situ of crystalline cholesterol and calcium phosphate hydroxyapatite in human atherosclerotic plaques by solid-state magic angle spinning NMR. *Arteriosclerosis, Thrombosis, and Vascular Biology* **20**(6)**:** 1630-1636.

Halliwell, B., and Gutteridge, J. M. C. (1999). "Free radicals in biology and medicine." Clarendon Press, Oxford.

Hay, D. R. (2004). Cardiovascular disease in New Zealand, 2004 *Technical Report No. 82* New Zealand Heart Foundation

Hegyi, L., Skepper, J. N., Cary, N. R. B., and Mitchinson, M. J. (1996). Foam cell apoptosis and the development of the lipid core of human atherosclerosis. *Journal of Pathology* **180**(4)**:** 423-429.

Heinecke, J. W., Baker, L., Rosen, H., and Chait, A. (1986). Superoxide-mediated modification of low density lipoprotein by arterial smooth muscle cells. *Journal of Clinical Investigation* **77**(3)**:** 757-761.

Heinecke, J. W., Li, W., Daehnke Iii, H. L., and Goldstein, J. A. (1993). Dityrosine, a specific marker of oxidation, is synthesized by the myeloperoxidase-hydrogen peroxide system of human neutrophils and macrophages. *Journal of Biological Chemistry* **268**(6)**:** 4069-4077.

Heinecke, J. W. (1999). Mass spectrometric quantification of amino acid oxidation products in proteins: Insights into pathways that promote LDL oxidation in the human artery wall. *FASEB Journal* **13**(10)**:** 1113-1120.

Helderman, F., Segers, D., De Crom, R., Hierck, B. P., Poelmann, R. E., Evans, P. C., and Krams, R. (2007). Effect of shear stress on vascular inflammation and plaque development. *Current Opinion in Lipidology* **18**(5)**:** 527-533.

Hennekens, C. H., and Schneider, W. R. (2008). The need for wider and appropriate utilization of aspirin and statins in the treatment and prevention of cardiovascular disease. *Expert Review of Cardiovascular Therapy* **6**(1)**:** 95-107.

Herpfer, I., Greilberger, J., Ledinski, G., Widner, B., Fuchs, D., and Jurgens, G. (2002). Neopterin and 7,8-dihydroneopterin interfere with low density lipoprotein oxidation mediated by peroxynitrite and/or copper. *Free Radical Research* **36**(5)**:** 509-520.

Hiramatsu, K., Rosen, H., and Heinecke, J. W. (1987). Superoxide initiates oxidation of low density lipoprotein by human monocytes. *Arteriosclerosis* **7**(1)**:** 55-60.

Hoffmann, G., Kenn, S., Wirleitner, B., Deetjen, C., Frede, S., Smolny, M., Rieder, J., Fuchs, D., Baier-Bitterlich, G., and Schobersberger, W. (1998). Neopterin induces nitric oxide-dependent apoptosis in rat vascular smooth muscle cells. *Immunobiology* **199:** 63-73.

Hoffmann, G., Gollnick, F., and Meyer, R. (2002). Neopterin inhibits ATP-induced calcium release in alveolar epithelial cell *in vitro*. *Mediators of Inflammation* **11:** 181-185.

Hoffmann, G., Wirleitner, B., and Fuchs, D. (2003). Potential role of immune system activation-associated production of neopterin derivatives in humans. *Inflammation Research* **52**(8)**:** 313-321.

Hughes, H., Mathews, B., Lenz, M. L., and Guyton, J. R. (1994). Cytotoxicity of oxidized LDL to porcine aortic smooth muscle cells is associated with the oxysterols 7-ketocholesterol and 7-hydroxycholesterol. *Arteriosclerosis and Thrombosis* **14**(7)**:** 1177-1185.

Jang, I. K., Lassila, R., and Fuster, V. (1993). Atherogenesis and inflammation. *European Heart Journal* **14**(Suppl. K)**:** 2-6.

Jessup, W., Rankin, S. M., De Whalley C.V., Hoult, R. S., Scott, J., and Leake, D. S. (1990). α-Tocopherol consumption during low-density-lipoprotein oxidation *Biochemical Journal* **265**(1)**:** 399-403.

Jessup, W., and Brown, A. J. (2005). Novel routes for metabolism of 7-ketocholesterol. *Rejuvenation Research* **8**(1)**:** 9-12.

Kojima, S., Icho, T., Kajiwara, Y., and Kubota, K. (1992). Neopterin as an endogenous antioxidant. *FEBS Letters* **304**(2,3)**:** 163-166.

Kritharides, L., Jessup, W., Gifford, J., and Dean, R. T. (1993). A method for defining the stages of low density lipoprotein oxidation by the separation of cholesterol and cholesteryl ester oxidation products using HPLC. *Analytical Biochemistry* **213:** 79-98.

Kritharides, L., Jessup, W., and Dean, R. T. (1995). Macrophages require both iron and copper to oxidize low-density lipoprotein in Hank's Balanced Salt solution. *Archives of Biochemistry and Biophysics* **323**(1): 127-136

Kruth, H. S., Huang, H. W., Ishii, I., and Zhang, W.-Y. (2002). Macrophage foam cell formation with native low density lipoprotein *Journal of Biochemical Chemistry* **277**(37)**:** 23573-34580.

Larsson, D. A., Baird, S., Nyhalah, J. D., Yuan, X. M., and Li, W. (2006). Oxysterol mixtures, in atheroma-relevant proportions, display synergistic and proapoptotic effects. *Free Radical Biology and Medicine* **41**(6)**:** 902-910.

Larsson, H., Bottiger, Y., Iuliano, L., and Diczfalusy, U. (2007). In vivo interconversion of 7B-hydroxycholesterol and 7-ketocholesterol, potential surrogate markers for oxidative stress. *Free Radical Biology and Medicine* **43**(5)**:** 695-701.

Lassila, R. (1993). Inflammation in atheroma: Implications for the plaque ruture and platelet-collagen interaction. *European Heart Journal* **14**(Suppl. K)**:** 94-97.

Leeuwenburgh, C., Rasmussen, J. E., Hsu, F. F., Mueller, D. M., Pennathur, S., and Heinecke, J. W. (1997). Mass spectrometric quantification of markers for protein oxidation by tyrosyl radical, copper, and hydroxyl radical in low density lipoprotein isolated from human atherosclerotic plaques. *Journal of Biological Chemistry* **272**(6)**:** 3520-3526.

Li, W., Ostblom, M., Xu, L. H., Hellsten, A., Leanderson, P., Liedberg, B., Brunk, U. T., Eaton, J. W., and Yuan, X. M. (2006). Cytocidal effects of atheromatous plaque components: The death zone revisited. *FASEB Journal* **20**(13)**:** 2281-2290.

Libby, P. (2002a). Inflammation in atherosclerosis. *Nature* **420**(6917)**:** 868-874.

Libby, P. (2002b). Atherosclerosis: The new view. *Scientific American* **286**(5)**:** 46.

Libby, P., Ridker, P. M., and Maseri, A. (2002). Inflammation and atherosclerosis. *Circulation* **105**(9)**:** 1135-1143.

Ling, L. J. (2003). Peroxyl radical mediated protein oxidation in plasma. *Masters of Science*. University of Canterbury, Christchurch, New Zealand.

Lizard, G., Monier, S., Cordelet, C., Gesquiere, L., Deckert, V., Gueldry, S., Lagrost, L., and Gambert, P. (1999). Characterization and comparison of the mode of cell death, apoptosis versus necrosis, induced by 7β-hydroxycholesterol and 7-ketocholesterol in the cells of the vascular wall. *Arteriosclerosis, Thrombosis, and Vascular Biology* **19**(5)**:** 1190-1200.

Martinet, W., Knaapen, M. W. M., De Meyer, G. R. Y., Herman, A. G., and Kockx, M. M. (2002). Elevated levels of oxidative DNA damage and DNA repair enzymes in human atherosclerotic plaques. *Circulation* **106**(8)**:** 927-932.

Neuzil, J., and Stocker, R. (1993). Bilrubin attenuates radical-mediated damage to serum albumin. *FEBS* **331**(3)**:** 281-284.

Neuzil, J., Thomas, S. R., and Stocker, R. (1996). Requirement for, promotion, or inhibition by α-tocopherol of radical- induced initiation of plasma lipoprotein lipid peroxidation. *Free Radical Biology and Medicine* **22**(1-2)**:** 57-71.

Nishi, K., Uno, M., Fukuzawa, K., Horiguchi, H., Shinno, K., and Nagahiro, S. (2002). Clinicopathological significance of lipid peroxidation in carotid plaques. *Atherosclerosis* **160**(2)**:** 289-296.

Nishio, E., Arimura, S., and Watanabe, Y. (1996). Oxidized LDL induces apoptosis in cultured smooth muscle cells: A possible role for 7-ketocholesterol. *Biochemical and Biophysical Research Communications* **223**(2)**:** 413-418.

Niu, X., Zammit, V., Upston, J. M., Dean, R. T., and Stocker, R. (1999). Coexistence of oxidized lipids and α-tocopherol in all lipoprotein density fractions isolated from advanced human atherosclerotic plaques. *Arteriosclerosis, Thrombosis, and Vascular Biology* **19**(7)**:** 1708-1718.

Oettl, K., Dikalov, S., Freisleben., H.-J., Mlekusch, W., and Reibnegger, G. (1997). Spin trapping study of antioxidant properties of neopterin and 7,8-dihydroneopterin. *Biochemical and Biophysical Research Communications* **234**(3)**:** 774-778.

Oettl, K., Wirleitner, B., Baier-Bitterlich, G., Grammer, T., Fuchs, D., and Reibnegger, G. (1999). Formation of oxygen radicals in solutions of 7,8-dihydroneopterin. *Biochemical and Biophysical Research Communications* **264**(1)**:** 262-267.

Osborn, A. (2006). Measurements of human plasma oxidation. *Master of Science*. Univeristy of Canterbury, Christchurch, New Zealand.

Patterson, R. A., Horsley, E. T. M., and Leake, D. S. (2003). Prooxidant and antioxidant properties of human serum ultrafiltrates toward LDL: important role of uric acid. *Journal of Lipid Research* **44:** 512-521.

Pearson, J. (2002). Oxidative modification of apolipoprotein B-100. *Master of Science*. University of Canterbury, Christchurch, New Zealand.

Pietzsch, J. (2000). Measurement of 5-hydroxy-2-aminovaleric acid as a specific marker of iron mediated oxidation of proline and arginine side chain residues of low density lipoprotein apolipoprotein B-100. *Biochemical and Biophysical Research Communications* **270:** 852-857.

Prunet, C., Petit, J. M., Ecarnot-Laubriet, A., Athias, A., Miguet-Alfonsi, C., Rohmer, J. F., Steinmetz, E., Neel, D., Gambert, P., and Lizard, G. (2006). High circulating levels of 7β- and 7α-hydroxycholesterol and presence of apoptotic and oxidative markers in arterial lesions of normocholesterolemic atherosclerotic patients undergoing endarterectomy. *Pathologie Biologie* **54**(1)**:** 22-32.

Quinlan, G. J., Evans, T. W., and Gutteridge, J. M. C. (1994). Oxidative damage to plasma proteins in adult respiratory distress syndrome. *Free Radical Research* **20**(5)**:** 289-298.

Quinn, M. T., Parthasarathy, S., Fong, L. G., and Steinberg, D. (1987). Oxidatively modified low density lipoproteins: A potential role in recruitment and retention of monocyte/macrophages during atherogenesis. *Proceedings of the National Academy of Sciences of the United States of America* **84**(9)**:** 2995-2998.

Rakjavashisth, T. B., Andalibi, A., Territo, M. C., Berliner, J. A., Navab, M., Fogelman, A. M., and Lusis, A. J. (1990). Induction of endothelial cell expression of granulocyte and macrophage colony-stimulating factors by modified low-density lipoproteins. *Nature* **344**(6263)**:** 254-257.

Reibnegger, G., Krainer, M., Herold, M., Ludwig, H., Wachter, H., and Huber, H. (1991). Predictive value of interleukin-6 and neopterin in patients with multiple myeloma. *Cancer Research* **51**(23)**:** 6250-6253.

Requena, J. R., Chao, C.-C., Levine, R. L., and Stradman, E. R. (2001). Glutamic and aminoadipic semialdehydes are the main carbonyl products of metal catalyzed oxidation of proteins. *Proceedings of the National Academy of Sciences of the United States of America* **98**(1)**:** 69-74.

Resnick, N., Yahav, H., Shay-Salit, A., Shushy, M., Schubert, S., Zilberman, L. C. M., and Wofovitz, E. (2003). Fluid shear stress and the vascular endothelium: For better and for worse. *Progress in Biophysics and Molecular Biology* **81**(3)**:** 177-199.

Rodgers, K. J., and Dean, R. T. (2000). Metabolism of protein-bound DOPA in mammals. *International Journal of Biochemistry and Cell Biology* **32**(9)**:** 945-955.

Rodriguez, I. R., Alam, S., and Lee, J. W. (2004). Cytotoxicity of oxidized low-density lipoprotein in cultured RPE cells is dependent on the formation of 7-ketocholesterol. *Investigative Ophthalmology and Visual Science* **45**(8)**:** 2830-2837.

Ross, R., and Glomset, J. A. (1973). Atherosclerosis and the arterial smooth muscle cell: proliferation of smooth muscle is a key event in the genesis of the lesions of atherosclerosis. *Science* **180**(4093)**:** 1332-1339.

Roubal, W. T., and Tappel, A. L. (1966). Polymerization of proteins induced by free-radical lipid peroxidation. *Archives of Biochemistry and Biophysics* **113**(1)**:** 150-155.

Savenkova, M. I., Mueller, D. M., and Heinecke, J. W. (1994). Tyrosyl radical generated by myeloperoxidase is a physiological catalyst for the initiation of lipid peroxidation in low density lipoprotein. *Journal of Biological Chemistry* **269**(32)**:** 20394-20400.

Schoedon, G., Troppmair, J., Fontana, A., Huber, C., Curtius, H. C., and Niederwieser, A. (1987). Biosynthesis and metabolism of pterins in peripheral blood mononuclear cells and leukemia lines of man and mouse. *European Journal of Biochemistry* **166**(2)**:** 303-310.

Scott, J. (2004). Pathophysiology and biochemistry of cardiovascular disease. *Current Opinion in Genetics and Development* **14**(3)**:** 271-279.

Simpson, J. A., Narita, S., Gieseg, S., Gebicki, S., Gebicki, J. M., and Dean, R. T. (1992). Long-lived reactive species on free-radical-damaged proteins. *Biochemical Journal* **282**(3)**:** 621-624.

Smith, C., Mitchinson, M. J., Aruoma, O. I., and Halliwell, B. (1992). Stimulation of lipid peroxidation and hydroxyl-radical generation by the contents of human atherosclerotic lesions. *Biochemical Journal* **286:** 901-905.

Stadler, N., Lindner, R. A., and Davies, M. J. (2004). Direct detection and quantification of transition metal ions in human atherosclerotic plaques: Evidence for the presence of elevated levels of iron and copper. *Arteriosclerosis Thrombosis and Vascular Biology* **24**(5)**:** 949-954.

Stanley, N., Stadler, N., Woods, A. A., Bannon, P. G., and Davis, M. D. (2006). Concentrations of iron correlate with the extent of protein, but not lipid, oxidation in advanced atherosclerotic lesions. *Free Radical Biology and Medicine* **40**(9)**:** 1636-1643.

Stary, H. C., Blankenhorn, D. H., Chandler, A. B., Glagov, S., Insull Jr, W., Richardson, M., Rosenfeld, M. E., Schaffer, S. A., Schwartz, C. J., Wagner, W. D., and Wissler, R. W. (1992). A definition of the intima of human arteries and of its atherosclerosis-prone regions: a report from the Committee on Vascular Lesions of the Council on Arteriosclerosis, American Heart Foundation. *Circulation* **85**(1)**:** 391-405.

Stary, H. C., Chandler, A. B., Glagov, S., Guyton, J. R., Insull Jr, W., Rosenfeld, M. E., Schaffer, S. A., Schwartz, C. J., Wagner, W. D., and Wissler, R. W. (1994). A definition of initial, fatty streak, and intermediate lesions of atherosclerosis: A report from the committee on vascular lesions of the council on arteriosclerosis, American Heart Association. *Arteriosclerosis and Thrombosis* **14**(5)**:** 840-856.

Stary, H. C., Chandler, A. B., Dinsmore, R. E., Fuster, V., Glagov, S., Insull Jr, W., Rosenfeld, M. E., Schwartz, C. J., Wagner, W. D., and Wissler, R. W. (1995). A definition of advanced types of atherosclerotic lesions and a histological classification of atherosclerosis: A report from the Committee on Vascular Lesions of the Council on Arteriosclerosis, American Heart Association. *Arteriosclerosis, Thrombosis, and Vascular Biology* **15**(9)**:** 1512-1531.

Steffen, Y., Wiswedel, I., Peter, D., Schewe, T., and Sies, H. (2006). Cytotoxicity of myeloperoxidase/nitrite-oxidized low-density lipoprotein toward endothelial cells is due to a high 7β-hydroxycholesterol to 7-ketocholesterol ratio. *Free Radical Biology and Medicine* **41**(7)**:** 1139-1150.

Steinberg, D., Parthasarathy, S., Carew, T. E., Khoo, J. C., and Witztum, J. L. (1989). Beyond cholesterol: Modifications of low-density lipoprotein that increase its atherogenicity. *New England Journal of Medicine* **320**(14)**:** 915-924.

Steinbrecher, U. P. (1988). Role of superoxide in endothelial-cell modification of low-density lipoproteins. *Biochimica et Biophysica Acta - Lipids and Lipid Metabolism* **959**(1)**:** 20-30.

Steinbrecher, U. P., Lougheed, M., Kwan, W. C., and Dirks, M. (1989). Recognition of oxidized low density lipoprotein by the scavenger receptor of macrophages results from derivatization of apolipoprotein B by products of fatty acid peroxidation. *Journal of Biological Chemistry* **264**(26)**:** 15216-15223.

Stocker, R., and Keaney, J. F. (2004). Role of oxidative modifications in atherosclerosis. *Physiological Reviews* **84**(4)**:** 1381-1478.

Suarna, C., Dean, R. T., May, J., and Stocker, R. (1995). Human atherosclerotic plaque contains both oxidized lipids and relatively large amounts of α-tocopherol and ascorbate. *Arteriosclerosis, Thrombosis, and Vascular Biology* **15**(10)**:** 1616-1624.

Sutherland, W. H. F., Gieseg, S. P., Walker, R. J., de Jong, S., A.,, Firth, C. A., and Scott, N. (2003). Serum protein bound 3,4-dihydroxyphenylalanine and related products of protein oxidation and chronic hemodialysis. *Renal Failure* **25**(6)**:** 997-1009.

Tang, F. T., Chen, S. R., Wu, X. Q., Wang, T. Q., Chen, J. W., Li, J., Bao, L. P., Huang, H. Q., and Liu, P. Q. (2006). Hypercholesterolemia accelerates vascular calcification induced by excessive vitamin D via oxidative stress. *Calcified Tissue International* **79:** 326-339.

Tanimura, A., McGregor, D. H., and Anderson, H. C. (1983). Matrix vesicles in atherosclerotic calcification. *Proceedings of the Society for Experimental Biology and Medicine* **172**(2)**:** 173-177.

Tatzber, F., Rabl, H., Koriska, K., Erhart, U., Puhl, H., Waeg, G., Krebs, A., and Esterbauer, H. (1991). Elevated serum neopterin levels in atherosclerosis. *Atherosclerosis* **89**(2-3)**:** 203-208.

Tricot, O., Mallat, Z., Heymes, C., Belmin, J., Lesèche, G., and Tedgui, A. (2000). Relation between endothelial cell apoptosis and blood flow direction in human atherosclerotic plaques. *Circulation* **101**(21)**:** 2450-2453.

Upston, J. M., Niu, X., Brown, A. J., Mashima, R., Wang, H., Senthilmohan, R., Kettle, A. J., Dean, R. T., and Stocker, R. (2002a). Disease stage-dependent accumulation of lipid and protein oxidation products in human atherosclerosis. *American Journal of Pathology* **160**(2)**:** 701-710.

Upston, J. M., Terentis, A. C., Morris, K., Keaney Jr, J. F., and Stocker, R. (2002b). Oxidized lipid accumulates in the presence of α-tocopherol in atherosclerosis. *Biochemical Journal* **363**(3)**:** 753-760.

van Reyk, D. M., Brown, A. J., Hulten, L. M., Dean, R. T., and Jessup, W. (2006). Oxysterols in biological systems: Sources, metabolism and pathophysiological relevance. *Redox Report* **11**(6)**:** 255-262.

Walpola, P. L., Gotlieb, A. I., Cybulsky, M. I., and Langille, B. L. (1995). Expression of ICAM-1 and VCAM-1 and monocyte adherence in arteries exposed to altered shear stress. *Arteriosclerosis, Thrombosis, and Vascular Biology* **15**(1)**:** 2-10.

Walter, R. B., Fuchs, D., Weiss, G., Walter, T. R., and Reinhart, W. H. (2003). HMG-CoA reductase inhibitors are associated with decreased serum neopterin levels in stable coronary artery disease. *Clinical Chemistry and Laboratory Medicine* **41**(10)**:** 1314-1319.

Weiss, G., Fuchs, D., Hausen, A., Reibnegger, G., Werner, E. R., Werner-Felmayer, G., Semenitz, E., Dierich, M. P., and Wachter, H. (1993). Neopterin modulates toxicity mediated by reactive oxygen and chloride species. *FEBS Letters* **321**(1)**:** 89-92.

Weiss, G., Willeit, J., Kiechl, S., Fuchs, D., Jarosch, E., Oberhollenzer, F., Reibnegger, G., Tilz, G. P., Gerstenbrand, F., and Wachter, H. (1994). Increased concentrations of neopterin in carotid atherosclerosis. *Atherosclerosis* **106**(2)**:** 263-271.

Wells, S., Broad, J., and Jackson, R. (2006). Estimated prevalence of cardiovascular disease and distribution of cardiovascular risk in New Zealanders: Data for healthcare planners, funders, and providers. *New Zealand Medical Journal* **119**(1232).

Widner, B., Mayr, C., Wirleitner, B., and Fuchs, D. (2000). Oxidation of 7,8-dihydroneopterin by hypochlorous acid yields neopterin. *Biochemical and Biophysical Research Communications* **275**(2)**:** 307-311.

Williams, K. J., and Tabas, I. (1995). The response-to-retention hypothesis of early atherogenesis. *Arteriosclerosis, Thrombosis, and Vascular Biology* **15**(5)**:** 551-562.

Wilson, P. W. F., Kannel, W. B., Silbershatz, H., and D'Agostino, R. B. (1999). Clustering of metabolic factors and coronary heart disease. *Archives of Internal Medicine* **159**(10)**:** 1104-1109.

Wirleitner, B., Obermoser, G., Bock, G., Neurauter, G., Schennach, H., Sepp, N., and Fuchs, D. (2003). Induction of apoptosis in human blood T cells by 7,8-dihydroneopterin: The difference between healthy controls and patients with systemic lupus erythematosus. *Clinical Immunology* **107:** 152-159.

Wirleitner, B., Schroecksnadel, K., Winkler, C., and Fuchs, D. (2005). Neopterin in HIV-1 infection. *Molecular Immunology* **42**(2)**:** 183-194.

Woll, E., Weiss, G., Fuchs, D., Lang, F., and Wachter, H. (1993). Effect of Pteridine Derivatives on Intracellular Calcium-Concentration in Human Monocytic Cells. *Febs Letters* **318**(3)**:** 249-252.

Yang, Y. (2005). Inhibition of protein oxidation in plasma. *Masters of Science*. Univeristy of Canterbury, Christchurch, New Zealand.

Yoshida, Y., Tsuchiya, J., and Niki, E. (1994). Interaction of α-tocopherol with copper and its effect on lipid peroxidation. *Biochimica et Biophysica Acta - General Subjects* **1200**(2)**:** 85-92.

Yuan, X. M., Li, W., Brunk, U. T., Dalen, H., Chang, Y. H., and Sevanian, A. (2000). Lysosomal destabilization during macrophage damage induced by cholesterol oxidation products. *Free Radical Biology and Medicine* **28**(2)**:** 208-218.

Appendix I

Table I. Summary of the average overall concentration of protein, cholesterol, neopterin and α-tocopherol in plaques A-N

Plaques A-E analysed this study, G-H in Firth (2006) and I-N in Flavall (2008). Plaque name includes laboratory code. Data represents the mean ± SEM of the sections averages. Chol – cholesterol

Plaque	Protein	Cholesterol	Neopterin	A-Tocopherol
	mg/g plaque	µmole/g plaque	nmole/g plaque	nmole/g plaque mmole/mol chol
A **RB040407a**	69.23 ± 7.06	7.85 ± 0.38	2.34 ± 0.41	21.84 ± 1.66 0.83 ± 0.04
B **RB040407b**	45.16 ± 6.02	6.68 ± 0.69	1.57 ± 0.16	9.64 ± 1.79 0.77 ± 0.10
C **MD260407**	104.29 ± 6.14	43.39 ± 4.94	2.02 ± 0.15	161.70 ± 16.27 1.47 ± 0.14
D **MLA130607**	120.47 ± 4.10	64.21 ± 2.43	1.93 ± 0.15	95.40 ± 5.25 2.28 ± 0.15
E **BB050507**	186.59 ± 22.78	44.86 ± 4.46	2.00 ± 0.29	200.56 ± 25.30 4.39 ± 0.29
F **TE120704**	91.76 ± 4.04	92.61 ± 0.41	0.72 ± 0.01	360.20 ± 24.74 0.73 ± 0.02
G **DLB011203**	77.62 ± 4.49	37.15 ± 5.01	0.21 ± 0.01*****	32. 33 ± 4.96 2.34 ± 0.12
H **ADC100903**	66.71 ± 4.02	84.75 ± 12.10	0.16 ± 0.01*****	44.69 ± 2.84 3.91 ± 0.33
I **IH120704**	70.30 ± 6.19	75.82 ± 8.21	0.09 ± 0.00*****	57.04 ± 6.57 2.84 ± 0.18
J **HW290304**	92.04 ± 5.13	80.89 ± 6.38	0.21 ± 0.01*****	37.94 ± 5.72 1.59 ± 0.25
K **WC210604**	64.26 ± 2.20	57.95 ± 4.47	1.59 ± 0.11	127.09 ± 6.84 3.89 ± 0.27
L **MS200405**	92.14 ± 3.22	47.42 ± 3.28	1.79 ± 0.15	213.09 ± 6.84 3.97 ± 0.20
M **ES020407**	94.78 ± 13.10	25.81 ± 2.20	1.26 ± 0.18	60.00 ± 5.54 1.55 ± 0.12
N **GP050407**	140.33 ± 5.45	59.31 ± 3.95	0.92 ± 0.06	152.27 ± 10.42 4.28 ± 0.15
Overall Average	**93.98 ± 6.71**	**52.05 ± 4.21**	**1.61 ± 0.17**	**112.41 ± 10.09** **2.49 ± 0.19**

***** The neopterin detected within plaques G-J were analysed by the TCA method. This has been replaced by the ACN method (2.2.4). Therefore the data was not included within the overall average value or the combined plaque analysis.

Table II. Summary of the average overall concentrations of TBARS, protein carbonyls, DOPA and dityrosine in plaques A-N

Plaques A-E analysed this study, G-H in Firth (2006) and I-N in Flavall (2008). Plaque name includes laboratory code. Data represents the mean ± SEM of the sections averages
Chol – cholesterol, prot – protein, ND – not detected

Plaque	TBARS	Prot. carbonyls	DOPA	Dityrosine
	nmole/g plaque	nmole/g plaque	nmole/g plaque	nmole/g plaque
	nmole/mol chol	µmole/g prot	nmole/g prot	nmole/g prot
A RB040407a	21.31 ± 4.41	266.54 ± 62.89	6.44 ± 0.76	0.05 ± 0.03
	2797.65 ± 534.76	3.77 ± 0.66	110.54 ± 14.15	1.04 ± 0.59
B RB040407b	76.32 ± 16.49	159.63 ± 47.15	7.01 ± 0.81	ND
	13830.54 ± 4173.3	3.38 ± 0.65	168.09 ± 18.81	
C MD260407	12.31 ± 1.24	369.50 ± 29.29	25.41 ± 2.04	9.11 ± 2.35
	387.99 ± 75.31	4.01 ± 0.33	263.27 ± 26.34	116.43 ± 39.12
D MLA130607	12.16 ± 0.30	137.32 ± 30.96	16.22 ± 1.08	9.86 ± 1.21
	193.75 ± 7.75	3.08 ± 0.78	124.78 ± 8.34	77.94 ± 7.69
E BB050507	4.20 ± 0.29	434.20 ± 35.63	13.86 ± 1.47	2.27 ± 0.61
	100.60 ± 5.15	3.13 ± 0.39	89.85 ± 9.44	14.12 ± 3.94
F TE120704	9.84 ± 0.68	256.10 ± 56.94	16.24 ± 1.63	3.94 ± 0.12
	106.28 ± 7.34	2.79 ± 0.62	176.96 ± 17.79	42.97 ± 1.35
G DLB011203	4.59 ± 0.70	161.52 ± 25.88	12.79 ± 0.66	0.50 ± 0.10
	128 ± 12.74	2.23 ± 0.35	170.77 ± 11.39	5.85 ± 0.93
H ADC100903	3.39 ± 0.41	357 ± 19.78	11.58 ± 0.67	4.86 ± 1.21
	54.65 ± 8.30	5.56 ± 0.32	177.49 ± 10.61	60.63 ± 13.49
I IH120704	7.48 ± 0.77	310 ± 32.37	15.66 ± 0.71	0.59 ± 0.14
	115.09 ± 15.10	4.79 ± 0.51	245.19 ± 19.87	9.35 ± 1.55
J HW290304	7.43 ± 1.13	140.86 ± 13.26	29.13 ± 3.45	11.62 ± 2.92
	86.41 ± 8.95	5.00 ± 0.37	340.54 ± 40.16	149.26 ± 44.23
K WC210604	4.53 ± 0.85	287.52 ± 25.25	4.93 ± 0.61	0.91 ± 0.15
	77.34 ± 14.97	4.43 ± 0.33	79.08 ± 11.12	14.15 ± 2.26
L MS200405	7.13 ± 1.15	445.04 ± 50.85	15.50 ± 3.47	8.86 ± 1.54
	178.09 ± 35.48	4.82 ± 0.52	179.90 ± 43.20	101.77 ± 18.95
M ES020407	14.28 ± 1.59	276.18 ± 46.51	7.59 ± 1.96	ND
	607.55 ± 79.84	3.02 ± 0.47	84.60 ± 16.17	
N GP050407	15.49 ± 1.61	389.90 ± 38.25	10.08 ± 0.70	9.19 ± 0.89
	255.54 ± 17.66	2.76 ± 0.22	72.06 ± 4.74	66.85 ± 7.23
Overall Average	**14.32 ± 2.26**	**287.09 ± 36.79**	**13.75 ± 1.43**	**4.41 ± 0.81**
	191.01 ± 24.05	**3.77 ± 0.47**	**163.08 ± 18.01**	**47.17 ± 10.09**

Appendix II

The invited review entitled “Potential to inhibit plaque growth of atherosclerotic plaque development through the modulation of macrophage neopterin/7,8-dihydroneopterin/neopterin synthesis” was published within the British Journal of Pharmacology. Figure 2 titled ‘Concentration of neopterin across the length of a carotid atherosclerotic plaque’ displays neopterin data from a plaque analysed during the research.

The second paper, a short communication paper, entitled ‘Dissociation of neopterin and 7,8-dhydroneopterin from plasma components before HPLC analysis” was published in the Journal of Chromatography B. The linearity of neopterin detection between 5 nM and 2 μM for the presented HPLC system was calculated during the course of the study.

The third paper, a research paper, entitled “Macrophage mediated protein hydroperoxide formation and lipid oxidation in low density lipoprotein are inhibited by the inflammation marker 7,8-dihydroneopterin” was published in Biochimica et Biophysica Acta. Table 1 titled “Total neopterin levels in atherosclerotic plaques” lists the overall neopterin content within plaques analysed over the course of this research.